# IDENTIFICATION OF STIFFNESS REDUCTIONS USING PARTIAL NATURAL FREQUENCY DATA

by

Thea Sokheang

A Thesis

Submitted to the Faculty of Purdue University

In Partial Fulfillment of the Requirements for the degree of

Master of Science in Civil Engineering
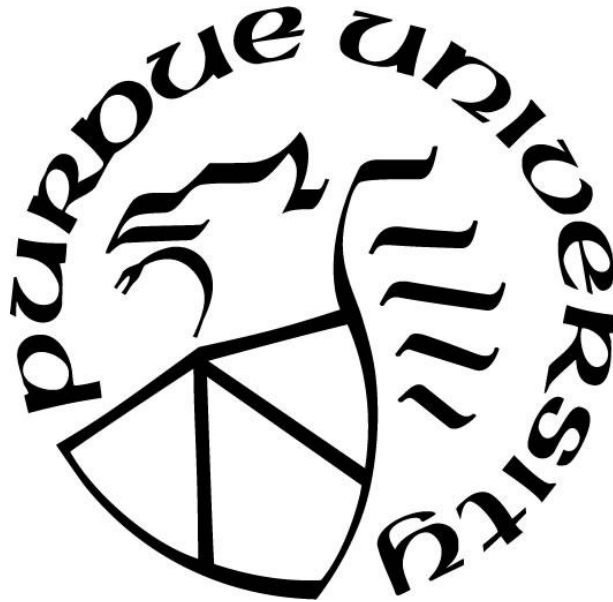
Lyles School of Civil Engineering

West Lafayette, Indiana

May 2019

THE PURDUE UNIVERSITY GRADUATE SCHOOL
STATEMENT OF COMMITTEE APPROVAL

Dr. Ayhan Irfanoglu, Chair

Lyles School of Civil Engineering

Dr. Arun Prakash

Lyles School of Civil Engineering

Dr. Santiago Pujol

Lyles School of Civil Engineering

Approved by:

Dr. Dulcy M. Abraham

Head of the Graduate Program

*To my parents who give me mass, my educators who give me stiffness,
and my wife with whom I share the dynamics of joy.*

ACKNOWLEDGMENTS

I wish to express my sincere gratitude to my advisor and my committee chair, Professor Ayhan Irfanoglu for his support throughout my academic years at Purdue. I appreciate his advice, time, effort and encouragement that I received for this project. I also would like to thank my committee members, Professor Arun Prakash and Professor Santiago Pujol, for their constructive feedbacks on the research.

I am grateful to my teammates for CE 575 class, Jonathan Chi and Shubham Agrawal, for their assistance with the experiment. Professor Santiago Pujol, Professor Shirley Dyke and CE department provided me with materials, equipment and working space for the experiment. I want to thank Mr. Kevin Brower, Mr. Harry Tidrick and Ms. Alana Lund for their help at the Bowen Laboratory. I am grateful to Ms. Molly A. Stetler and Ms. Jenny Ricksy for their assistance on the administrative procedures.

This is possible due to the Fulbright Scholarship by the US Department of State and Purdue University, which provided me with financial support and tuition award for the two-year MSCE program.

Last, my wife Taing Siv Huong has sacrificed her productive two years with me at Purdue where we share both joy and sorrow. My sisters help us adapt and explore the US. This made an unforgettable memory that we have never dreamt of, coming from a developing country, Cambodia.

TABLE OF CONTENTS

LIST OF TABLES

APPENDIX C Tables:

APPENDIX D Tables:

LIST OF FIGURES

APPENDIX C Figures:

APPENDIX D Figures:

ABSTRACT

Author: Thea, Sokheang. MSCE
Institution: Purdue University
Degree Received: May 2019
Title: Identification of Stiffness Reductions Using Partial Natural Frequency Data
Committee Chair: Ayhan Irfanoglu

In vibration-based damage detection in structures, often changes in the dynamic properties such as natural frequencies, modeshapes, and derivatives of modeshapes are used to identify the damaged elements. If only a partial list of natural frequencies is known, optimization methods may need to be used to identify the damage. In this research, the algorithm proposed by Podlevskyi & Yaroshko (2013) is used to determine the stiffness distribution in shear building models. The lateral load resisting elements are presented as a single equivalent spring, and masses are lumped at floor levels. The proposed method calculates stiffness values directly, i.e., without optimization, from the known partial list of natural frequency data and mass distribution. It is shown that if the number of stories with reduced stiffness is smaller than the number of known natural frequencies, the stories with reduced stiffnesses can be identified. Numerical studies on building models with two stories and four stories are used to illustrate the solution method. Effect of error or noise in given natural frequencies on stiffness estimates and, conversely, sensitivity of natural frequencies to changes in stiffness are studied using 7-, 15-, 30-, and 50-story numerical models. From the studies, it is learnt that as the number of stories increases, the natural frequencies become less sensitive to stiffness changes. Additionally, eight laboratory experiments were conducted on a five-story aluminum structural model. Ten slender columns were used in each story of the specimen. Damage was simulated by removing columns in one, two, or three stories. The method can locate and quantify the damage in cases presented in the experimental studies. It is also applied to a 1/3 scaled 18-story steel moment frame building tested on an earthquake simulator (Suita et al., 2015) to identify the reduction in the stiffness due to fractures of beam flanges. Only the first two natural frequencies are used to determine the reductions in the stiffness since the third mode of the tower is torsional and no reasonable planar spring-mass model can be developed to present all of the translational modes. The method produced possible cases of the softening when the damage was assumed to occur at a single story.

1. INTRODUCTION

1.1 Background and Previous Research

1.1.1 Vibration-based Damage Identification Methods and Their Classifications

Dynamic properties of a system such as frequencies and modeshapes have been used to determine variations in the physical parameters of the system such as its mass and stiffness. To locate cavity in a floor or wall, for example, we just knock on them and listen for distinctive response sounds. Obviously, the dynamic responses of the system are related to its physical properties. Changes in its physical properties result in changes in its response. Researchers have been using differences observed in the dynamic responses of a system to determine the changes in its stiffness and mass. This characteristic has many applications in damage detection and structural health monitoring.

During the 1970s and early 1980s, researchers, especially in offshore oil industries, began to study and investigate the response-based damage identification techniques (Doebling et al., 1998). These methods use different dynamic responses and properties to locate and quantify defects. The techniques themselves differ. Global methods use the dynamic responses of the structures to locate and quantify the damage (Doebling et al., 1998), whereas the local methods such as ultrasound and X-ray usually require access to vicinity of the damage which means damage locations are known a priori (Kong, Cai, & Hu, 2017). Rytter (1993) classified the techniques into four levels of damage identification. Level 1 aims to detect that damage exists. Level 2 aims to detect the presence of the damage and its location(s). Level 3 includes Level 2 and quantifies the damage severity, and Level 4 includes Level 3 and estimates the remaining useful life of the system.

Early reviews of the methods were given in Salawu (1997) and Doebling et al. (1998), whereas more recent reviews can be found in Das et al. (2017) and Kong et al. (2017). In addition, Gomes et al. (2018) discusses the application of optimization algorithm and artificial intelligence in the field of damage identification. Kong et al. (2017) categorizes the techniques as Time Domain Methods, Frequency Domain Methods and Modal Domain Methods depending on the type of data used and the analysis procedures. These methods have both advantages and disadvantages. Time Domain Methods use the time series of response directly and thus preserve most information

including the nonlinearity (Kong, Cai, & Hu, 2017). Frequency Domain Methods, on the other hand, transform the time series into frequency domain and usually focus on the ratio of the output signals (acceleration, velocity or displacement) over the input signals (forcing frequencies), which are Frequency Response Functions. For Modal Domain Methods where modal properties such as natural frequencies or periods, and modeshapes and their derivatives are used to determine the system physical properties. The benefits are that the physical properties describe the structure directly and are easy to interpret, while the drawbacks are that much information such as time series of the signal was lost or abandoned and they are sensitive to environmental noise and uncertainty (Kong, Cai, & Hu, 2017).

1.1.2   Methods that Primarily Use Frequency Data

Doebling et al. (1998) categorized the methods using frequency shifts to identify damage as either a forward problem or an inverse problem. The forward problems employ mathematical models to simulate damage and compare the results with the measured frequencies, which means it is a Level 1 type of detection (Doebling, Farrar, & Prime, 1998). On the other hand, the inverse problems, usually Level 2 or 3, compute the damages directly from the frequency changes (Doebling, Farrar, & Prime, 1998). One of the early researches on the forward problems that used shifts in frequencies to identify defects was conducted by Cawley and Adam in 1979. They were able to locate and quantify the damages to an aluminum plate and a carbon-fiber-reinforced plastic plate by using the original modeshape data as well as changes in frequencies before and after the damages were introduced, along with finite-element models. Nevertheless, they only accounted for a single damage location, not multiple locations. Lifshiftz and Rotem (1969) published a journal article on the inverse problem to detect damages using frequency changes. Stubbs and Osegueda (1987) improved upon the work of Cawley and Adam, and incorporated modeshape data to help determine the location of the defects as well the magnitude of the defects (Hassiotis & Jeong, 1995; Doebling, Farrar, & Prime, 1998).

1.1.3   Methods that Primarily Use Modeshapes and their Derivatives

Modeshape change and its derivatives have also been used detect defects. West (1984) was probably the first to use modeshape changes to locate damage by introducing modal assurance criteria (MAC) that established the extent of correlation between the modeshapes of a specimen

when it was undamaged and damaged (Doebling, Farrar, & Prime, 1998). Slope of modeshape, its curvature and higher order derivatives (up to fourth order) prove to be more sensitive to changes in the physical properties of the system (Whalen, 2008). Pandey et al. (1991) used the curvature of the modeshape to pinpoint the damage location estimated from the changes in the curvature, and the severity by the amount of changes occurred. They demonstrated the procedure using finite-element models of cantilevered and simply supported beams. Zhu et al. (2011) did numerical simulations of an eight-story shear building and did an experimental study on a three-story model using changes in the fundamental modeshape slope (CFMSS). They were able to assess and locate the amount of the damages using an iterative scheme. Roy and Chaudhuri (2013) developed an approximate closed-form mathematical solution that relates the fundamental modeshape and its derivatives to the damage location. They did not estimate the magnitude of the damage but mentioned that mathematical correlation can be made to do so. Roy's more recent paper (2017) also included an experiment conducted on a six-story steel frame using the same method.

Strain energy methods are among the other techniques that employ modeshape data for damage estimation analysis. Stubbs et al. (1995) conducted numerous experiments and field testing on a 423 feet three-span bridge. They developed a method which uses the modeshape and stiffness matrices to locate the damage. Shi et al. (1998) introduced modal strain energy (MSE) method, which also used the modeshape data. Modal strain energy change ratio (MSECR), the ratio of the absolute difference of damaged MSE and undamaged MSE over the undamaged MSE, was used to locate and quantify the damage. Other studies on the modal strain energy include but not limited to Cornwell et al. (1999), Alvandi and Cremona (2006), Guan and Karrbhari (2008), and Dawari et al. (2015).

1.1.4   Methods that Use Optimization Techniques and Partial Frequency Data

Many of the methods described above assume that the frequency data are abundant, and that the modeshape information are available. Nonetheless, acquiring reliable and adequate data for vibration-based methods can be challenging, and buildings may be instrumented intermittently. Obtaining all the dynamic properties is improbable. In some cases, especially when the system is not sufficiently instrumented, modeshape data are harder to obtain and appear more susceptible to statistical disparity due to environmental noise (Doebling, Farrar, & Goodman, 1997).

Hassiotis and Jeong (1995) proposed a method to obtain the reduction in stiffness by using only a partial list of natural frequencies. They applied the method to a numerical model of a ten-story steel moment frame, and a cantilevered beam laboratory specimen. Their method was successful in locating and quantifying the amount of damage at more than one location. Since there are not enough input frequencies to solve the equation uniquely, an optimization approach was applied. Their optimization approach involves minimizing a cost function which includes a linear relationship between changes in stiffness and changes in the eigenvalues, and inequality constraints that stiffness coefficients are not allowed to increase, i.e. the elements either remain as before or soften. They introduced three criteria for the cost function: least total change in the element stiffnesses, minimization of the norm of the change in the global stiffness matrix, and minimization of eigenvalue problem residuals. The criteria did not have any physics reasoning rather they were mathematical devices to obtain a unique solution. Lee et al. (2004) extended the method by adding measured changes in modeshape, and Esfandiari et al. (2013) by introducing the modeshape of the original structure into the linear constraint.

1.1.5   Linear Parameterized Inverse Eigenvalue Problem (LiPIEP)

Many buildings or structures may be instrumented sparsely and therefore only partial frequency data before and after an event may be known, and most probably without any modeshape information. For spring-mass systems, if all frequencies and masses are known, the stiffnesses can be calculated directly without using optimization methods or linearizing the equations, eliminating potential errors. However, in an n-degree of freedom system, if only a partial set of frequencies (say, m number of frequencies) are known as opposed to the complete spectrum, i.e. n number of frequencies, and no modeshape information is given, it may not be possible to reach a solution without some sort of comprises. For example, optimization methods, with their inherent biases, may be used. Or, the number of softened stories may be limited to fewer than m. In this case, all possible softened cases need to be investigated and the extra frequency or frequencies from the known set of frequency can be used to choose the solution which fits the measured frequencies best. The problems in which elements of the matrices are calculated from the known eigenvalues are called Inverse Eigenvalue Problem (IEP). There are many different types of IEPs depending on the properties of the to-be-constituted matrix and the known eigenvalues and eigenvectors. In

case of spring-mass systems, which are used to model building structures, the problem is classified as Linear Parameterized Inverse Eigenvalue Problem (LiPIEP).

1.2   Objectives and Scope of Research

The current research project aims to use the solution to LiPIEP of spring-mass systems to determine the reduction in the stiffnesses of a building model using only a partial set of natural frequency data. Theoretical and mathematical background are presented in the following chapter. Numerical studies and experiments on a five-degree-of-freedom shear building model are made to illustrate how the method works. Next, the method will be applied to a building. Finally, it is summarized and concluded in the last chapter.

2. METHOD FOR CALCULATING STIFFNESSES FROM PARTIAL NATURAL FREQUENCY DATA

2.1 Spring-Mass System Idealization

Many structural systems may be idealized as spring-mass-damper systems. One example of those is the water tank supported by concrete or steel pillars. It can be regarded as a single-degree-of-freedom system where the lumped mass (water tank) is held by a linear spring (concrete or steel pillars). The damper is the energy dissipation device and it should always exist since the system always loses energy somehow. Often, the damping is small. In such structures, characteristic dynamic properties such as modal periods and modeshapes are estimated using only a spring-mass (Figure 2-1). It is not limited to a single degree of freedom. For example, a building is a multiple-degree-of-freedom system where each floor is considered as a lumped mass connected by columns which were thought to be springs.

The multiple-degree-of-freedom-system equation of motion for free vibration without damping is

$$M\ddot{u} + Ku = 0 \tag{2-1}$$

where

M and K are the mass and stiffness matrix.

$\ddot{u}$ and u are the acceleration and displacement.

Let the solution of the Equation 2-1 be

$$u(t) = q_n(t)\phi_n \tag{2-2}$$

$q_n(t)$ is the displacement in generalized coordinates for mode n, and a harmonic function of time t and natural cyclic frequency ω_n. It is given by

$$q_n(t) = A_n \cos(\omega_n t) + B_n \sin(\omega_n t) \tag{2-3}$$

Modeshape n is given by ϕ_n. Substitute Equation 2-3 into Equation 2-2, we obtain

$$u(t) = [A_n \cos(\omega_n t) + B_n \sin(\omega_n t)]\phi_n \tag{2-4}$$

Taking time derivatives and substitute into Equation 2-1, after simplification it becomes

$$[-\omega_n^2 M\phi_n + K\phi_n]q_n(t) = 0 \tag{2-5}$$

The non-trivial solution is given by

$$(K - \omega_n^2 M)\phi_n = 0 \tag{2-6}$$

Equation 2-6 is an eigenvalue problem. If $\lambda_n = \omega_n^2$ is the eigenvalue, ϕ_n will be the corresponding eigenvector. Nontrivial ϕ_n exists if

$$\det(K - \lambda_n M) = 0 \tag{2-7}$$

Equation 2-7, usually called the 'characteristic equation', has n real and positive roots of λ_n since M and K are positive symmetric and positive definite if the structure is properly restrained against rigid-body motion (Chopra, 2012).

2.2 Direct Stiffness Determination of a Spring-mass System from Mass and Frequency Data

2.2.1 Two-Degree-Of-Freedom System

For two-degree-of-freedom system (Figure 2-1), if the coordinates are chosen as the displacements of the two lumped masses, the mass matrix and stiffness matrices are

$$M = \begin{bmatrix} m_1 & 0 \\ 0 & m_2 \end{bmatrix} \tag{2-8}$$

$$K = \begin{bmatrix} k_1 + k_2 & -k_2 \\ -k_2 & k_2 \end{bmatrix} \tag{2-9}$$

The characteristic equation for this structure is given by

$$\det \begin{bmatrix} k_1 + k_2 - \lambda_n m_1 & -k_2 \\ -k_2 & k_2 - \lambda_n m_2 \end{bmatrix} = 0 \tag{2-10}$$

Expanding and simplifying Equation 2-10, we obtain

$$k_1 + \left(\frac{m_1 + m_2}{m_1}\right)k_2 - \frac{k_1 k_2}{\lambda_n m_1} = m_2 \lambda_n \tag{2-11}$$

For mode 1, i.e., fundamental mode,

$$k_1 + \left(\frac{m_1 + m_2}{m_1}\right)k_2 - \frac{k_1 k_2}{\lambda_1 m_1} = m_2 \lambda_1 \tag{2-12}$$

For mode 2,

$$k_1 + \left(\frac{m_1 + m_2}{m_1}\right)k_2 - \frac{k_1 k_2}{\lambda_2 m_1} = m_2 \lambda_2 \tag{2-13}$$

Taking the difference of Equation 2-13 and Equation 2-12 and solving for k_1, it gives

$$k_1 = \frac{\lambda_1 \lambda_2 m_1 m_2}{k_2} \qquad (2\text{-}14)$$

Substituting Equation 2-14 into Equation 2-12, it gives

$$(m_1 + m_2)k_2^2 - m_1 m_2(\lambda_1 + \lambda_2)k_2 + m_1 m_2^2 \lambda_1 \lambda_2 = 0 \qquad (2\text{-}15)$$

If masses (m_1 and m_2) and both natural frequencies (ω_1 and ω_2) are known, we can calculate the stiffness coefficients directly from Equations 2-14 and 2-15. Since Equation 2-15 is a quadratic equation, there will be two pairs of stiffnesses k_1 and k_2. It has two real positive roots if and only if

$$(\lambda_2 - \lambda_1)^2 > 4 \frac{m_1}{m_2} \lambda_1 \lambda_2 \qquad (2\text{-}16)$$

However, if only one of the cyclic natural frequencies is given, say ω_1, we will not be able to find the solutions as there will be three unknowns and two equations. In that case, assuming that k_2 is given, k_1 can be directly determined from Equation 2-14 and the solution will be unique. These provide means to calculate the stiffnesses directly from the given frequencies.

2.2.2 Three-Degree-of-Freedom System

As illustrated in the section above for two-degree-of-freedom system, stiffness coefficients can be calculated directly from known frequencies. Choosing a coordinate system which is based on the position of the masses, and following steps similar to those for the two-degree-of-freedom system, the mass and stiffness matrices for the three-degree-of-freedom system (Figure 2-1) are

$$\boldsymbol{M} = \begin{bmatrix} m_1 & 0 & 0 \\ 0 & m_2 & 0 \\ 0 & 0 & m_3 \end{bmatrix} \qquad (2\text{-}17)$$

$$\boldsymbol{K} = \begin{bmatrix} k_1 + k_2 & -k_2 & 0 \\ -k_2 & k_2 + k_3 & -k_3 \\ 0 & -k_3 & k_3 \end{bmatrix} \qquad (2\text{-}18)$$

The characteristic equation will be given by

$$det \begin{bmatrix} k_1 + k_2 - \lambda_n m_1 & -k_2 & 0 \\ -k_2 & k_2 + k_3 - \lambda_n m_2 & -k_3 \\ 0 & -k_3 & k_3 - \lambda_n m_1 \end{bmatrix} = 0 \qquad (2\text{-}19)$$

Expanding the expression above for different λ_n, n = 1, 2, 3

$$k_1 + \frac{m_1 + m_2}{m_2}k_2 + \frac{m_1(m_2 + m_3)}{m_2 m_3}k_3 - \frac{k_1 k_2}{\lambda_1 m_2} - \frac{(m_2 + m_3)}{\lambda_1 m_2 m_3}k_1 k_3 - \frac{m_1 + m_2 + m_3}{\lambda_1 m_2 m_3}k_2 k_3$$
$$+ \frac{k_1 k_2 k_3}{\lambda_1^2 m_2 m_3} = \lambda_1 m_1 \tag{2-20}$$

$$k_1 + \frac{m_1 + m_2}{m_2}k_2 + \frac{m_1(m_2 + m_3)}{m_2 m_3}k_3 - \frac{k_1 k_2}{\lambda_2 m_2} - \frac{(m_2 + m_3)}{\lambda_2 m_2 m_3}k_1 k_3 - \frac{m_1 + m_2 + m_3}{\lambda_2 m_2 m_3}k_2 k_3$$
$$+ \frac{k_1 k_2 k_3}{\lambda_2^2 m_2 m_3} = \lambda_2 m_1 \tag{2-21}$$

$$k_1 + \frac{m_1 + m_2}{m_2}k_2 + \frac{m_1(m_2 + m_3)}{m_2 m_3}k_3 - \frac{k_1 k_2}{\lambda_3 m_2} - \frac{(m_2 + m_3)}{\lambda_3 m_2 m_3}k_1 k_3 - \frac{m_1 + m_2 + m_3}{\lambda_3 m_2 m_3}k_2 k_3$$
$$+ \frac{k_1 k_2 k_3}{\lambda_3^2 m_2 m_3} = \lambda_3 m_1 \tag{2-22}$$

Solving Equations 2-20, 2-21 and 2-22 simultaneously with known masses and frequencies, we will find the values for the stiffness coefficients k_1, k_2 and k_3. Similarly, if the number of known frequencies is smaller than the number of the degrees of freedom, the equations cannot be solved for unique stiffness values. Nonetheless, if some of the stiffness coefficients are known along with frequencies and the total of known variables equal to or greater than the degrees of freedom, unknown stiffness coefficients can be found.

2.2.3 Linear Parameterized Inverse Eigenvalue Problem (LiPIEP) Solution by Newton Method

For systems with the degrees of freedom more than three, expanding the characteristic equation and solving the simultaneous equations can be formidable. Nevertheless, as there are mathematical algorithms to calculate the eigenvalues and eigenvectors from a matrix, there are also methods to solve for the original matrix from the known eigenvalues and eigenvectors. Those kinds of problems are called Inverse Eigenvalue Problem (IEP). Chu and Golub (2005) classified those problems into different categories mostly depending on the initial matrix properties. For a spring-mass system, if the coordinate system is based on the locations of the masses, the mass matrix $\boldsymbol{M}$ of the system will be a diagonal matrix with the masses as the diagonal entries and the stiffness matrix $\boldsymbol{K}$ is a tri-band matrix. The eigenvalues and eigenvectors of the system can be calculated from the matrix $\boldsymbol{M^{-1}K}$. The $\boldsymbol{M^{-1}K}$ can be written in a linear combination of other matrices in which the stiffness of each degree of freedom is the coefficient or parameter. Due to this characteristic property, Chu and Golub (2005) categorized the problem as 'Linear Parameterized

Inverse Eigenvalue Problem (LiPIEP)'. Beigler-Konig (1981) and Kublanovskaya (2003) proposed an algorithm that is based on the Newton's method and iteration scheme. Podlevskyi & Yaroshko (2013) suggested two algorithms that use fewer mathematical operations the first of which will be used in this study and described below.

Let $A(m, k) = M^{-1}K.$ It can be written as

$$A(m, k) = \sum_{i=1}^{n} k_i A_i(m) \qquad (2\text{-}23)$$

where

   $k = (k_1, k_2, \ldots, k_n)^T$ is the stiffness vector.

   $m = (m_1, m_2, \ldots, m_n)^T$ is the mass vector.

   n is the number of the degree of freedom.

   $A_i(m)$ are matrices that are function of the mass alone.

   $A(m, k)$ has the eigenvalues of $\lambda_1 = \omega_1^2, \lambda_2 = \omega_2^2, \ldots, \lambda_n = \omega_n^2.$

Let $F(k)$ be the characteristic equations, I is the identity matrix and masses m are given. $F(k)$ can be expressed as

$$F(k) = \begin{bmatrix} \det(A(k) - \lambda_1 I) \\ \vdots \\ \det(A(k) - \lambda_n I) \end{bmatrix} = \begin{bmatrix} F_1(k) \\ \vdots \\ F_n(k) \end{bmatrix} \qquad (2\text{-}24)$$

Solving $F(k) = 0$, stiffness coefficients $k's$ will be obtained. Nevertheless, the equations involve finding the determinant of $n \times n$ matrix and solving n nonlinear polynomial equations simultaneously. To find the roots, Newton's iterative process is used which involves finding the partial derivatives of $F(k)$ with respect to k_i. Let

$$g_{ij}(k) = \frac{\partial F_i(k)}{\partial k_j} \qquad (2\text{-}25)$$

Let $J(k)$ be the Jacobian matrix of which g_{ij}'s are the components

$$J(k) = \{g_{ij}(k)\}_{i,j=1}^{n} \qquad (2\text{-}26)$$

Podlevskyi & Yaroshko (2013) further proposed to use trace theorem (Lancaster, 1966) to calculate those derivatives.

$$g_{ij}(k) = \frac{\partial F_i(k)}{\partial k_j} = F_i(k) \cdot tr\left[(A(k) - \lambda_i I)^{-1} \cdot \frac{\partial(A(k) - \lambda_i I)}{\partial k_j}\right]$$
$$= F_i(k) \cdot tr\left[(A(k) - \lambda_i I)^{-1} \cdot A_{ij}\right] \qquad (2\text{-}27)$$

where

$$A_{ij} = \frac{\partial(A(k) - \lambda_i I)}{\partial k_j} \qquad (2\text{-}28)$$

The iteration scheme for the Newton's method will be

$$k^{(p+1)} = k^{(p)} - \left[J\left(k^{(p)}\right)\right]^{-1} F\left(k^{(p)}\right), \qquad p = 0,1,2,\dots \qquad (2\text{-}29)$$

Using the trace theorem above, $J(k)$ can be written as

$$J(k) = diag\left(F_1(k), F_2(k), \dots, F_n(k)\right) \cdot H(k) \qquad (2\text{-}30)$$

where

$$H_{ij}(k) = tr\left[(A(k) - \lambda_i I)^{-1} \cdot A_{ij}\right] \qquad (2\text{-}31)$$

Equation 2-29 can be then rewritten as

$$k^{(p+1)} = k^{(p)} - [H(k)]^{-1} e, \qquad p = 0,1,2,\dots \qquad (2\text{-}32)$$

where

$$e = (1,1,\dots,1)^T$$

Podlevskyi & Yaroshko (2013) suggested the following algorithm to solve the LiPIEP.

1. Set the initial estimate for $k^{(0)} = \left(k_1^{(0)}, k_2^{(0)}, \dots, k_n^{(0)}\right)^T$

2. Iterate $p = 0,1,2\dots$ until convergence

    a. Determine $\left(A\left(k^{(p)}\right) - \lambda_i I\right), i = 1,2,\dots,n$

    b. Determine $\left(A\left(k^{(p)}\right) - \lambda_i I\right)^{-1}, i = 1,2,\dots,n$

    c. Use Equation 2-31 to assemble the matrix $H\left(k^{(p)}\right)$

    d. Determine the next iteration $k^{(p+1)}$ by solving $H\left(k^{(p)}\right)\left(k^{(p+1)} - k^{(p)}\right) = -e$

    e. Use $k^{(p+1)}$ for the next iteration of m. Go to Step 2.a.

3. End after convergence

Chu & Golub (2005) proved that there are at most n! solutions in the complex set. Since the stiffnesses are real and positive, the number of solutions will be fewer than n!. To illustrate the algorithm, an example of a two-degree-of-freedom system will be solved in the Appendix A.

2.3   Implementation of the Method

The presented method of calculating stiffness directly from the frequencies and many methods discussed in Chapter 1 assume that the systems can be modelled as spring-mass systems behaving linearly under small amplitude excitations, and the damage causes only reductions in the stiffness. It is assumed that masses and stiffnesses of the original structures can be estimated. The reductions in the stiffnesses are determined by the difference in the stiffnesses between the initial system and the softened one.

The preceding sections only discuss how to calculate the stiffnesses from the complete set of frequencies. If the number of known frequencies is smaller than the number of the degrees of freedom and other information such as the modeshapes cannot be obtained, it is not possible to calculate the stiffnesses or the reductions in stiffness values without using some form of optimization or making some compromises such as by reserving at least one frequency to help select the most likely case.

Suppose that the number of the degrees of freedom is n and the number of known frequencies is m with $m<n$. Based on this information, the number of the characteristic equations obtained is m, while the number of stiffness coefficients is the same as the degrees of freedom, i.e., n. It is improbable to solve this since there are n unknowns and only m equations unless we assume that m-n stiffness coefficients do not change from the original structure and, therefore, are known. Even though we can solve for the stiffness coefficient with this approach, finding the correct solution is unachievable since the solution is not unique. However, if at least one frequency is reserved for independent verification, the most likely solution may be found. This approach allows up to m-1 stiffness coefficients to change, and the most likely stiffness vectors must produce the frequency that is matching the reserved ones. Accordingly, this approach limits the number of the softened elements to be smaller than the number of known frequencies, which is a compromise we need to make because of limited amount of information. The stiffness coefficient values corresponding to softened elements (or stories) must also be real, positive and less than the original stiffness values. All the cases that have the number of softened elements smaller than m-1 must also be explored, and the 'correct' solution is chosen based on the criteria explained above.

3. NUMERICAL STUDIES

3.1 Introduction

Numerical studies of a two-degree-of-freedom (2-DOF) system and a four-degree-of-freedom system (4-DOF) will be discussed to demonstrate the use of partial frequency data and LiPIEP solution algorithm to identify the reduction in the stiffness. All the masses used in the numerical models are set to unit mass, and the stiffness values are 2500 for 2-DOF system, 2000 for 4-DOF system. Additionally, a 7-DOF system (with k=1800), a 15-DOF system (with k=1700), and 30-DOF and 50-DOF systems (with k=1600) are also considered. The units of the mass and the stiffness are consistent. This choice of *m* and *k*'s is chosen to make the fundamental period of the systems to equal, approximately, to the number of the degree of freedom over ten. The stiffness k_1 is referred to as story 1 stiffness, k_2 as story 2 stiffness and so on. It is assumed that the building can be idealized as shown in Figure 2-1. The reduction in stiffness in a story is called 'softening' and the corresponding structure is called 'softened structure.' How frequencies change with variations in stiffness of a single story will be explored throught 2-DOF, 4-DOF, 7-DOF, 15-DOF, 30-DOF and 50-DOF system examples. The effects of errors in frequency estimates, also called noise, will also be explained using the same systems.

3.2 Two-Degree-Of-Freedom System

With the stiffnesses ($k_1=k_2=2000$) and masses ($m_1=m_2=1$) as stated in the previous section, the system will have a fundamental period of $T_1 = 0.203s$ and $T_2 = 0.078s$. This corresponds to $f_1 = 4.918Hz$ and $f_2 = 12.876Hz$. It should be noted that the use of high number of significant figures, even though may not be realistic in an actual measurement, is necessary to avoid numerical errors. Effect of inaccuracies in frequency "measurements" will be discussed later in this chapter.

Assume that the natural frequencies of the softened structure are $f_1^* = 4.243\ Hz$ and $f_2^* = 11.845\ Hz$. The cyclic frequencies will then be $\omega_1^* = 2\pi f_1^* = 26.660\ rad/s$ and $\omega_1^* = 2\pi f_1^* = 74.424\ rad/s$, with the eigenvalues $\lambda_1^* = \omega_1^{*2} = 710.732\ rad^2/s^2$ and $\lambda_2^* = \omega_2^{*2} = 5538.981\ rad^2/s^2$. Substitute these values into Equation 2-15, we obtain

$$2k_2^{*2} - 6249.712k_2^* + 3.936 = 0$$

Solving the equation above:

$$k_2^* = \begin{bmatrix} 874.8 \\ 2250 \end{bmatrix}$$

Substituting k_2^* into Equation 2-14

$$k_1^* = \begin{bmatrix} 4500 \\ 1749.6 \end{bmatrix}$$

Hence, there are two pairs of solutions: $(k_1^*, k_2^*) = (4500, 874.8)$ and $(1749.6, 2250)$. The first pair can be easily eliminated since the reduced stiffness in the softened structure $k_1^* = 4500$ cannot be higher than the original stiffness $k_1 = 2500$. Therefore, the reduced stiffnesses are $k_1^* = 1749.6$ and $k_2^* = 2250$, which are approximately 70% of k_1 and 90% of k_2, respectively. In other words, there is 30% reduction in stiffness for k_1 and 10% reduction in k_2.

Nevertheless, if only one natural frequency of the softened structure (f_1^* or f_2^*) is known, to find a unique answer, we need additional information, for example either the stiffness for story 1 or the stiffness for story 2 remains the same before and after the event; that is $k_1^* = k_1$ or $k_2^* = k_2$. With these, the stiffness can be calculated from the known frequency and stiffness by using either Equation 2-12 or Equation 2-13.

3.3   Four-Degrees-Of-Freedom System

3.3.1   The Original System

The system will have the fundamental period of 0.4 second with unit masses and uniform stiffnesses of 2000. The four natural frequencies are:

- $f_1 = 2.472\ Hz$
- $f_2 = 7.118\ Hz$
- $f_3 = 10.905\ Hz$
- $f_4 = 13.377\ Hz$

The Mathcad routines used in this section are given in Appendix B.

3.3.2   Case of Two Known Frequencies

Assume that the two given frequencies are $f_1^* = 2.267\ Hz$ and $f_2^* = 6.715\ Hz$. We are to determine which story may have reduced stiffness and by how much. In a "damage detection"

setting, this could be considered as finding the softened story and the amount of the softening, i.e., reduction in stiffness. Since only two frequencies are known, one frequency (f_1^*) will be used to determine the amount of the reduction in the stiffness and another frequency (f_2^*) will be used select the most likely case. All possible softening scenarios, listed in Table 3-1, are explored where the relative stiffness is defined as $kr = \dfrac{k^*}{k}$. The stiffness estimates obtained are then used to determine the corresponding frequencies. These frequencies (f^c), listed in Table 3-2, are compared with the measured (known) frequencies (f_1^* and f_2^*) and the case where the frequencies match correspond to the softened structure. Table 3-3 shows the relative difference between f^c and f^*, where $\Delta fr^* = \dfrac{f^c - f^*}{f^*}$. From Table 3-3, case 1 fits the measured frequencies exactly, which translates to 30% reduction in the first story stiffness. Again, because only two frequencies are known in a 4-DOF system, estimate is limited to a single story.

3.3.3   Case of Three Known Frequencies

If three frequencies are provided, the method can be used to determine the cases where the softening may be presented in one or, at most, two stories. Let $f_1^* = 2.192\ Hz$, $f_2^* = 6.835\ Hz$ and $f_3^* = 9.838\ Hz$. All softening cases are explored including the cases where the softening happens only at one story. These are shown in Table 3-4 and Table 3-5. The frequencies resulting from the calculated stiffnesses for all the considered cases are presented in Table 3-6 and Table 3-7, and the relative frequency changes are given in Table 3-8 and Table 3-9. One frequency (f_1^*) will be used determine the reduced story stiffness for cases where softening occurs in only one story. This leaves two frequencies (f_2^*, f_3^*) which can be used to select the softened story through comparison with the calculated frequencies from the stiffnesses. For cases where softening happens in two stories, on the other hand, two frequencies (f_1^*, f_2^*) will be used to quantify the softening and one frequency (f_3^*) for selecting the most likely case. Other combinations of frequencies such as (f_2^*, f_3^*) and (f_1^*, f_3^*) can also be used to quantify the softening , and f_1^* and f_2^* to select the correct case. Nevertheless, (f_1^*, f_2^*) combination and (f_3^*) were used on the rationale that the system should satisfy the fundamental frequency and lower modes first. The fundamental frequency and lower modes can also be determined more accurately than higher modes.

From the tables, Case 6 is the most likely softening scenario; that is $kr_2 = 60\%$ and $kr_3 = 80\%$, or 40% stiffness reduction in story 2 and 20% in story 3. Also, for Cases 8 and 9 to be possible, the resulting stiffness estimates are required to be larger than the original stiffnesses to suit the measured frequencies. This is physically unlikely, and it is one of the criteria for case elimination. For Case 7, there are no real and positive stiffness k_3^* and k_4^* to fit the given frequencies. Case 5 also seems to be a good candidate since the relative change in story 3 frequency $\Delta fr_3^* = -0.1\%$. This may be because the mass and stiffness of the system are uniform. If mode 4 frequency is known, the solution will converge to the Case 6 as shown in Table 3-10.

3.3.4   Case of Four Known-Frequencies

If all four softened structure natural frequencies are known, all cases can be considered. The given frequencies are

- $f_1^* = 2.233\ Hz$
- $f_2^* = 6.634\ Hz$
- $f_3^* = 10.256\ Hz$
- $f_4^* = 12.666\ Hz$

All possible scenarios are shown in Table 3-11 through Table 3-14, and the frequencies calculated from the stiffnesses in Table 3-15 through

18. Those frequencies were compared with the given frequencies above and are presented in Table 3-19 through Table 3-22. From the tables, Case 15 fits the measured frequencies exactly. The result indicates that there is 25% reduction in stiffness for story 1 ($kr_1 = 75\%$), 15% reduction in stiffness for story 2 ($kr_2 = 85\%$), 10% reduction in stiffness for story 3 ($kr_3 = 10\%$) and 2% reduction in stiffness for story 4 ($kr_4 = 2\%$).

3.4   Sensitivity of Frequency Changes to Stiffness Changes

For 2-DOF system, if the stiffness for story 2 before and after a damaging event remain the same, that is $k_2 = k_2^*$, we can study how frequencies change if k_1^* varies. Let the relative change in frequencies be defined as $\Delta fr = \frac{f - f^*}{f}$. Figure 3-1 shows the relative change in frequencies (Δfr) for both mode 1 and mode 2 versus the relative stiffness kr_1. It indicates that variations in k_1 produce larger, quadratic changes in mode 1 frequency compared to linear changes in mode 2

frequency. Figure 3-2 illustrates the case where k_2 changes ($k_1^* = k_1$) result in bigger shifts in mode 2 frequencies compared to in mode 1 frequency. In both cases, nevertheless, it takes over 20% reduction in stiffness to generate over 10% change in frequencies.

Similarly, Figure 3-3 through Figure 3-6 shows how the frequencies change for a 4-DOF system when each story stiffness is allowed to vary in turn. For the case where k_2^* changes (Figure 3-4), it is interesting to note that mode 2 frequency remains constant. This means that if mode 2 frequency is used to determine the stiffness variations, there will be infinitely many answers. This happens because all four stiffnesses are the same. Other cases with uniform mass and stiffness up to 20-DOF system in which stiffness change in a particular story does not lead to changes in some of the natural frequencies are shown in Table 3-22. Also, Mode 1 frequency becomes less sensitive to changes in stiffness as the reduction in stiffness appears in higher story.

Figure 3-7 to Figure 3-13 presents the cases for 7-DOF system. We can see similar trends as observed in the 2-DOF and 4-DOF system. When kr_1 varies, mode 1 frequency is more sensitive compared to that of mode 2, mode 2 frequencies are more sensitive than mode 3 frequency and so on. Besides, as all the stories are made to have similar stiffnesses, some modal frequencies are insensitive to kr changes as can be seen in Figure 3-8, Figure 3-9 and Figure 3-11. Figure 3-14 to Figure 3-17 illustrate the case for 15-DOF system, Figure 3-18 to Figure 3-21 for 30-DOF system and Figure 3-22 to Figure 3-27 for 50-DOF system. Only the first ten modes and selected cases are shown. From these figures, as the number of degrees of freedom increases, each mode becomes less and less sensitive to a single-story stiffness change. A 50% reduction in the first story stiffness for a 50-DOF only lead to less than 2% decrease in mode 1 frequency while for a 4-DOF system the drop in the first mode frequency is up to approximately 18%.

3.5 Effect of Errors in Frequency Estimates to the Calculated Stiffnesses

For 2-DOF system, let the reduction in stiffness for story 1 be 80% ($kr_1 = 20\%$) and k_2 remains the same. If f_1^* is used to determine k_1^* and there is no noise (i.e. no error), the resulting kr_1 estimate will be exactly 20%. Nonetheless, f_1^* obtained from measurements is always not accurate and it will affect the calculated k_1^* depending on the amount of error. Figure 3-28 shows the calculated kr_1 in relation to the error level introduced to f_1^*, and Figure 3-29 the percent difference

from 20%. From the figures, +/-5% error to f_1^* will result in approximately 18% and 22% of k_1, or roughly 2% deviation from $kr_1 = 20\%$. Nevertheless, if $kr_1 = 90\%$ to begin with, 5% error will lead up to 10% deviations (Figure 3-30 and Figure 3-31). Figure 3-32 illustrates the effect of error in frequency estimate for different cases of kr_1. It appears that the smaller reductions in stiffness are more sensitive to error. Figure 3-33 shows the case where f_1^* is used to determine kr_2 assuming $k_1^* = k_1$. From the graph, kr_2 is much more sensitive to error especially when it is on the positive side. If f_2^* is used to determine kr_1 and kr_2 assuming k_2 and k_1 remain the same respectively, the results are the reverse which can be seen in Figure 3-34 and Figure 3-35.

Figure 3-36 to Figure 3-39 shows the same plots for a 4-DOF system. They also follow the same trends as the 2-DOF system. The more initial reduction in stiffness the less sensitive it is to the error in frequency estimate. The graphs are not symmetric around the zero point and the negative parts are less sensitive. The effect of error also increases dramatically as the erroneous f_1^* is used to determine higher story stiffness especially for the positive error (estimate higher than actual frequency). For example, for the case where $kr = 50\%$, 2% error to f_1^* produces around 4% difference from $kr_1 = 50\%$ whereas around 30% difference from $kr_4 = 50\%$. Figure 3-40 to Figure 3-43 illustrates the similar graphs for 7-DOF, 15-DOF, 30-DOF and 50-DOF system for kr_1 and error in f_1^* cases. As previously noted, as the number of the degree of freedom increases, the error becomes more influential.

3.6   Considerations in the Application of the Method

The presented sensitivity and insensitivity of the stiffness change to frequency change and vice versa are inherent to all damage detection methods that use frequency data to determine the stiffness reductions. Errors in the frequency estimates are always present and therefore errors in the stiffness calculations are expected. The proposed method calculates the stiffness directly from the given partial list of natural frequencies without using optimization techniques which often introduce additional errors to the stiffness estimates. This method presents the use of given limited frequency data to assess the reductions in the stiffness in the structures.

Table 3-23 and Table 3-24 show the percentage of noise introduced to f_1 to produce less than 10% errors in the estimate of kr_1 for different structures with uniform mass and stiffness. As can be

seen, structures with fewer degrees of freedom and with higher reduction in the stiffness can tolerate more error in the estimated frequencies. In this research, because the fundamental and lower mode frequencies can be determined from the response data with greater confidence compared with higher modes, fundamental and, where possible and necessary, lower mode frequencies are used to determine the stiffness reductions, while the higher mode frequencies are used to choose the most likely case.

Since all possible cases are to be explored, the amount of computational operations can rise dramatically as the number of the degrees of freedom increases. For instance, for a 4-DOF system, if all modal frequencies are known, there will be 4 possible cases of softening at one story, 6 cases of softening at two stories, 4 cases of softening at three stories and one case of softening at all (four) stories. The total cases for the 4-DOF will be 15. For 10-DOF, following the same logic, there will be up to 1013 cases. Nonetheless, since not all modal frequencies are known, the maximum number of stories with reduced stiffness that can be considered is limited and, as such, total number of possible cases investigated is usually smaller than the maximum total if all modal frequencies are known.

4. EXPERIMENTAL STUDIES

4.1 Introduction

An experiment was proposed to determine whether partial set of frequency data could be used to determine the reduction in the stiffness in a physical laboratory model using the method described in Chapter 2 and illustrated using numerical simulations. A small scale five-story shear building model was built out of aluminum. The structure is idealized as a five-DOF spring-mass system. The floors of the model is stiff to achieve the shear building assumptions. The damping is also small so the undamped natural frequencies are almost the same as the damped ones. Ten columns were used to support each floor. To simulate various levels of reduction in stiffness, different numbers of columns were removed. A unidirectional earthquake simulator, also known as a shake table, was used to feed harmonic signals to the base of the model. The frequencies of the models before and after the softening can then be obtained by studying response data. The frequencies are then used to determine where and how much reductions in the story stiffnesses occur.

4.2 Experimental Programs

4.2.1 Modal Description

The aluminum model was constructed as shown in Figure 4-1. The floors are made of 0.375 in. thick 6 in. x 6 in. plates. They are supported by 7-in. tall columns on two sides of the plates (5 columns on each side). The columns were clamped and bolted through angles and plates (Figure 4-2), creating ideally fixed-fixed boundary conditions for the columns. The specified dimensions of the aluminum elements and bolts for the models are shown in Table C-1 in Appendix C. Thicker plates (0.04 in.) are used for the four corner columns while thinner plates (0.032 in.) for the inner columns. Two plates of the same type are bundled together to create the columns for the lower three stories; hence, the stiffness for story 1 through story 3 are about twice the stiffness for story 4 and story 5.

4.2.2 Test Setup

The test set up is shown in Figure 4-3 and Figure 4-4. To measure the displacements, two OptiTrack cameras were placed perpendicular to the plane of motion of the model. The specimen

was attached to the shake table which provided uniaxial motion in the flexible directions of the supporting columns. The cameras were able to sample at 250 points per second. Reflective tapes were cut into circular shapes and fixed on various locations on the floor plates to track the movement as shown in Figure 4-4. To determine the individual story stiffness, the specimen was dissembled into its single stories and set up as shown in Figure 4-4 and Figure 4-6. The equipment specifications and calibration, and data acquisition system are described in the Appendix C.

4.2.3   Test Procedures

The properties of the original system such as mass and stiffness are determined first. The mass can be measured directly from components of the model while the stiffness can be calculated from the applied force and observed displacement. The frequencies of the original system can also be obtained from the displacement signals. The shake table is used to provide harmonic motions at the base of the specimen and at excitation frequencies near all five natural frequencies of the structure. The model is then let freely vibrate and the natural frequencies are extracted from the displacement signals at similar amplitudes by using Fourier Spectra of the displacement signal (using Fast Fourier Transform). The frequencies obtained are used to determine the stiffness which will be compared with the stiffness obtained from other tests.

To simulate the damage and reduce the stiffness of the system, columns are removed from the structure. The change in the mass is assumed to be negligible and ignored. The softened model is then shaken to determine the softened structure natural frequencies which will be used to determine the amount of reduction in stiffness by comparing the reduced stiffness with the original one. Different softening scenarios are explored. As discussed before, the number of frequencies obtained should be larger than the number of the softened stories so that the softened case can be identified. The columns and floor plates were also labeled so that the removed columns and the plates can be placed back at the same locations and orientation as the original system to minimize errors. The columns were removed in pairs and in such a way that no torsion is introduced to the structure.

4.2.3.1   Measuring Displacements

Two OptiTrack cameras were used to track the motion of the specimen. They were placed at different heights and angles facing the model. Reflective tape was cut into circular polygons and taped on the following locations on the aluminum tower:

- Three evenly spaced on every floor plate
- Two on the shake table

These are the tracking points for the cameras and shown in Figure 4-4. The sampling frequencies of the system was 250 Hz whereas the highest expected frequency measured is around 14 Hz. Therefore, aliasing is not be an issue.

4.2.3.2   Measuring Mass

The mass of one story was defined with the following parts:

- Floor plate (1)
- Angle sections (4)
- Bar sections (4)
- Column Plates (10/20)
- ¼" ⌀ 1" LG bolt and nut (4)
- ⅛" ⌀ ½" LG bolt, nut, and washer (10)

Mass of the columns in a given story is assumed to be distributed equally between the floor below and the floor above. The top floor mass is lighter than other floors since the two bar sections, bolts, nuts and washers are not present. The combined mass of each story is measured by the Ohaus SP6000 scale and shown in Table 4-1.

4.2.3.3   Determining Stiffness from Force and Displacement

Two types of test were made to determine the story stiffnesses. In the first type, the model was disassembled, and each story was tested individually. Lateral load was applied incrementally and resulting lateral displacement was recorded. The slope of the force-displacement curve gave the stiffness of the story. The second test, on the other hand, was carried out on the full model. The load was applied slowly ("quasi-statically") to avoid generating dynamic forces. The load was applied at one floor at a time and the displacements were recorded for every floor. The resulting

displacements were used to assemble the flexibility matrix for the whole structure. The stiffness can be calculated from the inverse of the flexibility matrix.

For the first test, a crude, but effective, method was devised using a dial gage, load cell, and two steel beams. The Federal dial gage was used to measure the displacements while the CALT load cell was used to measure the load. The butterfly screw can be turned to push or release the load cell, locking the screw in place. The story stiffnesses obtained are summarized in Table 4-2. The story stiffnesses were measured again for various column configurations. Two columns were removed successively in each case and the story stiffness relative to the original stiffness for the lower three stories are listed in Table 4-3 and for the upper two stories in Table 4-4. From the tables, removing a pair of columns results in approximately 17% reduction in the story stiffness. This number would have been 20% if identical strips were used as column plates. However, as mentioned above, thicker strips were used at the four corners of the model.

Using quasi-static loading, five tests were conducted. In each test, the model was loaded three times. Since the force and displacements were known, the stiffness can be calculated and averaged for all the trials. The results are shown in the Table 4-5. These values differ from those obtained from the first test in which individual stories were loaded. This may be because the two models, full model and individual stories as single-story specimens do not have the same boundary conditions. The variations in stiffness values are less than 15% as shown in Table 4-6.

4.2.3.4 Determining Frequencies from Displacement Signals

The model was shaken at near resonance frequency one mode at a time and then let vibrate freely. The displacement signals with similar amplitudes were used in all tests. They were decomposed to determine what the frequency contents are using the Fast Fourier Transform function in Matlab. Several tests were conducted for different softening scenarios. Even though the frequencies obtained from each scenario were similar, they were averaged before being used to determine the stiffness values.

4.3 Results and Discussions

4.3.1 System Identification of the Original Model

A total number of 44 tests were made on the original model to identify all natural frequencies. The full results were shown in Table 4-7, and the summary is given below.

- Mode 1: 2.07 Hz, 0.41% damping ratio
- Mode 2: 5.23 Hz, 0.28% damping ratio
- Mode 3: 8.73 Hz, 0.26% damping ratio
- Mode 4: 10.61 Hz, 0.41% damping ratio
- Mode 5: 13.98 Hz, 0.82% damping ratio

The damping ratios for the modes are small and therefore the damped natural frequencies determined will be very close the undamped natural frequencies. The free vibration signals to determine the damping ratios are shown in Figure 4-7 to Figure 4-11

Using the stiffness determined by the "quasi-static" test and mass obtained earlier, the frequencies do not match with frequencies determined by the dynamic test exactly. Using the LiPIEP algorithm with the measured frequencies as the input, the stiffness of each story is estimated and shown in Table 4-9. The input frequencies also needed to be adjusted so that they are close to the measured frequencies and the differences in the stiffness are minimal. Differences are occurring naturally because of the discrete model representation of an actual structure. It shows that the difference between the stiffness are within 3% while the differences in frequencies are below 0.7%. The stiffness estimates based on dynamic tests, given in Table 4-9, will therefore be used for the following tests.

4.3.2 Experiment 1: Two Columns Removed from the First Story and Two Modes Known

Two columns were removed from the first story (Figure 4-12). This will result in approximately 17% reduction in the stiffness. Since two modes are known and the softening is only in one story, one frequency (the first mode) can be used to determine the severity of the softening and the other modal frequency (mode 2) to locate which story is the most likely story with the softening. 12 tests were conducted to determine the softened frequencies. From those, the two softened frequencies are

- Mode 1: 2.01 Hz

- Mode 2: 5.07 Hz

Results are shown in Table 4-10. Different cases in which the softening can happen in a single story are shown in Table 4-11, along with Table 4-12 which shows the frequencies corresponding to the softening cases. The relative frequency differences are listed in Table 4-13. From the table, it is likely that the softening happened at the first story with 19% reduction in stiffness, compared with the supposed reduction of approximately 17%.

4.3.3 Experiment 2: Four Columns Removed from the Third Story and Two Modes Known

Similar to the Experiment 1, with two modes known, the location and the amount of the softening can be determined. Nine tests were conducted after four columns were removed from the story 3 and the results are shown in Table 4-14. The first two modal frequencies are

- Mode 1: 1.93 Hz
- Mode 2: 5.14 Hz

There will be a total of five scenarios which are shown in Table 4-15, with the corresponding frequencies shown in Table 4-16. The differences between the frequencies are given in Table 4-17. From the table, the most likely case is Case 3 where the reduction in the stiffness happens at story 3 with a relative stiffness of 52.3%. With four columns removed from story 3, the relative stiffness should be 49.5%. This represents approximately 3% error.

4.3.4 Experiment 3: Two Columns Removed from the Third Story and Two Modes Known

A total of 9 tests were conducted and the measured frequencies are

- Mode 1: 2.03 Hz
- Mode 2: 5.12 Hz

The full test results are shown in Table 4-18. A process similar to Experiment 1 and Experiment 2 is followed, and all cases are shown in Table 4-19. Table 4-20 and Table 4-21 show the frequencies and relative changes, respectively. From the results, it appears that Case 2 (i.e., softening in second story) is the softening scenario. However, this was not the case, which may be due to noise in measurements. If mode 3 is also known, the frequencies and relative differences are presented in Table 4-22 and Table 4-23. From that Case 3 seems more likely with the relative stiffness of

approximately 77%, or 23% reduction in stiffness. The supposed reduction should be around 17%, nonetheless.

4.3.5 Experiment 4: Two Columns Removed from the First Story and the Second Story and Three Modes Known

For the Experiment 4, two softened stories were simulated by removing two columns from the first story and two from the second story. Since now three frequencies are known, it is assumed that the softening can happen in two stories or in a single story. The number of possible cases is 15. Twelve tests were conducted and shown in Table 4-24. The results are

- Mode 1: 1.95 Hz
- Mode 2: 5.06 Hz
- Mode 3: 8.59 Hz

All of the softening scenarios are shown in Table 4-25 to Table 4-27 with the corresponding frequencies given in Table 4-28 to Table 4-30. There are cases that are blank, which means there was no solution that meets the criteria or that at least one of the stiffness coefficients increases compared to the corresponding original stiffness value. These cases can be eliminated. The comparisons with the measured frequencies are shown in Table 4-31 to Table 4-33. From the tables, the most likely case was scenario 6 with the relative stiffness of 90.2% and 70.2% for the story 1 and story 2 respectively. The value, nonetheless, should be 82.6% for both stories.

4.3.6 Experiment 5: Six Columns Removed from the First Story, Four Columns Removed from the Second Stories and Three Modes Known

For Experiment 5, six columns were removed from the first story and four columns were removed from the second story. A total of 11 tests were conducted and the measured frequencies are

- Mode 1: 1.69 Hz
- Mode 2: 4.62 Hz
- Mode 3: 8.06 Hz

The full test results are shown in Table 4-34. All possible scenarios are shown in Table 4-34, Table 4-36 and Table 4-37. The corresponding natural frequencies and relative differences are listed in Table 4-38 to Table 4-43. From these results, the most likely scenario is Case 6 which is true in this experiment. The stiffnesses are 44.7% of original k_1 and 70.2% of original k_2, compared to 51.7% and 67.8%.

4.3.7   Experiment 6: Two Columns Removed from the Third Story, Four Columns from the Fourth Story, and Three Modes Known

This experiment simulated two-story softening in upper stories, story 3 and story 4. 12 tests were conducted to determine the softened structure natural frequencies. From those, the first two natural frequencies are

- Mode 1: 1.95 Hz
- Mode 2: 4.79 Hz
- Mode 3: 8.45 Hz

The full test results are shown in Table 4-44. Table 4-45 to Table 4-47 shows all softening cases with the corresponding frequencies given in Table 4-48 to Table 4-50. The relative frequency differences ae shown in Table 4-51 to Table 4-53. The most likely scenario is Case 8, which is the actual setting. The stiffnesses are 82.1% of original k_1 and 67% of original k_2, compared to 83.2.7% and 67.7%.

4.3.8   Experiment 7: Two Columns Removed from the First Story, Two Columns Removed from the Second Story, Two Columns from the Third Story and Four Modes Known

Three softened stories case was simulated in this experiment and therefore at least four known measured frequencies are necessary. 23 tests were conducted and shown in Table 4-54. The measured frequencies are

- Mode 1: 1.91 Hz
- Mode 2: 5.05 Hz
- Mode 3: 8.29 Hz
- Mode 4: 10.1 Hz

Since four modes are known, the cases where softening happened in at most three stories can be explored and the fourth mode can be used to locate the softening. The total number of cases is 25. All the considered cases were shown in Table 4-55 to Table 4-59 with the corresponding frequencies in Table 4-60 to Table 4-64. Those frequencies were compared with the measured frequencies and shown in Table 4-65 to Table 4-69. From that, the mostly likely case is Case 16 which indicates that the lower three stories have reductions in stiffness, which is indeed the actual setting. The relative stiffnesses are estimated to be 90.5%, 72.9% and 73.9% for story 1, story 2 and story 3, respectively. The value should be 82.6% for all those three stories.

4.3.9 Experiment 8: Two Columns Removed from the First Story, Four Columns Removed from the Second Story, Two Columns from the Third Story and Four Modes Known

This experiment is similar to the Experiment 7. Two additional columns were removed from the second story. A total of 14 tests were conducted and the measured frequencies are:

- Mode 1: 1.88 Hz

- Mode 2: 5.01 Hz

- Mode 3: 8.34 Hz

- Mode 4: 10.19 Hz

The full test results are shown in Table 4-70. All cases were shown in Table 4-71 to Table 4-75 with the accompanying frequencies in Table 4-76 to Table 4-80. The comparisons of the frequencies are presented in Table 4-81 to Table 4-85. From the tables, the most likely scenario is Case 16, which is true. The stiffnesses are 87.2% of original k_1 and 64.6% of original k_2 and 80.7% of original k_3, compared to 83.2.7%, 67.7% and 83.2.7% respectively.

5. APPLICATION TO A BUILDING

5.1 Introduction

Suita et al. (2015) tested a 1/3-scale 18-story steel moment frame building on E-Defense earthquake simulator. The building was subjected to several ground motions, with increasing intensity, along one of its principal axes. The scaled motion intensity was represented by the value of the nearly constant pseudo response velocity obtained for 5% viscous damping ratio. The excitations increased from small amplitude to the design level and then further to cause collapse of the building. The damage to the building starts with cracks at welded connections of the beam ends and fracturing at their flanges at lower stories. The data given by Suita et al. (2015) are used to determine the reductions in the stiffness using the natural frequency data before and after the first observable damage occurred. The building is modeled as a planar, multiple-degree-of-freedom spring-mass system.

5.2 Building Description and Damage Progression

The plan and elevation views of the building, along with information about its structural elements, are shown in Figure 5-1. The typical floor is 5m by 6m with 5cm-thick concrete slab supported by four steel beams. Along the Y-axis, there are two 3-bay steel frames each of which consists of four 200mm x 200mm square-hollow-section columns. The base input motion was only in the Y-direction. Table 5-1 lists the input motion level as well the progression of damage in the structure. As can be seen, cracks to the welded connections started to appear at the beam ends at 2nd to 5^{ft} floors when the pseudo response velocity was increased to 180 cm/s. The first observed fractures at the beam flanges occurred at the 2nd floor with the pseudo response velocity of 220 cm/s. The collapse of the building happened when the pseudo velocity response reached 420cm/s. The natural frequencies before and after the first fractures (at 220cm/s) were determined to identify the reduction in the stiffness that happened during the event.

5.3   Analysis Procedures

5.3.1   Estimating the Building Frequencies

The natural frequencies before the fractures occurred were determined by producing the transfer function of the response of the roof to ground input motion along the Y-direction at pseudo velocity response of 17cm/s. At this velocity, the building was undamaged and expected to remain linear. The frequencies obtained are taken to represent the natural frequencies of the original system. There were two accelerometers placed at the opposite corners of the building (Suita et al., 2015). The average acceleration recorded by these two accelerometers is used as the input. The resulting transfer function for translational motion are given in Figure 5-2 with 0.88Hz, 2.69Hz, 4.88Hz, and 7.03Hz identified as the natural frequencies for mode 1, mode 2, mode 3 and mode 4. Additionally, half of the difference of the accelerations recorded at the two opposite corners of the building are used to produce the transfer function associated with torsional motion (Figure 5-3). There torsional mode frequencies are found to be at 3.96Hz and 6.79Hz. A planar SAP2000 (CSI, 2019) computer model (Figure 5-4) was also built to compare the translational frequencies. Both sets of frequencies appear to agree well (Table 5-2). Similar procedures were followed for the response observed during the shaking at 220cm/s pseudo-velocity intensity. However, to limit nonlinearities in the transfer function estimate, only the last 80 seconds of the motion observed during the 220cm/s pseudo-velocity intensity input motion were considered. From Figure 5-5 and Figure 5-6, the first four translational frequencies are identified at 0.83Hz, 2.54Hz, 4.59Hz and 6.69Hz.

5.3.2   Estimating Building Mass and Story Stiffnesses

A spring-mass model, representing the behavior of the frames in the direction of the base excitation, is constructed. The building lumped mass can be estimated from the structural elements and is given in Table 5-3. The story stiffnesses can be calculated by combining the lateral stiffness of the individual columns or from the SAP2000 (CSI, 2019) computer model by finding the ratios of the story shears and story drifts. Using these stiffness values in the spring-mass model, however, do not produce natural frequencies matching all of the measured frequencies for the translational modes in the direction of the base excitation. This is because the building is three dimensional and has torsional response besides its translational response. If the stiffness values of the spring-mass

system representing the planar frame and translational response only are adjusted to produce the exact measured translational mode frequencies, they will lead to unreasonable stiffness distribution in the model. For this study, only the first two translational mode frequencies, along the same direction of the base excitation, were matched since the third mode of the building is a torsional one. The resulting stiffness distributions are shown in Table 5-3. To determine the reductions in stiffness in the building, only the first two translational frequencies are used.

5.3.3   Estimating the Reduction in the Stiffnesses

Since only two frequencies are used to determine reductions in the stiffness, there are only 16 possible cases of story softening. As fractures at the beam flanges were observed at 2nd floor, it is expected that the reductions in the stiffness should happen at the first and second stories. If the flange fractures changed all column boundary conditions from fixed-fixed to fixed-pinned in a story, the reduction in the lateral stiffness of columns in that story should be 50%, i.e. from $12IE/L^3$ to $6EI/L^3$ for each column.

5.4   Analysis Results and Discussion

Table 5-4 and Table 5-5 show the relative stiffness when the softening is assumed to happen at a single story. Table 5-6 and Table 5-7 show the relative natural frequency differences. From the overall trend, it appears that the softening is more likely to occur at lower stories than in the upper ones. If cases with no more than 2% difference between the observed and estimated natural frequencies are considered, the likely cases are Case 1, Case 2, Case 3 and Case 10 where the softening happens at story 1, story 2, story 3 and story 10, respectively. The reductions in the stiffnesses are 60% for story 1, 62% for story 2, 72% for story 3 and 65% for story 10 for those four likely cases. The cases that are closest to the measured frequencies are Case 2 (softening at story 2) and Case 10 (softening at story 10). If there was no other information, it would not be possible to pinpoint a unique case. However, this information may be useful as it also indicates a few likely locations to focus on during possible inspection. The challenge of applying the method to this building includes the fact that 1) the stiffness distribution of the building cannot represent all the measured translational modes as the building is three dimensional and has torsional modes, and 2) in a system with large number of degrees of freedom like this structure, small variations in

natural frequencies can lead to large changes in stiffness (Table 3-24 and 3-25). The application of the method to a 7-story RC building is shown in Appendix D.

6. SUMMARY AND CONCLUSION

6.1 Summary

Vibration-based structural monitoring methods use changes in dynamic properties of the system, such as changes in its natural frequencies and modeshapes, to detect the presence, location, and extent of damage in the structure. Because of limited instrumentation, not all natural frequencies and modeshapes can be obtained from dynamic response data. Modeshapes are harder to obtain when the instrument locations are spread sparsely over the building. Often, only a partial list of natural frequencies can be observed. Cheng (2017) developed a response-phase-difference-based technique to identify multiple natural frequencies of a building even if limited response data are available. If a partial list of natural frequencies is used to monitor changes in the structural system of a building, compromise needs to be made to discover and measure the locations and extent of softening in structural elements. Hassiotis and Jeong (1995) proposed a method to use an incomplete list of natural frequencies to determine the reduction in stiffness by using optimization method. In this research, the algorithm to solve Linear Parameterized Inverse Eigenvalue Problem provided by Podlevskyi & Yaroshko (2013) was adopted to determine the stiffness configuration of a structure directly, i.e., without optimization, where discrete spring-mass dynamic models may be used to represent the building.

The method was applied to 2-DOF and 4-DOF numerical models with various softened spring cases. The computed reduced stiffnesses were used to determine the corresponding natural frequencies. The case which produces the closest frequencies to the given frequencies is the most likely case. In these numerical model studies, the presented method can locate and quantify the reductions in the stiffness values correctly. Sensitivity of changes in natural frequency to changes in stiffness are also studied. For the case where the softening happens only in a single story, it appears that natural frequencies become less and less sensitive to the stiffness change as the number of the degrees of freedom increases, while the noise effects become more and more prominent. This means that the measured natural frequencies need to be accurate to produce correct stiffness especially for higher degree of freedom systems. In the case where the discretized

structural model has uniform mass and uniform stiffness throughout, stiffness changes in some of the springs, representing story structural elements collectively, do not always lead to changes in the frequencies in some of the natural modes (Table 3-23).

To test the technique, eight experiments were conducted on a small scale five-story aluminum laboratory model. The model was composed of 7 in. x 7 in. x 0.375 in. plates supported by 10 columns in each story. A small-scale earthquake simulator ("shake table") was used to provide harmonic excitation at the base of the model. Displacement responses of the specimen were recorded by two OptiTrack cameras. The acquired signals were examined to determine the natural frequencies of the model using Fast Fourier Transform. To simulate reduction in stiffness, various combinations of columns were removed from the model. The natural frequencies before and after removal of columns were obtained and used to determine the reductions in the stiffness of the structure. Cases where damage was introduced in up to three stories were studied. The proposed method can locate and quantify the extent of damage in the studied cases.

The method was also applied to study a 1/3 scaled 18-story moment resisting frame to identify the reduction in the stiffness due to the fractures at the beam flanges at the 2nd floor. The building was subjected to ground motions with increased intensity until collapse. The natural frequencies before and after the fractures occurred were identified. Only the first two translational modal frequencies are used to determine the reductions in the stiffness since the third mode of the tower is torsional and no reasonable stiffness distribution can represent all of the measured translational modes. The method produces possible cases of the softening assumed to occur at a single story.

6.2   Conclusion

The proposed method can identify reductions in the stiffness of spring-mass systems using only partial natural frequency data, as illustrated with the presented numerical and experimental studies. If the number of known frequencies is larger than the number of the softened stories, the method offers a set of stiffness configurations. In some cases of structures with uniform stiffness and mass, certain modes could be insensitive to variations in stiffness at particular locations (Table 3-23). If those modes are used to determine the reductions in the stiffness at those particular locations, many possible solutions might be found. Nonetheless, this can be mitigated by using modes that are

sensitive to stiffness changes at those positions instead. The method can also be applied to buildings. Nonetheless, the challenges include 1) the presence of torsional modes which cannot be captured by a spring-mass model representing in-plane response of frame and 2) the measured frequencies might be influenced by soil-structure interaction or nonlinearities in the response of the buildings.

TABLES

Table 3-1 4-DOF (Two known frequencies): Cases of Single Softened Story

Case	1	2	3	4
kr_1	**70%**	100%	100%	100%
kr_2	100%	**64%**	100%	100%
kr_3	100%	100%	**51%**	100%
kr_4	100%	100%	100%	**25%**

Table 3-2 4-DOF (Two known frequencies): Single Softened Story Frequencies

Case	1	2	3	4
f_1^c (Hz)	2.267	2.267	2.267	2.267
f_2^c (Hz)	6.716	7.118	6.235	4.801
f_3^c (Hz)	10.614	9.985	10.651	9.196
f_4^c (Hz)	13.286	12.761	12.132	12.890

Table 3-3 4-DOF (Two known frequencies): Relative Frequency Difference

Case	1	2	3	4
Δfr_1^*	**0.0%**	0.0%	0.0%	0.0%
Δfr_2^*	**0.0%**	6.0%	-7.2%	-28.5%

Table 3-4 4-DOF (Three known frequencies): Cases of Single Softened Story

Case	1	2	3	4
kr_1	**62%**	100%	100%	100%
kr_2	100%	**56%**	100%	100%
kr_3	100%	100%	**42%**	100%
kr_4	100%	100%	100%	**20%**

Table 3-5 4-DOF (Three known frequencies): Cases of Two Softened Stories

Case	5	6	7	8	9	10
kr_1	**79%**	100%	100%	**61%**	**59%**	100%
kr_2	**68%**	**60%**	100%	100%	100%	**57%**
kr_3	100%	**80%**	-	100%	**128%**	100%
kr_4	100%	100%	-	**139%**	100%	**81%**

Table 3-6 4-DOF (Three known frequencies): Single Story Softened Frequencies

Case	1	2	3	4
f_1^c (Hz)	2.192	2.192	2.192	2.192
f_2^c Hz)	6.592	7.118	5.996	4.458
f_3^c (Hz)	10.541	9.681	10.572	9.116
f_4^c (Hz)	13.266	12.665	11.973	12.875

Table 3-7 4-DOF (Three known frequencies): Two Story Softened Frequencies

Case	5	6	7	8	9	10
f_1^c (Hz)	2.192	2.192	-	2.192	2.192	2.192
f_2^c (Hz)	6.835	6.835	-	6.835	6.834	6.835
f_3^c (Hz)	9.832	9.839	-	11.266	10.532	9.47
f_4^c (Hz)	12.789	12.062	-	14.012	14.121	12.264

Table 3-8 4-DOF (Three known frequencies): Single Story Softened Frequency Difference

Case	1	2	3	4
Δfr_1^* (%)	0.0%	0.0%	0.0%	0.0%
Δfr_2^* (%)	-3.6%	4.1%	-12.3%	-34.8%
Δfr_3^* (%)	7.1%	-1.6%	7.5%	-7.3%

Table 3-9 4-DOF (Three known frequencies): Two Stories Softened Frequency Difference

Case	5	6	7	8	9	10
Δfr_1^* (%)	0.0%	**0.0%**	-	0.0%	0.0%	0.0%
Δfr_2^* (%)	0.0%	**0.0%**	-	0.0%	0.0%	0.0%
Δfr_3^* (%)	-0.1%	**0.0%**	-	14.5%	7.1%	-3.7%

Table 3-10 4-DOF (Three known frequencies): Additional Fourth Frequency Known

Case	11
kr_1	100%
kr_2	**60%**
kr_3	**80%**
kr_4	100%

Table 3-11 4-DOF (Four known frequencies): Single Softened Story Cases

Case	1	2	3	4
kr_1	**66%**	100%	100%	100%
kr_2	100%	**60%**	100%	100%
kr_3	100%	100%	**46%**	100%
kr_4	100%	100%	100%	**23%**

Table 3-12 4-DOF (Four known frequencies): Two Softened Stories Cases

Case	5	6	7	8	9	10
kr_1	**64%**	100%	100%	**66%**	**67%**	100%
kr_2	**106%**	**71%**	100%	100%	100%	**62%**
kr_3	100%	**69%**	-	100%	**98%**	100%
kr_4	100%	100%	-	**98%**	100%	**72%**

Table 3-13 4-DOF (Four known frequencies): Three Softened Stories Cases

Case	11	12	13	14
kr_1	**78%**	**65%**	**70%**	100%
kr_2	**83%**	100%	**91%**	**71%**
kr_3	**86%**	**117%**	100%	**68%**
kr_4	100%	**86%**	**93%**	**104%**

Table 3-14 4-DOF (Four known frequencies): Four Softened Stories

Case	15
kr_1	**75%**
kr_2	**85%**
kr_3	**90%**
kr_4	**98%**

Table 3-15 4-DOF (Four known frequencies): Single Softened Story Cases

Case	1	2	3	4
f_1^c (Hz)	2.233	2.233	2.233	2.233
f_2^c (Hz)	6.658	7.118	6.121	4.628
f_3^c (Hz)	10.579	9.842	10.613	9.154
f_4^c (Hz)	13.277	12.713	12.051	12.882

Table 3-16 4-DOF (Four known frequencies): Two Softened Stories Cases

Case	5	6	7	8	9	10
f_1^c (Hz)	2.233	2.233	-	2.233	2.233	2.233
f_2^c (Hz)	6.634	6.634	-	6.634	6.634	6.634
f_3^c (Hz)	10.693	10.185	-	10.519	10.58	9.486
f_4^c (Hz)	13.402	11.850	-	13.243	13.206	12.188

Table 3-17 4-DOF (Four known frequencies): Three Softened Stories Cases

Case	11	12	13	14
f_1^c (Hz)	2.233	2.233	2.233	2.233
f_2^c (Hz)	6.634	6.634	6.634	6.634
f_3^c (Hz)	10.256	10.256	10.256	10.256
f_4^c (Hz)	12.540	13.621	13.016	11.910

Table 3-18 4-DOF (Four known frequencies): Four Softened Stories

Case	15
f_1^c (Hz)	2.233
f_2^c (Hz)	6.634
f_3^c (Hz)	10.256
f_4^c (Hz)	12.666

Table 3-19 4-DOF (Four known frequencies): Single Story % Difference

Case	1	2	3	4
Δfr_1^* (%)	0.0%	0.0%	0.0%	0.0%
Δfr_2^* (%)	0.4%	7.3%	-7.7%	-30.2%
Δfr_3^* (%)	3.1%	-4.0%	3.5%	-10.7%
Δfr_4^* (%)	4.8%	0.4%	-4.9%	1.7%

Table 3-20 4-DOF (Four known frequencies): Two Stories % Difference

Case	5	6	7	8	9	10
Δfr_1^* (%)	0.0%	0.0%	-	0.0%	0.0%	0.0%
Δfr_2^* (%)	0.0%	0.0%	-	0.0%	0.0%	0.0%
Δfr_3^* (%)	4.3%	-0.7%	-	2.6%	3.2%	-7.5%
Δfr_4^* (%)	5.8%	-6.4%	-	4.6%	4.3%	-3.8%

Table 3-21 4-DOF (Four known frequencies): Three Stories % Difference

Case	11	12	13	14
Δfr_1^* (%)	0.0%	0.0%	0.0%	0.0%
Δfr_2^* (%)	0.0%	0.0%	0.0%	0.0%
Δfr_3^* (%)	0.0%	0.0%	0.0%	0.0%
Δfr_4^* (%)	-1.0%	7.5%	2.8%	-6.0%

Table 3-22 4-DOF (Four known frequencies): Four Stories % Difference

Case	15
Δfr_1^* (%)	**0.0%**
Δfr_2^* (%)	**0.0%**
Δfr_3^* (%)	**0.0%**
Δfr_4^* (%)	**0.0%**

Table 3-23 System with Insensitive Frequencies to Stiffness Change

DOF	Story at which stiffness variation does not lead to change in natural frequency of one or more modes	Mode with frequency not changing
4	2	2
7	5	3
	3	2,5
	2	3
10	8	4
	5	4
	4	2,5,8
	2	4
12	8	3,8
	3	3,8
13	11	5
	8	5
	5	2,5,11
	2	5
16	14	6
	11	6
	8	6
	6	2,5,8,11,14
	5	6
	2	6
17	13	4,11
	11	3,8,13
	8	4,11
	4	3,8,13
	3	4,11
19	17	7
	14	7
	11	7
	8	7
	7	2,5,8,11,14,17
	5	7
	2	7

Table 3-24 Percent of Noise Introduced to f_1 to Produce less than 10% Error in kr_1 ($kr_1 = 50\%$)

% Noise Introduced to f_1					
2-DOF	**4-DOF**	**7-DOF**	**15-DOF**	**30-DOF**	**50-DOF**
-9% to 8%	-7% to 6%	-5% to 4%	-3% to 2%	-2% to 1%	-1% to 1%

Table 3-25 Percent of Noise Introduced to f_1 to Produce less than 10% Error in kr_1 ($kr_1 = 90\%$)

% Noise Introduced to f_1					
2-DOF	**4-DOF**	**7-DOF**	**15-DOF**	**30-DOF**	**50-DOF**
-5% to 4%	-3% to 2%	-2% to 1%	-1% to 1%	-0.5% to 0.3%	-0.3% to -0.1%

Table 4-1 Floor Mass

	Mass (g)				
Story	1	2	3	4	5
Floor Plate	1009.2	1006.0	1007.8	1002.6	931.3
Columns	74.9	74.8	75.0	37.5	37.4
Total	1084.1	1080.9	1064.1	1040.1	950.0

Table 4-2 Individual Story Stiffnesses from the Individual Story Tests

Story Stiffness	Stiffness N/m
k_1	2703.6
k_2	2325.4
k_3	2753.2
k_4	1347.5
k_5	1313.7

Table 4-3 Relative Stiffness from the Individual Story Tests (Story 1 to Story 3)

Number Columns	Stiffness N/m	Relative Stiffness, kr
10 Columns	1347.5	100.0%
8 Columns	1112.6	82.6%
6 Columns	911.8	67.7%
4 Columns	666.4	49.5%

Table 4-4 Relative Stiffness from the Individual Story Tests (Story 4 and Story 5)

Number Columns	Stiffness N/m	Relative Stiffness, kr
10 Columns	2703.6	100.0%
8 Columns	2249.7	83.2%
6 Columns	1832.5	67.8%
4 Columns	1398.3	51.7%

Table 4-5 Story Stiffnesses from Quasi-Static Test

Test Number	Story Stiffness				
	k_1 N/m	k_2 N/m	k_3 N/m	k_4 N/m	k_5 N/m
Test 1	2348.4				
Test 2	2362.6	2414.3			
Test 3	2398.9	2461.5	2497.9		
Test 4	2372.3	2396.5	2455.0	1205.8	
Test 5	2374.8	2444.1	2363.0	1215.8	1271.6
Average	**2371.4**	**2429.1**	**2438.6**	**1210.8**	**1271.6**

Table 4-6 Stiffness Comparison between Different Tests

Story Stiffness	Individual Story Stiffness N/m	Quasi-static Story Stiffness N/m	% Difference
k_1	2703.6	2371.4	-14.0%
k_2	2325.4	2429.1	4.3%
k_3	2753.2	2438.6	-12.9%
k_4	1347.5	1210.8	-11.3%
k_5	1313.7	1271.6	-3.3%

Table 4-7 Original System Modal Frequencies

Test Series		Mode 1 Hz	Mode 2 Hz	Mode 3 Hz	Mode 4 Hz	Mode 5 Hz
Mode 1	Test 1	2.06				
	Test 2	2.06				
	Test 3	2.06				
	Test 4	2.06				
Mode 2	Test 1	2.06	5.20			
	Test 2	2.06	5.20			
	Test 3	2.06	5.20			
	Test 4	2.06	5.20			
	Test 5	2.06	5.20			
	Test 6	2.06	5.20			
Mode 3	Test 1	2.07	5.25	8.72		
	Test 2	2.07	5.25	8.71		
	Test 3	2.07	5.23	8.72		
	Test 4	2.07	5.25	8.71		
	Test 5	2.06	5.25	8.71		
	Test 6	2.07	5.22	8.72		
	Test 7	2.06	5.23	8.72		
Mode 4	Test 1	2.07	5.21	8.72	10.57	
	Test 2	2.07	5.21	8.72	10.57	
	Test 3	2.07	5.22	8.72	10.56	
	Test 4	2.07	5.23	8.72	10.57	
	Test 5	2.07	5.23	8.73	10.56	
	Test 6	2.07	5.23	8.73	10.56	
	Test 7	2.07	5.24	8.72	10.57	
	Test 8	2.06	5.22	8.71	10.57	
	Test 9	2.07	5.24	8.72	10.55	
	Test 10	2.07	5.24	8.73	10.57	
	Test 11	2.07	5.23	8.73	10.58	

Table 4-8 Continue

	Test 1	2.14	5.26	8.74	10.64	14
	Test 2	2.12	5.27	8.74	10.64	13.97
	Test 3	2.01	5.22	8.73	10.63	13.98
	Test 4	2.07	5.27	8.75	10.65	13.99
	Test 5	2.08	5.26	8.75	10.63	13.99
	Test 6	2.10	5.26	8.74	10.64	13.97
	Test 7	2.06	5.25	8.75	10.64	13.97
Mode 5	Test 8	2.09	5.24	8.74	10.64	13.99
	Test 9	2.07	5.23	8.73	10.64	13.96
	Test 10	2.03	5.21	8.73	10.63	13.99
	Test 11	2.05	5.21	8.73	10.64	13.99
	Test 12	2.11	5.25	8.77	10.64	13.97
	Test 13	2.03	5.22	8.76	10.64	13.98
	Test 14	2.09	5.25	8.75	10.65	14
	Test 15	2.04	5.23	8.75	10.66	13.99
	Test 16	2.12	5.27	8.77	10.62	13.98
Average =		**2.07**	**5.23**	**8.73**	**10.61**	**13.98**

Table 4-9 Quasi-static and Dynamic Stiffness and Frequency Difference

Stiffness	Quasi-static		Dynamic		Measured Frequencies	Difference		
	Stiffness	*Frequency*	*Stiffness*	*Frequency*		*Stiffness*	*Frequency*	
	N/m	Hz	N/m	Hz	Hz	%	Quasi (%)	Dynamic (%)
k_1	2371.4	2.07	2377.3	2.09	2.07	0.2%	0.0%	-0.7%
k_2	2429.1	5.19	2506.9	5.20	5.23	3.2%	-0.8%	0.7%
k_3	2438.6	8.67	2506.5	8.72	8.73	2.8%	-0.7%	0.1%
k_4	1210.8	10.54	1207.0	10.60	10.61	-0.3%	-0.7%	0.1%
k_5	1271.6	13.79	1281.1	13.97	13.98	0.7%	-1.4%	0.1%

Table 4-10 Experiment 1: Vibration Test Modal Frequencies

Test Series		Mode 1 (Hz)	Mode 2 (Hz)	Mode 3 (Hz)
Mode 1	Test 1	2.00		
	Test 2	2.00		
	Test 3	2.00		
Mode 2	Test 1	2.00	5.05	
	Test 2	2.00	5.05	
	Test 3	2.00	5.05	
	Test 4	2.00	5.04	
Mode 3	Test 1	2.01	5.08	8.66
	Test 2	2.02	5.09	8.64
	Test 3	2.01	5.08	8.64
	Test 4	2.02	5.11	8.66
	Test 5	2.02	5.08	8.66
Average =		**2.01**	**5.07**	**8.65**

Table 4-11 Experiment 1: Single Story Softening Cases

Case	1	2	3	4	5
kr_1	**81.0%**	100%	100%	100%	100%
kr_2	100%	**77.0%**	100%	100%	100%
kr_3	100%	100%	**70.4%**	100%	100%
kr_4	100%	100%	100%	**73.5%**	100%
kr_5	100%	100%	100%	100%	**42.6%**

Table 4-12 Experiment 1: Single Story Softening Case Frequencies

Case	1	2	3	4	5
f_1^c (Hz)	2.01	2.01	2.01	2.01	2.01
f_2^c (Hz)	5.03	5.14	5.18	4.88	4.37

Table 4-13 Experiment 1: Single Story Softening Case Frequency Differences

Case	1	2	3	4	5
Δfr_1^*	0%	0%	0%	0%	0%
Δfr_2^*	**-0.8%**	1.4%	2.2%	-3.7%	-13.8%

Table 4-14 Experiment 2: Vibration Test Modal Frequencies

Test Series		Mode 1 (Hz)	Mode 2 (Hz)
Mode 1	Test 1	1.93	
	Test 2	1.93	
	Test 3	1.93	
	Test 4	1.92	
	Test 5	1.92	
	Test 6	1.92	
Mode 2	Test 1		5.13
	Test 2		5.14
	Test 3		5.14
Average =		**1.93**	**5.14**

Table 4-15 Experiment 2: Single Story Softening Cases

Case	1	2	3	4	5
kr_1	**66.0%**	100%	100%	100%	100%
kr_2	100%	**60.6%**	100%	100%	100%
kr_3	100%	100%	**52.3%**	100%	100%
kr_4	100%	100%	100%	**56.5%**	100%
kr_5	100%	100%	100%	100%	**27.2%**

Table 4-16 Experiment 2: Single Story Softening Case Frequencies (Mode 1, 2, 3 frequencies known)

Case	1	2	3	4	5
f_1^c(Hz)	1.93	1.93	1.93	1.93	1.93
f_2^c (Hz)	4.88	5.09	5.17	4.62	3.83
f_3^c (Hz)	8.49	8.66	7.87	8.52	6.81

Table 4-17 Experiment 2: One Story Softening Case Frequency Differences (Mode 1, 2 frequencies known)

Case	1	2	3	4	5
Δfr_1^*	0%	0%	0%	0%	0%
Δfr_2^*	-5.1%	-1.0%	**0.6%**	-10.1%	-25.5%

Table 4-18 Experiment 3: Vibration Test Modal Frequencies

Test Series		Mode 1 Hz	Mode 2 Hz	Mode 3 Hz
Mode 1	Test 1	2.02		
	Test 2	2.02		
	Test 3	2.02		
Mode 2	Test 1	2.03	5.12	
	Test 2	2.03	5.12	
	Test 3	2.04	5.13	
Mode 3	Test 1	2.03	5.13	8.42
	Test 2	2.03	5.12	8.42
	Test 3	2.03	5.12	8.42
Average =		**2.03**	**5.12**	**8.42**

Table 4-19 Experiment 3: Single Story Softening Cases

Case	1	2	3	4	5
kr_1	**85.0%**	100%	100%	100%	100%
kr_2	100%	**82.3%**	100%	100%	100%
kr_3	100%	100%	**76.7%**	100%	100%
kr_4	100%	100%	100%	**79.2%**	100%
kr_5	100%	100%	100%	100%	**42.6%**

Table 4-20 Experiment 3: Single Story Softening Case Frequencies (Mode 1, 2 frequencies known)

Case	1	2	3	4	5
f_1^c(Hz)	2.03	2.03	2.03	2.03	2.03
f_2^c (Hz)	5.08	5.16	5.19	4.96	4.56

Table 4-21 Experiment 3: Single Story Softening Case Frequency Differences (Mode 1, 2 frequencies known)

Case	1	2	3	4	5
Δfr_1*	0%	0%	0%	0%	0%
Δfr_2*	-0.8%	0.7%	**1.3%**	-3.2%	-11.0%

Table 4-22 Experiment 3: One Story Softening Case Frequencies (Mode 1, 2, 3 frequencies known)

Case	1	2	3	4	5
f_1^c(Hz)	2.03	2.03	2.03	2.03	2.03
f_2^c (Hz)	5.08	5.16	5.19	4.96	4.56
f_3^c (Hz)	8.63	8.7	8.44	8.64	7.34

Table 4-23 Experiment 3: One Story Softening Case Frequency Differences (Mode 1, 2, 3 frequencies known)

Case	1	2	3	4	5
Δfr_1*	0%	0%	0%	0%	0%
Δfr_2*	-0.8%	0.7%	**1.3%**	-3.2%	-11.0%
Δfr_3*	2.5%	3.3%	**0.2%**	2.6%	-12.8%

Table 4-24 Experiment 4: Vibration Test Modal Frequencies

Test Series		Mode 1 Hz	Mode 2 Hz	Mode 3 Hz
Mode 1	Test 1	1.95		
	Test 2	1.94		
	Test 3	1.94		
	Test 4	1.95		
Mode 2	Test 1	1.96	5.07	
	Test 2	1.95	5.05	
	Test 3	1.95	5.04	
	Test 4		5.05	
Mode 3	Test 1	1.97	5.08	8.62
	Test 2	1.95	5.06	8.58
	Test 3	1.96	5.07	8.58
	Test 4	1.95	5.06	8.58
Average =		**1.95**	**5.06**	**8.59**

Table 4-25 Experiment 4: Cases of Softening in a Single Story

Case	1	2	3	4	5
kr_1	**69.3%**	100%	100%	100%	100%
kr_2	100%	**64.2%**	100%	100%	100%
kr_3	100%	100%	**56.1%**	100%	100%
kr_4	100%	100%	100%	**60.1%**	100%
kr_5	100%	100%	100%	100%	**29.9%**

Table 4-26 Experiment 4: Cases of Softening in Two Stories (1)

Case	6	7	8	9	10
kr_1	**90.2%**	100%	100%	100%	**67.3%**
kr_2	**70.2%**	-	100%	100%	100%
kr_3	100%	-	**61.1%**	100%	100%
kr_4	100%	100%	**88.5%**	-	100%
kr_5	100%	100%	100%	-	**143.8%**

Table 4-27 Experiment 4: Cases of Softening in Two Stories (2)

Case	11	12	13	14	15
kr$_1$	**86.4%**	**65.0%**	100%	100%	100%
kr$_2$	100%	100%	**65.6%**	**68.3%**	100%
kr$_3$	**65.9%**	100%	100%	100%	**57.8%**
kr$_4$	100%	**120.5%**	**95.7%**	100%	100%
kr$_5$	100%	100%	100%	**93.6%**	**83.8%**

Table 4-28 Experiment 4: Frequencies – Cases of Softening in a Single Story

Case	1	2	3	4	5
f$_1^c$(Hz)	1.95	1.95	1.95	1.95	1.95
f$_2^c$ (Hz)	4.92	5.10	5.17	4.68	3.94
f$_3^c$ (Hz)	8.51	8.67	7.98	8.55	6.87

Table 4-29 Experiment 4: Frequencies – Cases of Softening in Two Stories (1)

Case	6	7	8	9	10
f$_1^c$(Hz)	1.95	-	1.95	-	1.95
f$_2^c$ (Hz)	5.06	-	5.06	-	5.06
f$_3^c$ (Hz)	8.60	-	8.12	-	9.21

Table 4-30 Experiment 4: Frequencies – Cases of Softening in Two Stories (2)

Case	11	12	13	14	15
f$_1^c$(Hz)	1.95	1.95	1.95	1.95	1.95
f$_2^c$ (Hz)	5.06	5.06	5.06	5.06	5.06
f$_3^c$ (Hz)	8.13	8.50	8.66	8.52	7.72

Table 4-31 Experiment 4: Difference in Estimated and Measured Frequencies – Cases of Softening in a Single Story

Case	1	2	3	4	5
Δfr$_1^*$	0%	0%	0%	0%	0%
Δfr$_2^*$	-2.8%	0.8%	2.2%	-7.5%	-22.1%
Δfr$_3^*$	-0.9%	0.9%	-7.1%	-0.5%	-20.0%

Table 4-32 Experiment 4: Difference in Estimated and Measured Frequencies – Cases of Softening in Two Stories (1)

Case	6	7	8	9	10
Δfr_1^*	0%	-	0%	-	0%
Δfr_2^*	0%	-	0%	-	0%
Δfr_3^*	**0.1%**	**-**	-5.5%	-	7.2%

Table 4-33 Experiment 4: Difference in Estimated and Measured Frequencies – Cases of Softening in Two Stories (2)

Case	11	12	13	14	15
Δfr_1^*	0%	0%	0%	0%	0%
Δfr_2^*	0%	0%	0%	0%	0%
Δfr_3^*	-5.4%	-1.0%	0.8%	-0.8%	-10.1%

Table 4-34 Experiment 5: Vibration Test Modal Frequencies

Test Series		Mode 1 Hz	Mode 2 Hz	Mode 3 Hz
Mode 1	Test 1	1.67		
	Test 2	1.69		
	Test 3	1.69		
	Test 4	1.69		
	Test 5	1.70		
Mode 2	Test 1	1.69	4.63	
	Test 2	1.68	4.60	
	Test 3	1.69	4.59	
Mode 3	Test 1	1.69	4.63	8.05
	Test 2	1.69	4.63	8.05
	Test 3	1.69	4.63	8.07
Average =		**1.69**	**4.62**	**8.06**

Table 4-35 Experiment 5: Cases of Softening in a Single Story

Case	1	2	3	4	5
kr_1	**39.0%**	100%	100%	100%	100%
kr_2	100%	**33.6%**	100%	100%	100%
kr_3	100%	100%	**26.6%**	100%	100%
kr_4	100%	100%	100%	**30.9%**	100%
kr_5	100%	100%	100%	100%	**13.1%**

Table 4-36 Experiment 5: Cases of Softening in Two Stories (1)

Case	6	7	8	9	10
kr_1	**44.7%**	100%	100%	100%	**39.0%**
kr_2	**70.2%**	-	100%	100%	100%
kr_3	100%	-	**34.4%**	100%	100%
kr_4	100%	100%	**56.6%**	-	100%
kr_5	100%	100%	100%	-	**120.1%**

Table 4-37 Experiment 5: Cases of Softening in Two Stories (2)

Case	11	12	13	14	15
kr_1	**58.1%**	**38.7%**	100%	100%	100%
kr_2	100%	100%	**36.3%**	**72.1%**	100%
kr_3	**38.4%**	100%	100%	100%	**28.4%**
kr_4	100%	**108%**	**75.3%**	100%	100%
kr_5	100%	100%	100%	**66.6%**	**52.4%**

Table 4-38 Experiment 5: Frequencies – Cases of Softening in a Single Story

Case	1	2	3	4	5
f_1^c(Hz)	1.69	1.69	1.69	1.69	1.69
f_2^c (Hz)	4.55	4.94	5.11	4.11	3.15
f_3^c (Hz)	8.25	8.47	6.84	8.35	6.57

Table 4-39 Experiment 5: Frequencies – Cases of Softening in Two Stories (1)

Case	6	7	8	9	10
f_1^c(Hz)	1.69	-	1.69	-	1.69
f_2^c (Hz)	4.62	-	4.62	-	4.62
f_3^c (Hz)	8.03	-	7.05	-	8.60

Table 4-40 Experiment 5: Frequencies – Cases of Softening in Two Stories (2)

Case	11	12	13	14	15
f_1^c(Hz)	1.69	1.69	1.69	1.69	1.69
f_2^c (Hz)	4.62	4.62	4.62	4.62	4.62
f_3^c (Hz)	7.09	8.25	8.48	7.79	6.21

Table 4-41 Experiment 5: Difference in Estimated and Measured Frequencies – Cases of Softening in a Single Story

Case	1	2	3	4	5
Δfr_1^*	0%	0%	0%	0%	0%
Δfr_2^*	-1.5%	7.0%	10.6%	-11.0%	-31.8%
Δfr_3^*	2.4%	5.1%	-15.1%	3.6%	-18.5%

Table 4-42 Experiment 5: Difference in Estimated and Measured Frequencies – Cases of Softening in Two Stories (1)

Case	6	7	8	9	10
Δfr_1^*	0%	-	0%	-	0%
Δfr_2^*	0%	-	0%	-	0%
Δfr_3^*	**-0.3%**	-	-12.5%	-	6.7%

Table 4-43 Experiment 5: Difference in Estimated and Measured Frequencies – Cases of Softening in Two Stories (2)

Case	11	12	13	14	15
Δfr_1^*	0%	0%	0%	0%	0%
Δfr_2^*	0%	0%	0%	0%	0%
Δfr_3^*	-12.0%	2.4%	5.3%	-3.3%	-22.9%

Table 4-44 Experiment 6: Vibration Test Modal Frequencies

Test Series		Mode 1 Hz	Mode 2 Hz	Mode 3 Hz
Mode 1	Test 1	1.94		
	Test 2	1.95		
	Test 3	1.95		
Mode 2	Test 1	1.96	4.79	
	Test 2	1.96	4.79	
	Test 3	1.96	4.79	
	Test 4	1.97	4.80	
Mode 3	Test 2	1.95	4.78	8.45
	Test 3	1.94	4.8	8.45
	Test 4	1.91	4.79	8.46
	Test 5	1.95	4.75	8.45
Average =		**1.95**	**4.79**	**8.45**

Table 4-45 Experiment 6: Cases of Softening in a Single Story

Case	1	2	3	4	5
kr_1	**69.3%**	100%	100%	100%	100%
kr_2	100%	**64.2%**	100%	100%	100%
kr_3	100%	100%	**56.1%**	100%	100%
kr_4	100%	100%	100%	**60.1%**	100%
kr_5	100%	100%	100%	100%	**29.9%**

Table 4-46 Experiment 6: Cases of Softening in Two Stories (1)

Case	6	7	8	9	10
kr_1	**46.9%**	100%	100%	100%	**71.1%**
kr_2	**174%**	-	100%	100%	100%
kr_3	100%	-	**82.1%**	100%	100%
kr_4	100%	100%	**67%**	-	100%
kr_5	100%	100%	100%	-	**79.3%**

Table 4-47 Experiment 6: Cases of Softening in Two Stories (2)

Case	11	12	13	14	15
kr_1	-	**76.0%**	100%	100%	100%
kr_2	100%	100%	**81.6%**	**72%**	100%
kr_3	-	100%	100%	100%	**62%**
kr_4	100%	**83%**	**71%**	100%	100%
kr_5	100%	100%	100%	**67%**	**61%**

Table 4-48 Experiment 6: Frequencies – Cases of Softening in a Single Story

Case	1	2	3	4	5
f_1^c(Hz)	1.95	1.95	1.95	1.95	1.95
f_2^c (Hz)	4.92	5.10	5.17	4.68	3.94
f_3^c (Hz)	8.51	8.67	7.98	8.55	6.87

Table 4-49 Experiment 6: Frequencies – Cases of Softening in Two Stories (1) Frequencies – Cases of Softening in Two Stories (1)

Case	6	7	8	9	10
f_1^c(Hz)	1.95	-	1.95	-	1.95
f_2^c (Hz)	4.79	-	4.79	-	4.79
f_3^c (Hz)	8.55	-	8.46	-	7.99

Table 4-50 Experiment 6: Frequencies – Cases of Softening in Two Stories (2)

Case	11	12	13	14	15
f_1^c (Hz)	-	1.95	1.95	1.95	1.95
f_2^c (Hz)	-	4.79	4.79	4.79	4.79
f_3^c (Hz)	-	8.53	8.59	7.80	7.29

Table 4-51 Experiment 6: Difference in Estimated and Measured Frequencies – Cases of Softening in a Single Story

Case	1	2	3	4	5
$\Delta fr_1{}^*$	0%	0%	0%	0%	0%
$\Delta fr_2{}^*$	2.7%	6.5%	7.9%	-2.3%	-17.7%
$\Delta fr_3{}^*$	0.7%	2.6%	-5.6%	1.2%	-18.7%

Table 4-52 Experiment 6: Difference in Estimated and Measured Frequencies – Cases of Softening in Two Stories (1)

Case	6	7	8	9	10
$\Delta fr_1{}^*$	0%	-	0%	-	0%
$\Delta fr_2{}^*$	0%	-	0%	-	0%
$\Delta fr_3{}^*$	1.2%	-	**0.1%**	-	-5.5%

Table 4-53 Experiment 6: Difference in Estimated and Measured Frequencies – Cases of Softening in Two Stories (2)

Case	11	12	13	14	15
$\Delta fr_1{}^*$	-	0%	0%	0%	0%
$\Delta fr_2{}^*$	-	0%	0%	0%	0%
$\Delta fr_3{}^*$	-	0.9%	1.6%	-7.7%	-13.8%

Table 4-54 Experiment 7: Vibration Test Modal Frequencies

Test Series		Mode 1 Hz	Mode 2 Hz	Mode 3 Hz	Mode 4 Hz
Mode 1	Test 1	1.91			
	Test 2	1.91			
	Test 3	1.91			
	Test 4	1.91			
	Test 5	1.92			
Mode 2	Test 1	1.92	5.04		
	Test 2	1.91	5.03		
	Test 3	1.92	5.03		
	Test 4	1.92	5.04		
	Test 5	1.92	5.04		
Mode 3	Test 1	1.92	5.05	8.36	
	Test 2	1.92	5.05	8.36	
	Test 3	1.91	5.06	8.36	
	Test 4	1.91	5.05	8.36	
	Test 5	1.92	5.04	8.36	
Mode 4	Test 1	1.91	5.05	8.29	10.12
	Test 2	1.91	5.05	8.26	10.11
	Test 3	1.91	5.05	8.27	10.11
	Test 4	1.91	5.06	8.22	10.11
	Test 5	1.90	5.03	8.29	10.10
	Test 6	1.91	5.05	8.20	10.11
	Test 7	1.91	5.06	8.28	10.11
	Test 8	1.91	5.05	8.22	10.11
Average =		**1.91**	**5.05**	**8.29**	**10.11**

Table 4-55 Experiment 7: Cases of Softening in a Single Story

Case	1	2	3	4	5
kr_1	**62.9%**	100%	100%	100%	100%
kr_2	100%	**57.4%**	100%	100%	100%
kr_3	100%	100%	**49.0%**	100%	100%
kr_4	100%	100%	100%	**53.3%**	100%
kr_5	100%	100%	100%	100%	**25.0%**

Table 4-56 Experiment 7: Cases of Softening in Two Stories (1)

Case	6	7	8	9	10
kr_1	**93.1%**	-	100%	-	**60.7%**
kr_2	**60.5%**	**-**	100%	-	100%
kr_3	100%	**-**	**52.9%**	-	100%
kr_4	100%	-	**88.0%**	**-**	100%
kr_5	100%	-	100%	**-**	**182.0%**

Table 4-57 Experiment 7: Cases of Softening in Two Stories (2)

Case	11	12	13	14	15
kr_1	**86.7%**	**58.5%**	100%	100%	100%
kr_2	100%	100%	**58.0%**	**57.6%**	100%
kr_3	**55.9%**	100%	100%	100%	**50.3%**
kr_4	100%	**128.7%**	**97.4%**	100%	100%
kr_5	100%	100%	100%	**96.0%**	**83.1%**

Table 4-58 Experiment 7: Cases of Softening in Three Stories (1)

Case	16	17	18	19	20
kr_1	**90.5%**	100%	100%	**57.9%**	**-**
kr_2	**72.9%**	**71.8%**	100%	100%	**-**
kr_3	**73.9%**	**69.5%**	**55.1%**	100%	100%
kr_4	100%	**94.4%**	**79.2%**	**138.3%**	100%
kr_5	100%	100%	**133.3%**	**93%**	**-**

Table 4-59 Experiment 7: Cases of Softening in Three Stories (2)

Case	21	22	23	24	25
kr_1	**61.6%**	**-**	100%	100%	**77.3%**
kr_2	100%	-	**55.6%**	**65.2%**	100%
kr_3	**86.1%**	100%	100%	**77.7%**	**62.7%**
kr_4	**127.3%**	**-**	**114.7%**	100%	100%
kr_5	100%	100%	**82.2%**	**93.6%**	**121.2%**

Table 4-60 Experiment 7: Frequencies – Cases of Softening in Two Stories (1)

Case	1	2	3	4	5
f_1^c(Hz)	1.91	1.91	1.91	1.91	1.91
f_2^c (Hz)	4.85	5.08	5.16	4.56	3.74
f_3^c (Hz)	8.46	8.65	7.77	8.50	6.77
f_4^c (Hz)	10.26	9.92	9.96	9.94	10.37

Table 4-61 Experiment 7: Frequencies – Cases of Softening in Two Stories (1)

Case	6	7	8	9	10
f_1^c(Hz)	1.91	-	1.91	-	1.91
f_2^c (Hz)	5.05	-	5.05	-	5.05
f_3^c (Hz)	8.59	-	7.89	-	9.35
f_4^c (Hz)	9.9	-	9.73	-	11.8

Table 4-62 Experiment 7: Frequencies – Cases of Softening in Two Stories (2)

Case	11	12	13	14	15
f_1^c(Hz)	1.91	1.91	1.91	1.91	1.91
f_2^c (Hz)	5.05	5.05	5.05	5.05	5.05
f_3^c (Hz)	7.88	8.44	8.65	8.56	7.52
f_4^c (Hz)	10.01	10.73	9.9	9.89	9.71

Table 4-63 Experiment 7: Frequencies – Cases of Softening in Three Stories (1)

Case	16	17	18	19	20
f_1^c(Hz)	1.91	1.91	1.91	1.91	-
f_2^c (Hz)	5.05	5.05	5.05	5.05	-
f_3^c (Hz)	8.29	8.29	8.29	8.29	-
f_4^c (Hz)	10.02	9.95	10.33	10.81	-

Table 4-64 Experiment 7: Frequencies – Cases of Softening in Three Stories (2)

Case	21	22	23	24	25
$f_1{}^c$(Hz)	1.91	-	1.91	1.91	1.91
$f_2{}^c$ (Hz)	5.05	-	5.05	5.05	5.05
$f_3{}^c$ (Hz)	8.29	-	8.29	8.29	8.29
$f_4{}^c$ (Hz)	10.68	-	9.89	9.95	10.44

Table 4-65 Experiment 7: Difference in Estimated and Measured Frequencies – Cases of Softening in a Single Story

Case	1	2	3	4	5
$\Delta fr_1{}^*$	0%	0%	0%	0%	0%
$\Delta fr_2{}^*$	-3.2%	1.3%	2.9%	-9.0%	-25.4%
$\Delta fr_3{}^*$	1.5%	3.7%	-6.8%	1.9%	-18.8%
$\Delta fr_4{}^*$	0.7%	-2.6%	-2.3%	-2.5%	1.8%

Table 4-66 Experiment 7: Difference in Estimated and Measured Frequencies – Cases of Softening in Two Stories (1)

Case	6	7	8	9	10
$\Delta fr_1{}^*$	0%	-	0%	-	0%
$\Delta fr_2{}^*$	0%	-	0%	-	0%
$\Delta fr_3{}^*$	3.0%	-	-5.4%	-	12.1%
$\Delta fr_4{}^*$	-2.8%	-	-4.5%	-	15.8%

Table 4-67 Experiment 7: Difference in Estimated and Measured Frequencies – Cases of Softening in Two Stories (2)

Case	11	12	13	14	15
$\Delta fr_1{}^*$	0%	0%	0%	0%	0%
$\Delta fr_2{}^*$	0%	0%	0%	0%	0%
$\Delta fr_3{}^*$	-5.5%	1.2%	3.7%	2.7%	-9.8%
$\Delta fr_4{}^*$	-1.8%	5.3%	-2.8%	-2.9%	-4.7%

Table 4-68 Experiment 7: Difference in Estimated and Measured Frequencies – Cases of Softening in Three Stories (1)

Cases	16	17	18	19	20
$\Delta fr_1{}^*$	0%	0%	-	0%	-
$\Delta fr_2{}^*$	0%	0%	-	0%	-
$\Delta fr_3{}^*$	0%	0%	-	0%	-
$\Delta fr_4{}^*$	**-0.9%**	-2.4%	-	6.1%	-

Table 4-69 Experiment 7: Difference in Estimated and Measured Frequencies – Cases of Softening in Three Stories (2)

Cases	21	22	23	24	25
$\Delta fr_1{}^*$	0%	-	0%	0%	0%
$\Delta fr_2{}^*$	0%	-	0%	0%	0%
$\Delta fr_3{}^*$	0%	-	0%	0%	0%
$\Delta fr_4{}^*$	4.8%	-	-2.9%	-2.4%	2.5%

Table 4-70 Experiment 8: Vibration Test Modal Frequencies

Test Series		Mode 1 Hz	Mode 2 Hz	Mode 3 Hz	Mode 4 Hz
Mode 1	Test 1	1.89			
	Test 2	1.87			
	Test 3	1.89			
Mode 2	Test 1	1.88	5.00		
	Test 2	1.88	5.00		
	Test 3	1.88	5.00		
Mode 3	Test 1	1.88	5.01	8.32	
	Test 2	1.88	5.02	8.32	
	Test 3	1.88	5.02	8.32	
	Test 4	1.88	5.01	8.33	
Mode 4	Test 1	1.89	5.02	8.35	10.18
	Test 2	1.89	5.00	8.34	10.18
	Test 3	1.89	5.03	8.36	10.19
	Test 4	1.89	5.03	8.36	10.21
Average =		**1.88**	**5.01**	**8.34**	**10.19**

Table 4-71 Experiment 8: Cases of Softening in a Single Story

Case	1	2	3	4	5
kr$_1$	**58.7%**	100%	100%	100%	100%
kr$_2$	100%	**53.0%**	100%	100%	100%
kr$_3$	100%	100%	**44.6%**	100%	100%
kr$_4$	100%	100%	100%	**49.0%**	100%
kr$_5$	100%	100%	100%	100%	**22.3%**

Table 4-72 Experiment 8: Cases of Softening in Two Stories (1)

Case	6	7	8	9	10
kr$_1$	**87.7%**	100%	100%	100%	**56.7%**
kr$_2$	**58.2%**	-	100%	100%	100%
kr$_3$	100%	-	**49.0%**	100%	100%
kr$_4$	100%	100%	**84.6%**	-	100%
kr$_5$	100%	100%	100%	-	**190.6%**

Table 4-73 Experiment 8: Cases of Softening in Two Stories (2)

Case	11	12	13	14	15
kr$_1$	**83.4%**	**54.9%**	100%	100%	100%
kr$_2$	100%	100%	**53.9%**	**56.2%**	100%
kr$_3$	**52.1%**	100%	100%	100%	**46.0%**
kr$_4$	100%	**129.2%**	**95.5%**	100%	100%
kr$_5$	100%	100%	100%	**93.1%**	**79.0%**

Table 4-74 Experiment 8: Cases of Softening in Three Stories (1)

Case	16	17	18	19	20
kr$_1$	**87.2%**	100%	100%	**54.7%**	-
kr$_2$	**64.6%**	**63%**	100%	100%	-
kr$_3$	**80.7%**	**73%**	-	100%	100%
kr$_4$	100%	**93.4%**	-	**132.9%**	100%
kr$_5$	100%	100%	-	**97%**	-

Table 4-75 Experiment 8: Cases of Softening in Three Stories (2)

Case	21	22	23	24	25
kr$_1$	**55.9%**	**-**	100%	100%	**71.0%**
kr$_2$	100%	-	**52.5%**	**56.9%**	100%
kr$_3$	**53.0%**	100%	100%	**85.5%**	**61.7%**
kr$_4$	**129.1%**	**-**	**106.6%**	100%	100%
kr$_5$	100%	100%	**86.0%**	**92.1%**	**135.1%**

Table 4-76 Experiment 8: Frequencies – Cases of Softening in a Single Story

Case	1	2	3	4	5
f$_1^c$(Hz)	1.88	1.88	1.88	1.88	1.88
f$_2^c$ (Hz)	4.80	5.06	5.16	4.48	3.61
f$_3^c$ (Hz)	8.43	8.63	7.61	8.48	6.72
f$_4^c$ (Hz)	10.23	9.81	9.92	9.89	10.36

Table 4-77 Experiment 8: Frequencies – Cases of Softening in Two Stories (1)

Case	6	7	8	9	10
f$_1^c$(Hz)	1.88	1.88	1.88	1.88	1.88
f$_2^c$ (Hz)	5.01	5.01	5.01	5.01	5.01
f$_3^c$ (Hz)	8.53	-	7.76	-	9.33
f$_4^c$ (Hz)	9.78	-	9.61	-	11.99

Table 4-78 Experiment 8: Frequencies – Cases of Softening in Two Stories (2)

Case	11	12	13	14	15
f$_1^c$(Hz)	1.88357	1.88	1.88	1.88	1.88
f$_2^c$ (Hz)	5.01273	5.01	5.01	5.01	5.01
f$_3^c$ (Hz)	7.74	8.41	8.63	8.48	7.31
f$_4^c$ (Hz)	9.96	10.71	9.79	9.76	9.58

Table 4-79 Experiment 8: Frequencies – Cases of Softening in Three Stories (1)

Case	16	17	18	19	20
f_1^c(Hz)	1.88	1.88	-	1.88	-
f_2^c (Hz)	5.01	5.01	-	5.01	-
f_3^c (Hz)	8.34	8.34	-	8.34	-
f_4^c (Hz)	9.89	9.87	-	10.74	-

Table 4-80 Experiment 8: Frequencies – Cases of Softening in Three Stories (2)

Case	21	22	23	24	25
f_1^c(Hz)	1.88	-	1.88	1.88	1.88
f_2^c (Hz)	5.01	-	5.01	5.01	5.01
f_3^c (Hz)	8.34	-	8.34	8.34	8.34
f_4^c (Hz)	10.70	-	9.75	9.81	10.72

Table 4-81 Experiment 8: Difference in Estimated and Measured Frequencies – Cases of Softening in a Single Story

Case	1	2	3	4	5
Δfr_1^*	0%	0%	0%	0%	0%
Δfr_2^*	-4.2%	0.9%	2.9%	-10.6%	-28.0%
Δfr_3^*	1.1%	3.5%	-8.7%	1.7%	-19.4%
Δfr_4^*	0.4%	-3.7%	-2.6%	-2.9%	1.7%

Table 4-82 Experiment 8: Difference in Estimated and Measured Frequencies – Cases of Softening in Two Stories (1)

Case	6	7	8	9	10
Δfr_1^*	0%	-	0%	-	0%
Δfr_2^*	0%	-	0%	-	0%
Δfr_3^*	2.3%	-	-6.9%	-	11.9%
Δfr_4^*	-4.0%	-	-5.7%	-	17.7%

Table 4-83 Experiment 8: Difference in Estimated and Measured Frequencies – Cases of Softening in Two Stories (2)

Case	11	12	13	14	15
Δfr_1^*	0%	0%	0%	0%	0%
Δfr_2^*	0%	0%	0%	0%	0%
Δfr_3^*	-7.2%	0.9%	3.5%	1.7%	-12.3%
Δfr_4^*	-2.3%	5.1%	-3.9%	-4.2%	-6.0%

Table 4-84 Experiment 8: Difference in Estimated and Measured Frequencies – Cases of Softening in Three Stories (1)

Cases	16	17	18	19	20
Δfr_1^*	0%	0%	-	0%	-
Δfr_2^*	0%	0%	-	0%	-
Δfr_3^*	0%	0%	-	0%	-
Δfr_4^*	**-2.9%**	-3.1%	-	5.4%	-

Table 4-85 Experiment 8: Difference in Estimated and Measured Frequencies – Cases of Softening in Three Stories (2)

Cases	21	22	23	24	25
Δfr_1^*	0%	-	0%	0%	0%
Δfr_2^*	0%	-	0%	0%	0%
Δfr_3^*	0%	-	0%	0%	0%
Δfr_4^*	5.0%	-	-4.3%	-3.7%	5.2%

Table 5-1 Input Level and Damage Progression (Suita et al., 2015)

Test	Input level		Description of input level	Max. disp. at the top (cm)	Max. story drift angle (floor)	Damage to specimen
	$_pS_v$ (cm/s)	% to pSv110				
pSv40	40	36.4	Design level 1	8.5	1/171 (14F)	None (elastic)
pSv80	81	73.6	Design level 2	15.3	1/110 (3,14F)	Full plastic of beam end (2-4F)
pSv110-1	110	100.0	Average of prediction	20.6	1/90 (14F)	Full plastic of beam end (2-7F) and column base (2-5F)
pSv110-2	110	100.0	Average of prediction	21.7	1/91 (14F)	ditto
pSv180-1	180	163.6	Max. of prediction	30.8	1/62 (11F)	Full plastic of beam end (2-14F), Crack initiation beam end (2-5F)
pSv180-2	180	163.6	Max. of prediction	31.7	1/55 (11F)	Crack progress beam end (2-5F)
pSv220	220	200.0	Over max. of prediction	34.7	1/48 (9F)	Fracture of beam flange (2F)
pSv250	250	227.3	Over max. of prediction	33.7	1/45 (2F)	Fracture of beam flange (2-3F)
pSv300	300	272.7	Over max. of prediction	37.4	1/30 (2F)	Fracture of beam flange (2-5F)
pSv340-1	340	310.0	Over max. of prediction	51.0	1/16 (2F)	Fracture of beam flange (upper Fl.) Local buckling of column base (1F)
pSv340-2	340	310.0	Over max. of prediction	56.3	1/13 (2F)	ditto
pSv420-1	420	381.8	Over max. of prediction	66.6	1/10 (2F)	Total fracture of beam end (2-5F)
pSv420-2	420	381.8	Over max. of prediction	100.0	1/6 (2F)	Fracture of column base (1F)
pSv420-3	420	381.8	Over max. of prediction	Collapse	Collapse	Collapse

Table 5-2 Measured Frequencies vs. SAP2000 Frequencies

Mode	Measured Frequencies	SAP2000 Frequencies	Percent Difference
	(Hz)	(Hz)	%
1	0.879	0.88	0%
2	2.686	2.767	3%
3	4.883	5.121	5%
4	7.030	7.446	6%
5	9.229	9.791	6%
6	11.572	12.098	5%

Table 5-3 Building Mass and Stiffness (Suita et al., 2015)

Story	Mass (kg)	Stiffness (N/m)
1	21210	1.15E+08
2	21210	1.28E+08
3	21210	1.14E+08
4	21210	9.93E+07
5	21210	8.66E+07
6	21210	7.66E+07
7	21210	7.04E+07
8	21210	6.86E+07
9	21210	7.04E+07
10	21210	7.56E+07
11	21210	8.29E+07
12	21010	8.99E+07
13	21010	9.39E+07
14	21010	8.93E+07
15	21010	8.62E+07
16	21010	8.04E+07
17	21010	7.41E+07
18	20600	7.24E+07

Table 5-4 Cases of Softening at One Story (1)

Case	1	2	3	4	5	6	7	8	9
kr_1	**40%**	100%	100%	100%	100%	100%	100%	100%	100%
kr_2	100%	**38%**	100%	100%	100%	100%	100%	100%	100%
kr_3	100%	100%	**28%**	100%	100%	100%	100%	100%	100%
kr_4	100%	100%	100%	**42%**	100%	100%	100%	100%	100%
kr_5	100%	100%	100%	100%	**44%**	100%	100%	100%	100%
kr_6	100%	100%	100%	100%	100%	**46%**	100%	100%	100%
kr_7	100%	100%	100%	100%	100%	100%	**46%**	100%	100%
kr_8	100%	100%	100%	100%	100%	100%	100%	**44%**	100%
kr_9	100%	100%	100%	100%	100%	100%	100%	100%	**40%**
kr_{10}	100%	100%	100%	100%	100%	100%	100%	100%	100%
kr_{11}	100%	100%	100%	100%	100%	100%	100%	100%	100%
kr_{12}	100%	100%	100%	100%	100%	100%	100%	100%	100%
kr_{13}	100%	100%	100%	100%	100%	100%	100%	100%	100%
kr_{14}	100%	100%	100%	100%	100%	100%	100%	100%	100%
kr_{15}	100%	100%	100%	100%	100%	100%	100%	100%	100%
kr_{16}	100%	100%	100%	100%	100%	100%	100%	100%	100%
kr_{17}	100%	100%	100%	100%	100%	100%	100%	100%	100%
kr_{18}	100%	100%	100%	100%	100%	100%	100%	100%	100%

Table 5-5 Cases of Softening at One Story (2)

Case	10	11	12	13	14	15	16	17	18
kr_1	100%	100%	100%	100%	100%	100%	100%	100%	100%
kr_2	100%	100%	100%	100%	100%	100%	100%	100%	100%
kr_3	100%	100%	100%	100%	100%	100%	100%	100%	100%
kr_4	100%	100%	100%	100%	100%	100%	100%	100%	100%
kr_5	100%	100%	100%	100%	100%	100%	100%	100%	100%
kr_6	100%	100%	100%	100%	100%	100%	100%	100%	100%
kr_7	100%	100%	100%	100%	100%	100%	100%	100%	100%
kr_8	100%	100%	100%	100%	100%	100%	100%	100%	100%
kr_9	100%	100%	100%	100%	100%	100%	100%	100%	100%
kr_{10}	**35%**	100%	100%	100%	100%	100%	100%	100%	100%
kr_{11}	100%	**29%**	100%	100%	100%	100%	100%	100%	100%
kr_{12}	100%	100%	**23%**	100%	100%	100%	100%	100%	100%
kr_{13}	100%	100%	100%	**18%**	100%	100%	100%	100%	100%
kr_{14}	100%	100%	100%	100%	**15%**	100%	100%	100%	100%
kr_{15}	100%	100%	100%	100%	100%	**11%**	100%	100%	100%
kr_{16}	100%	100%	100%	100%	100%	100%	**7%**	100%	100%
kr_{17}	100%	100%	100%	100%	100%	100%	100%	**4%**	100%
kr_{18}	100%	100%	100%	100%	100%	100%	100%	100%	**1%**

Table 5-6 Cases of Softening at One Story (1) – Relative Frequency Differences

Case	1	2	3	4	5	6	7	8	9
Δfr_1^*	0.0%	0.0%	0.0%	0.0%	0.0%	0.0%	0.0%	0.0%	0.0%
Δfr_2^*	**-1.3%**	**-0.4%**	**0.7%**	2.1%	3.6%	5.0%	5.8%	5.3%	3.5%

Table 5-7 Cases of Softening at One Story (1) – Relative Frequency Differences

Case	10	11	12	13	14	15	16	17	18
Δfr_1^*	0.0%	0.0%	0.0%	0.0%	0.0%	0.0%	0.0%	0.0%	0.0%
Δfr_2^*	**0.4%**	-3.5%	-7.7%	-12.3%	-17.4%	-23.3%	-30.3%	-39.0%	-50.5%

FIGURES
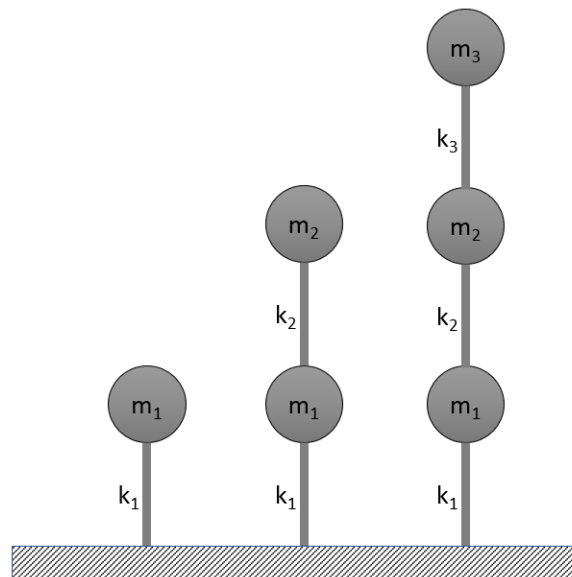
Figure 2-1 Spring-Mass System:

Single DOF, Two DOF, and Three DOF System
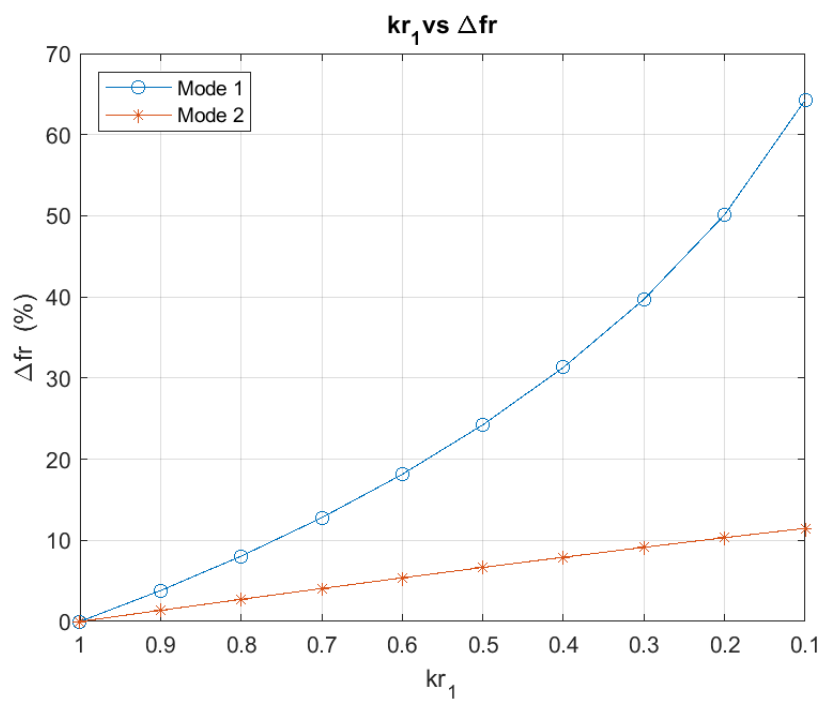
Figure 3-1 2-DOF System: Relative Stiffness (kr_1) vs. Relative Change in Frequencies
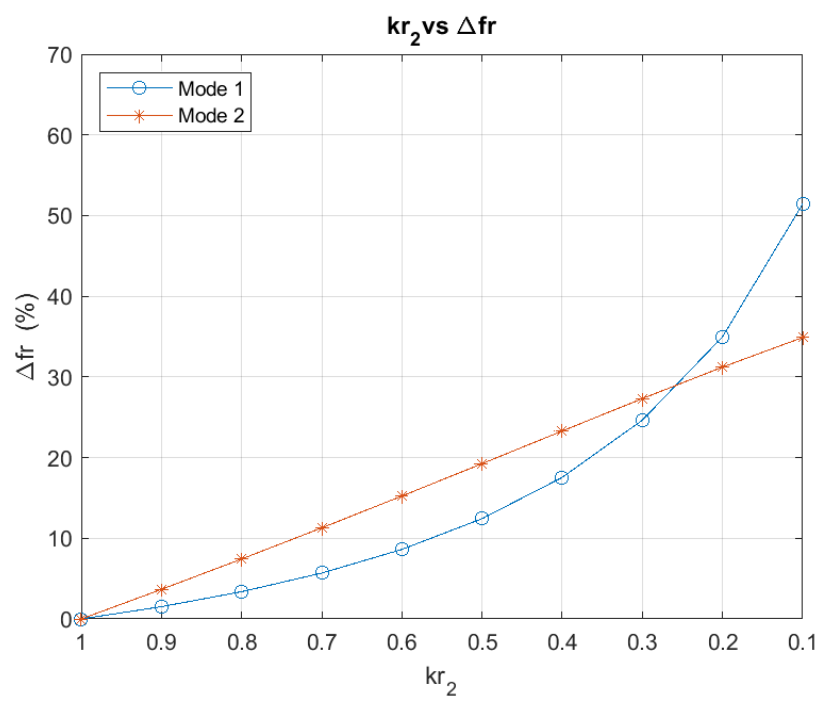
Figure 3-2 2-DOF System: Relative Stiffness (kr_2) vs. Relative Change in Frequencies
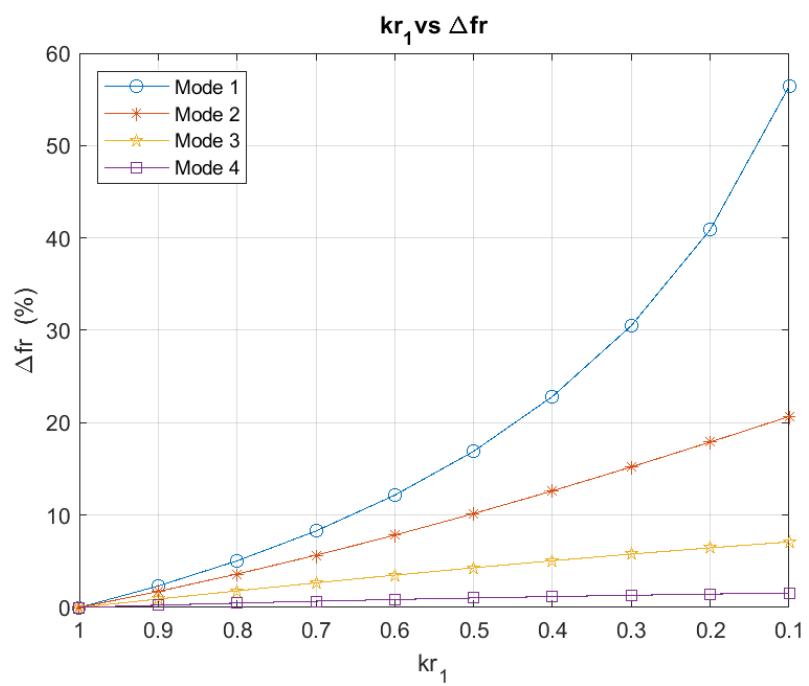
Figure 3-3 4-DOF System: Relative Stiffness (kr_1) vs. Relative Change in Frequencies
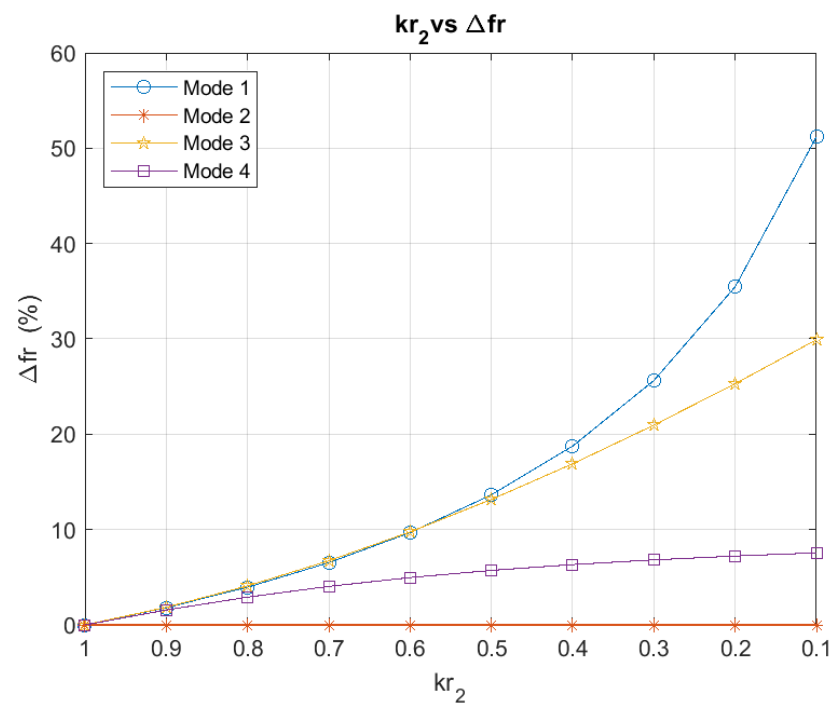
Figure 3-4 4-DOF System: Relative Stiffness (kr_2) vs. Relative Change in Frequencies
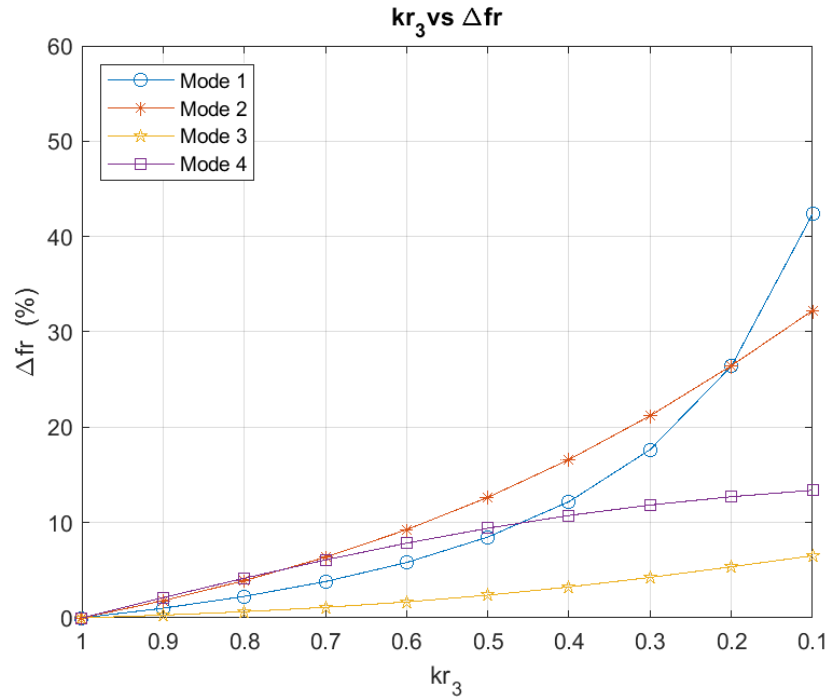
Figure 3-5 4-DOF System: Relative Stiffness (kr_3) vs. Relative Change in Frequencies
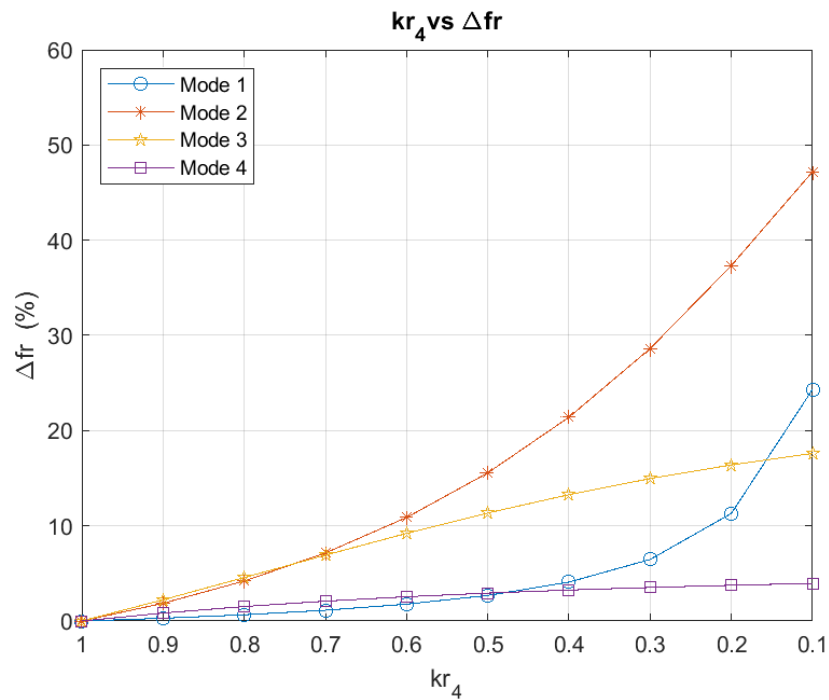
Figure 3-6 4-DOF System: Relative Stiffness (kr_4) vs. Relative Change in Frequencies
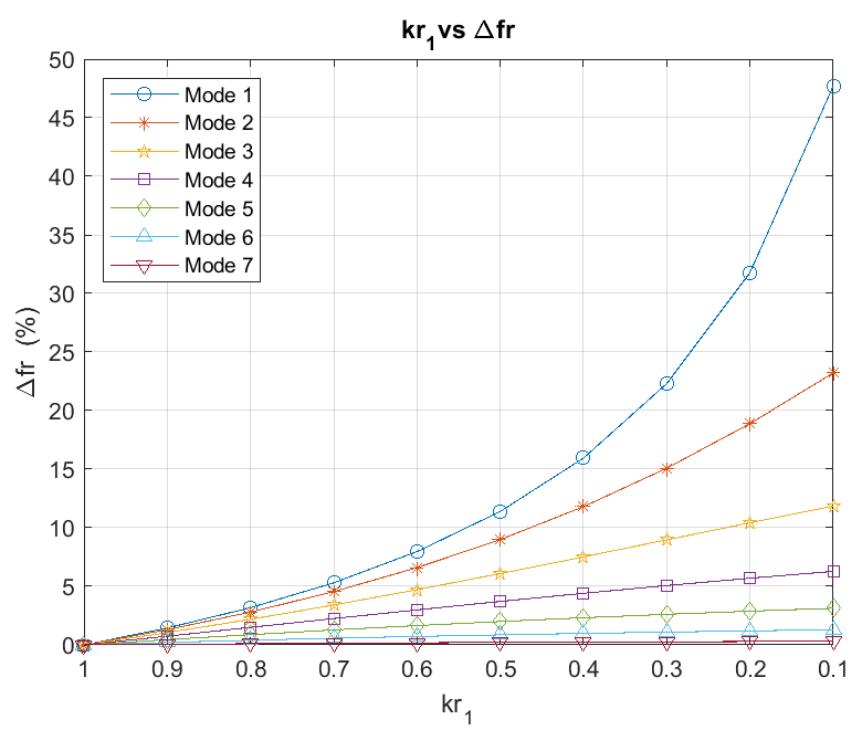
Figure 3-7 7-DOF System: Relative Stiffness (kr_1) vs. Relative Change in Frequencies
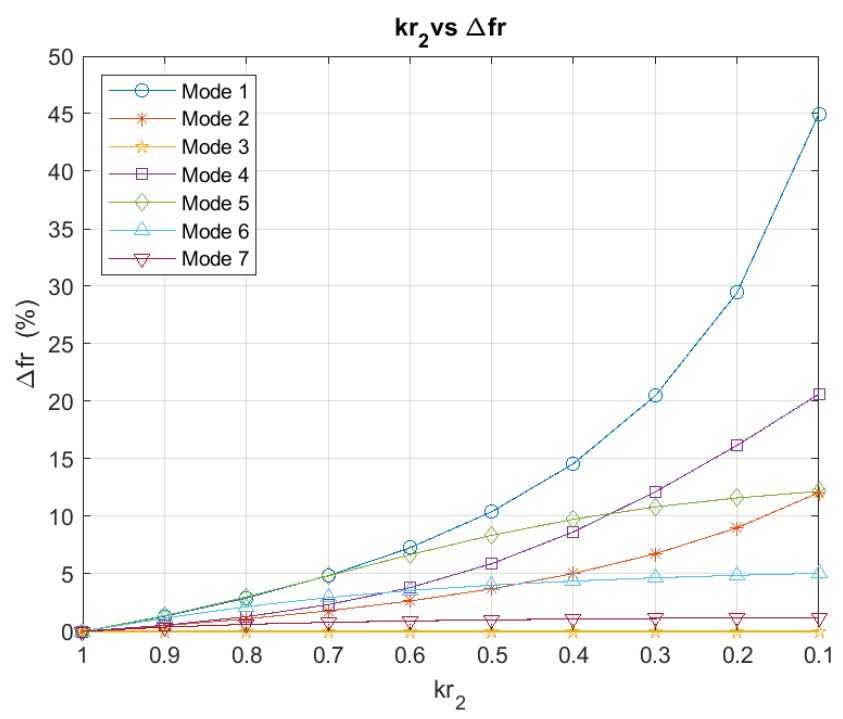

Figure 3-8 7-DOF System: Relative Stiffness (kr_2) vs. Relative Change in Frequencies
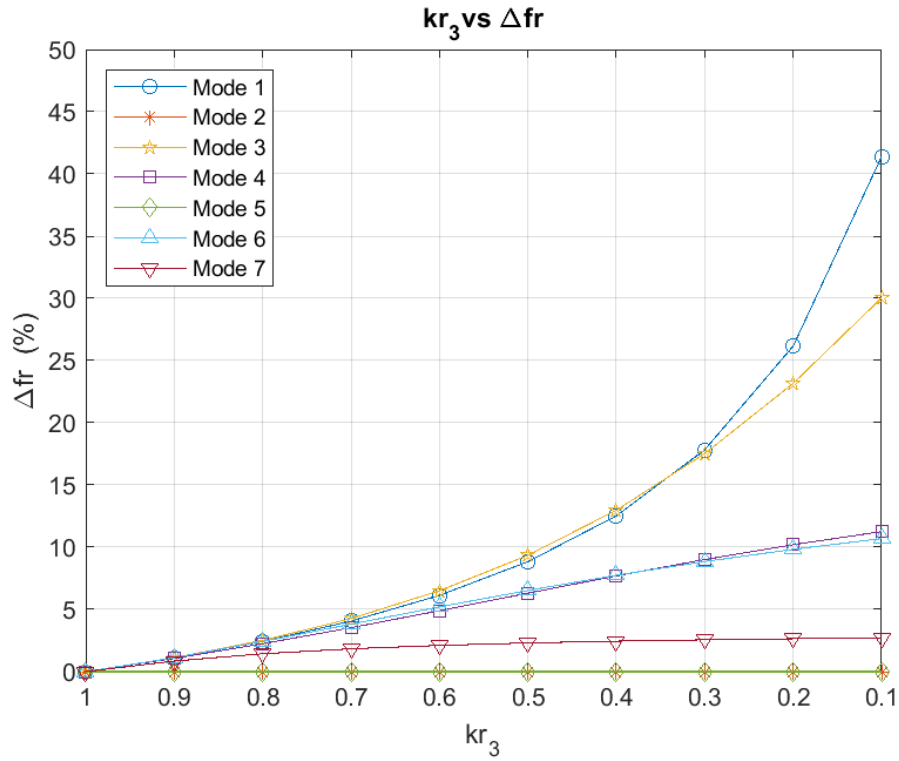
Figure 3-9 7-DOF System: Relative Stiffness (kr_3) vs. Relative Change in Frequencies
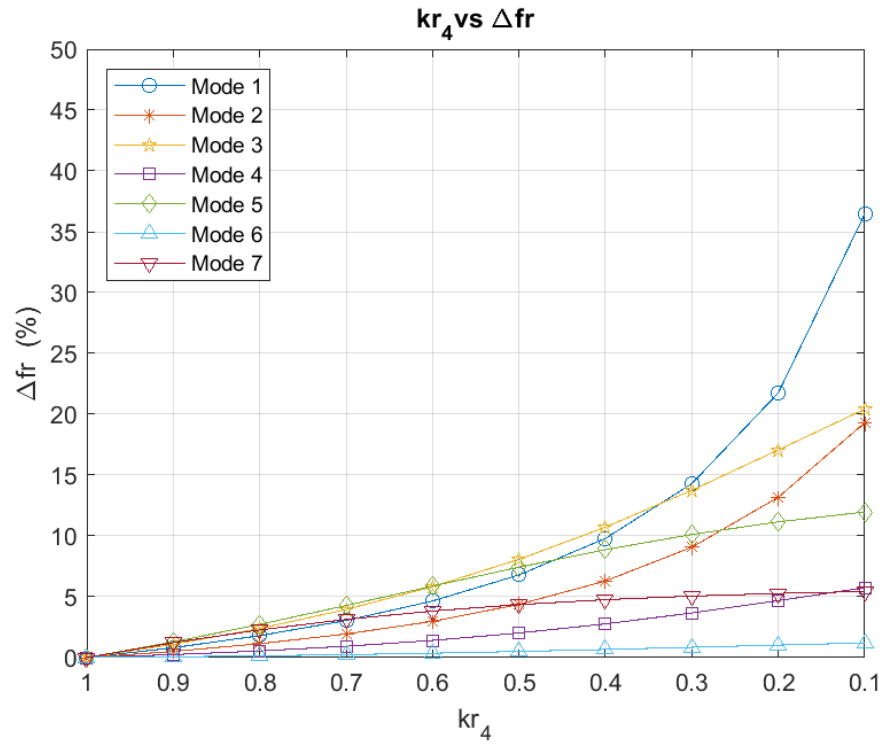
Figure 3-10 7-DOF System: Relative Stiffness (kr_4) vs. Relative Change in Frequencies
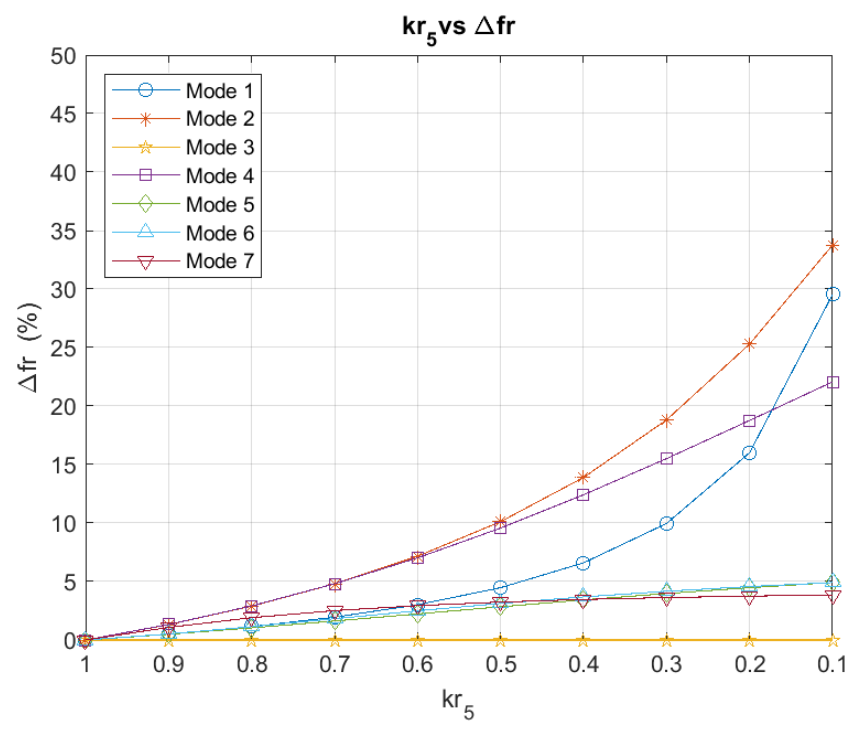
Figure 3-11 7-DOF System: Relative Stiffness (kr_5) vs.vs Relative Change in Frequencies

Figure 3-12 7-DOF System: Relative Stiffness (kr_6) vs. Relative Change in Frequencies
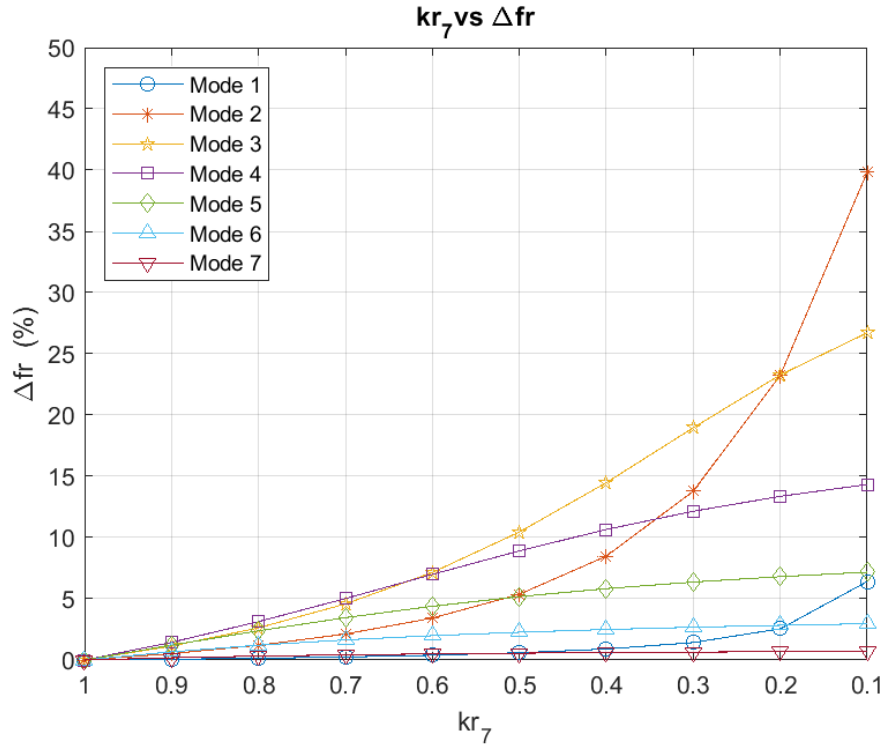
Figure 3-13 7-DOF System: Relative Stiffness (kr_7) vs. Relative Change in Frequencies
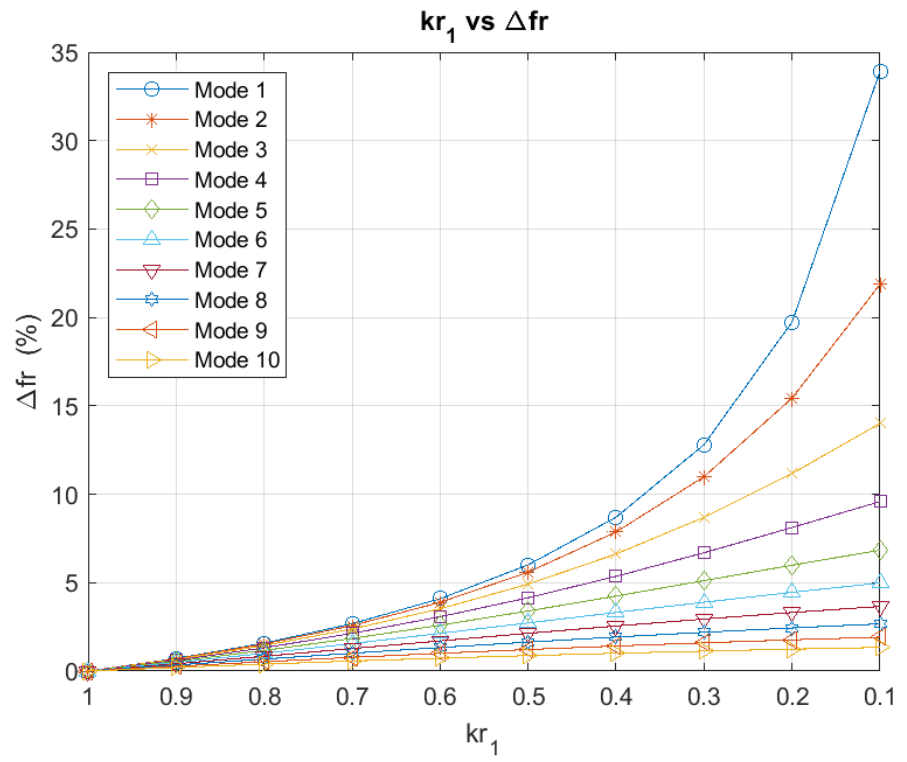
Figure 3-14 15-DOF System: Relative Stiffness (kr_1) vs. Relative Change in Frequencies
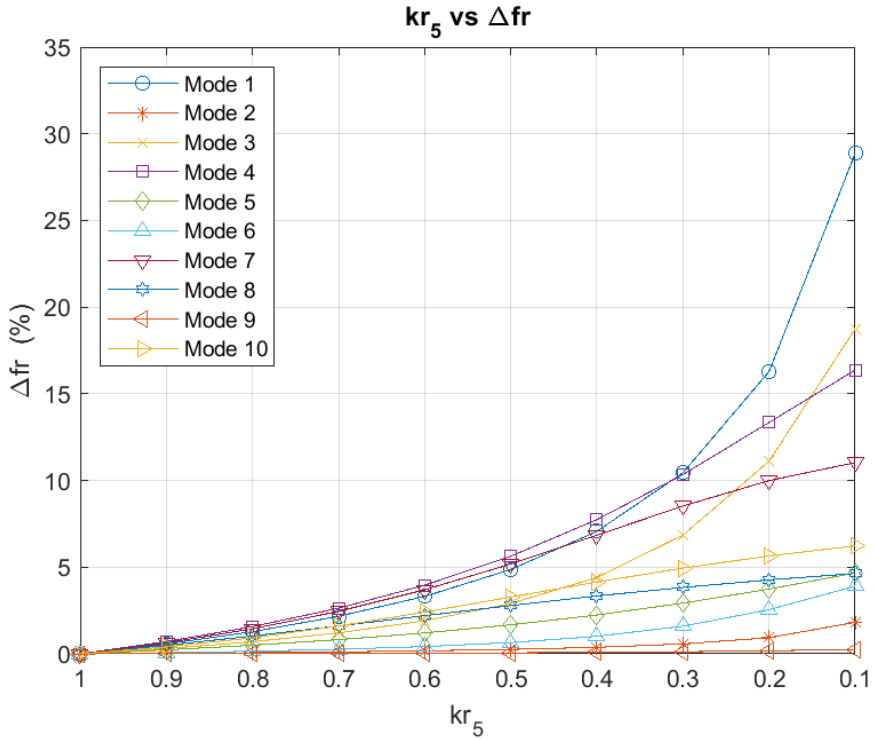
Figure 3-15 15-DOF System: Relative Stiffness (kr_5) vs. Relative Change in Frequencies
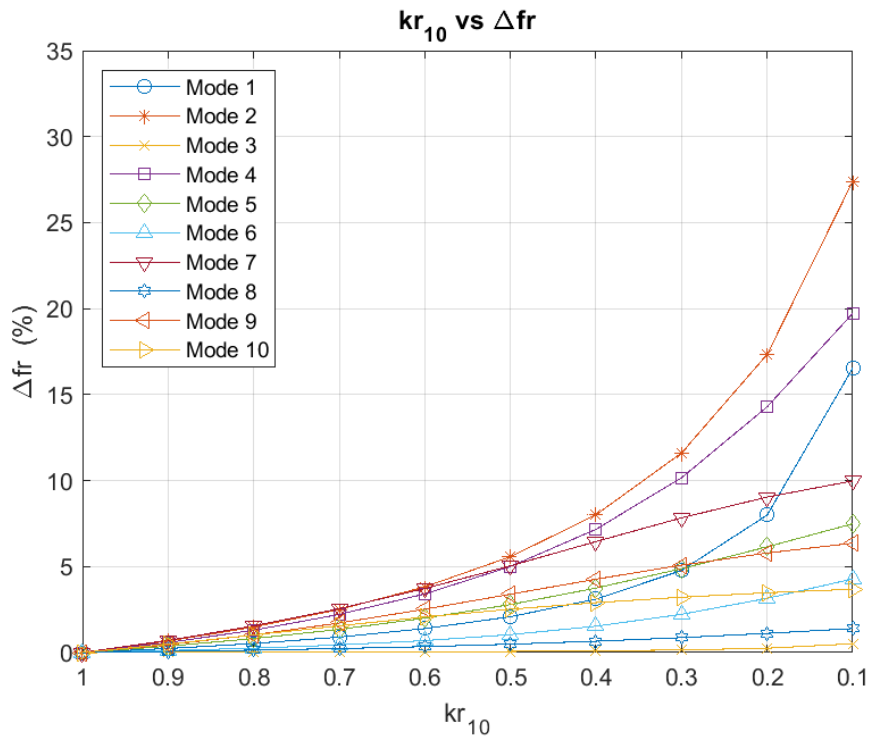
Figure 3-16 15-DOF System: Relative Stiffness (kr_{10}) vs. Relative Change in Frequencies
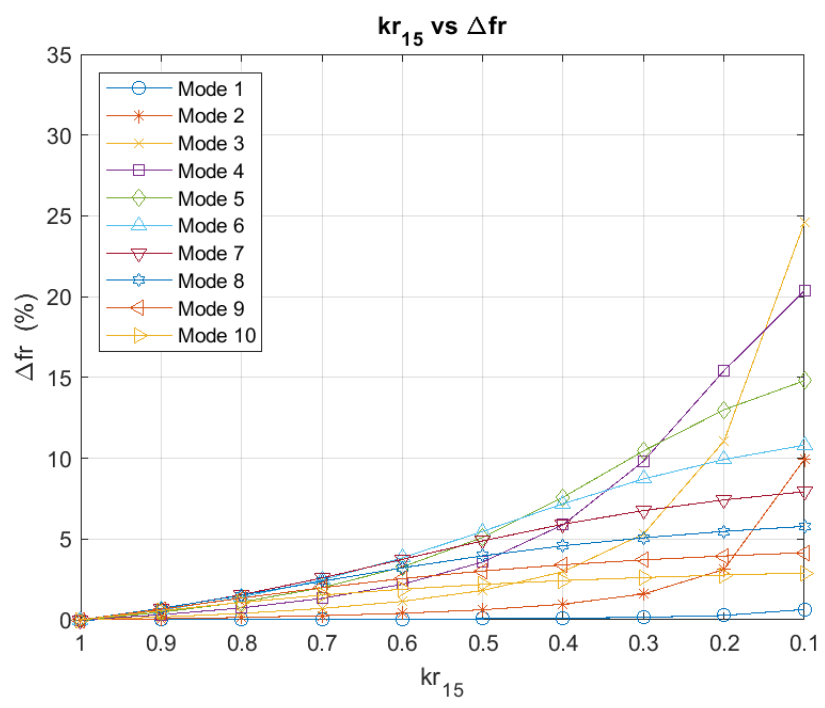
Figure 3-17 15-DOF System: Relative Stiffness (kr_{15}) vs. Relative Change in Frequencies
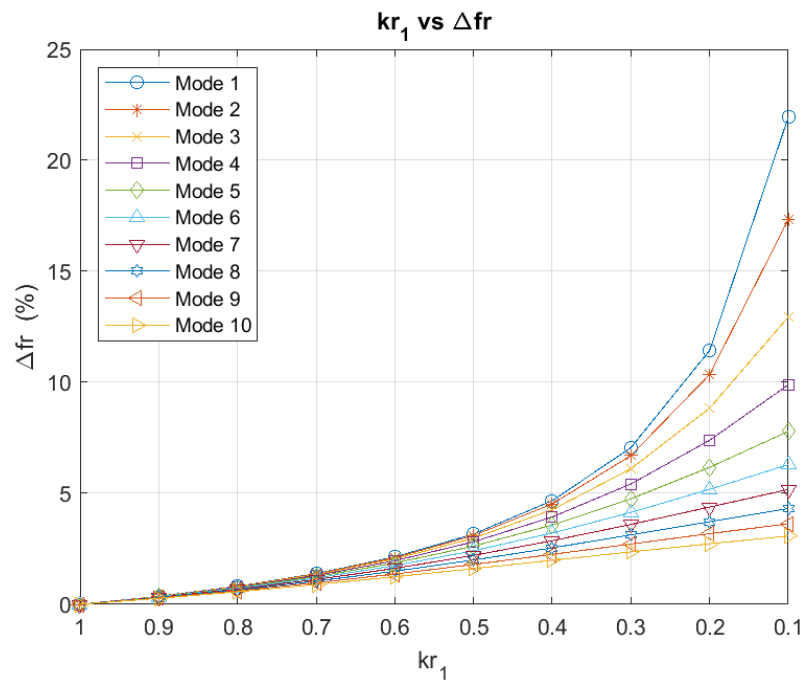
Figure 3-18 30-DOF System: Relative Stiffness (kr_1) vs. Relative Change in Frequencies
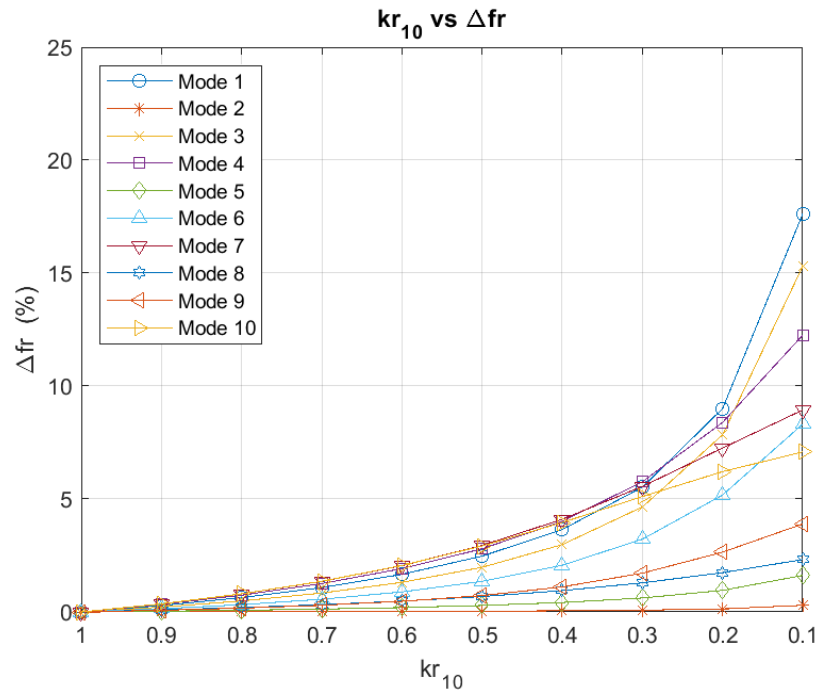
Figure 3-19 30-DOF System: Relative Stiffness (kr_{10}) vs. Relative Change in Frequencies
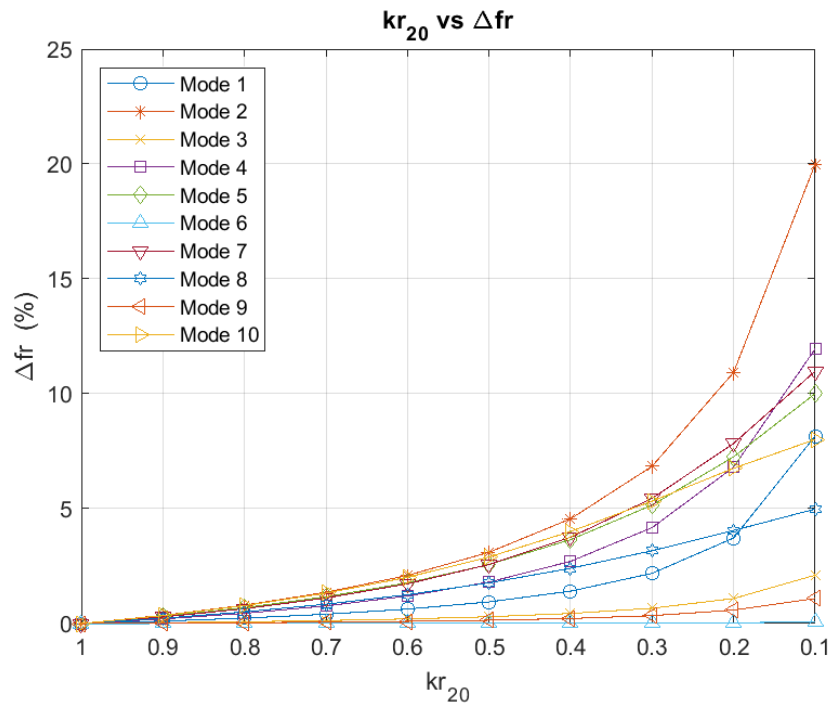
Figure 3-20 30-DOF System: Relative Stiffness (kr_{20}) vs. Relative Change in Frequencies
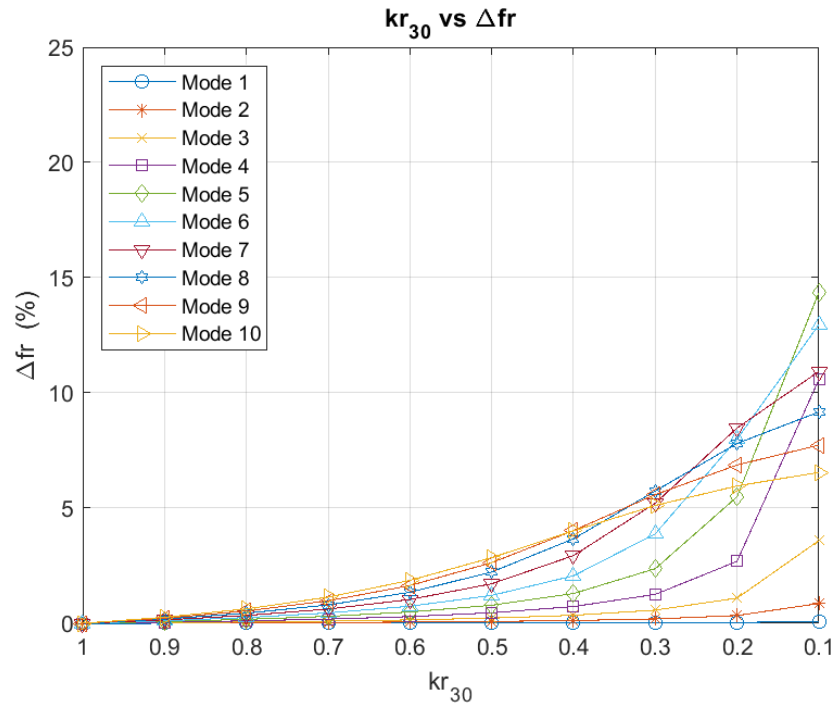
Figure 3-21 30-DOF System: Relative Stiffness (kr_{30}) vs. Relative Change in Frequencies
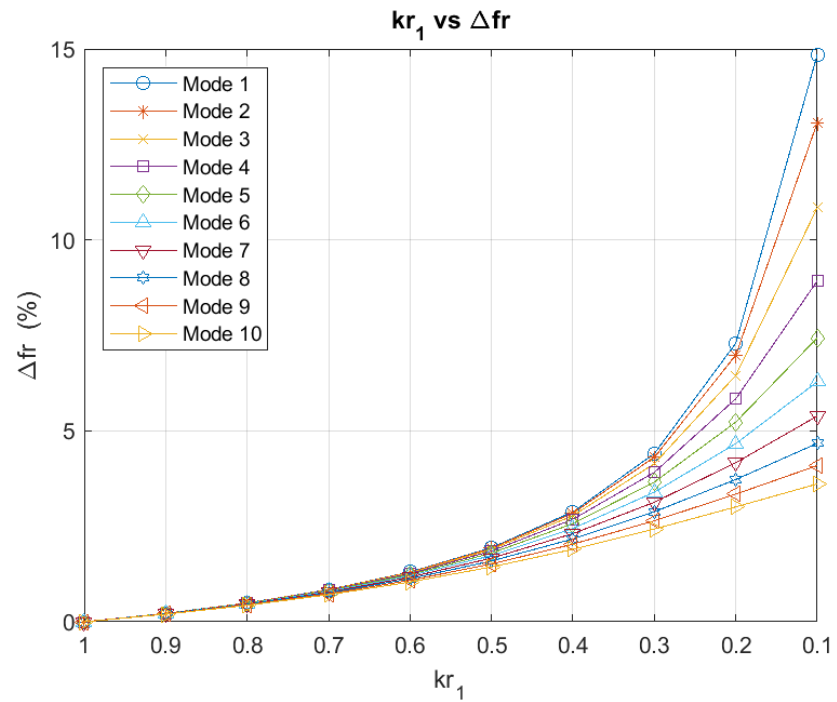
Figure 3-22 50-DOF System: Relative Stiffness (kr_1) vs. Relative Change in Frequencies
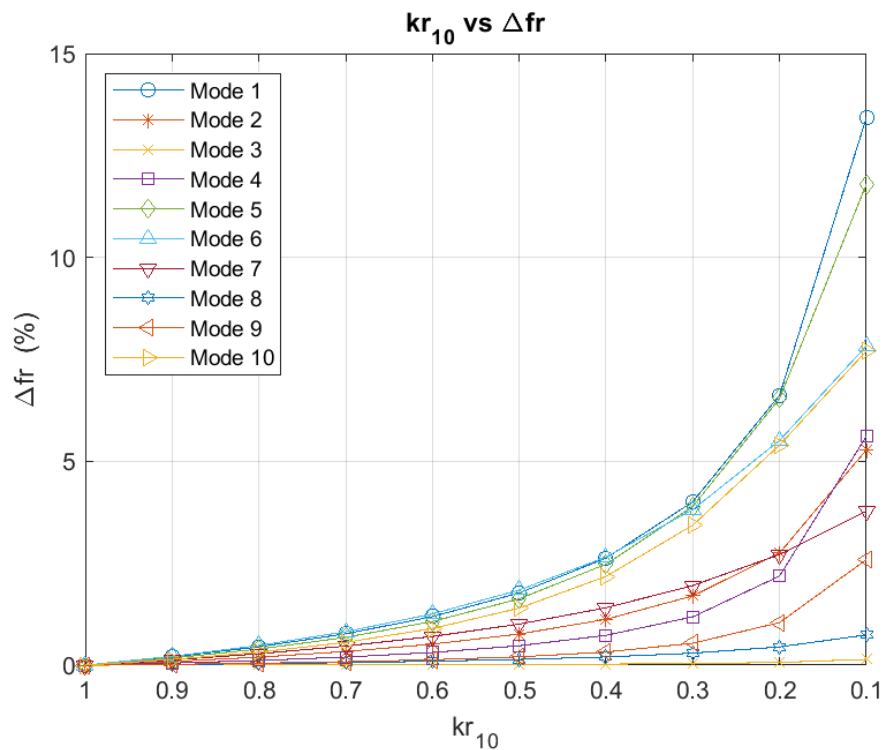
Figure 3-23 50-DOF System: Relative Stiffness (kr_{10}) vs. Relative Change in Frequencies
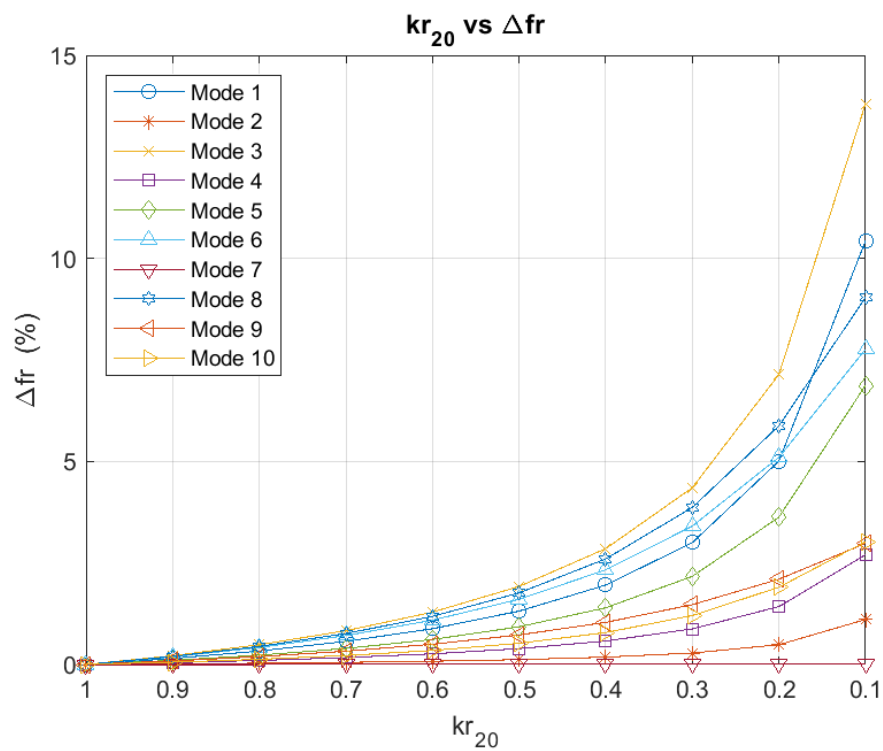
Figure 3-24 50-DOF System: Relative Stiffness (kr_{20}) vs. Relative Change in Frequencies
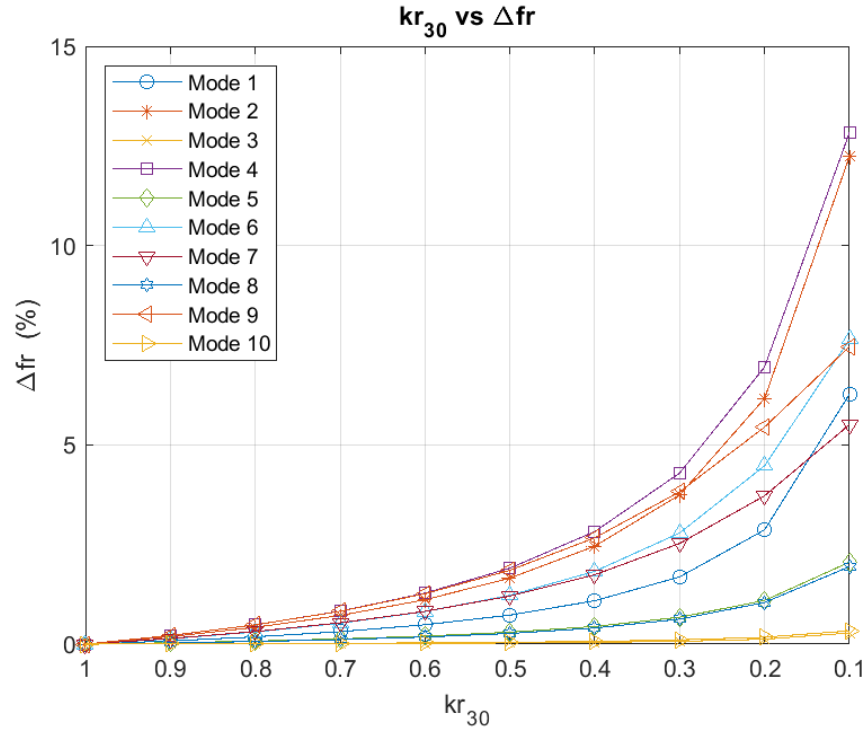
Figure 3-25 50-DOF System: Relative Stiffness (kr_{30}) vs. Relative Change in Frequencies
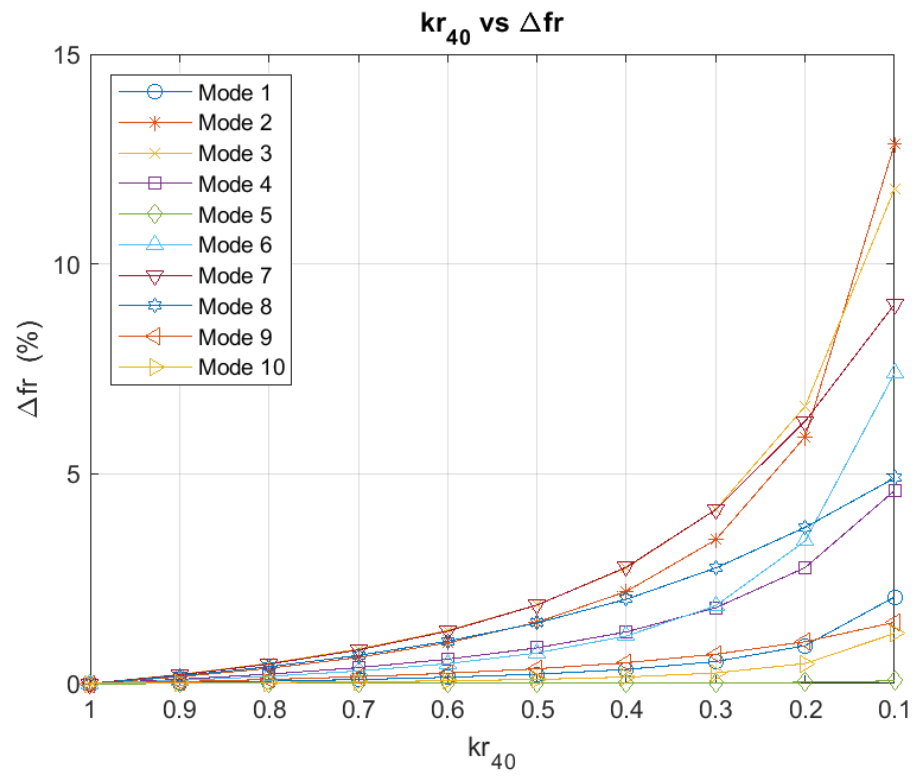
Figure 3-26 50-DOF System: Relative Stiffness (kr_{40}) vs. Relative Change in Frequencies
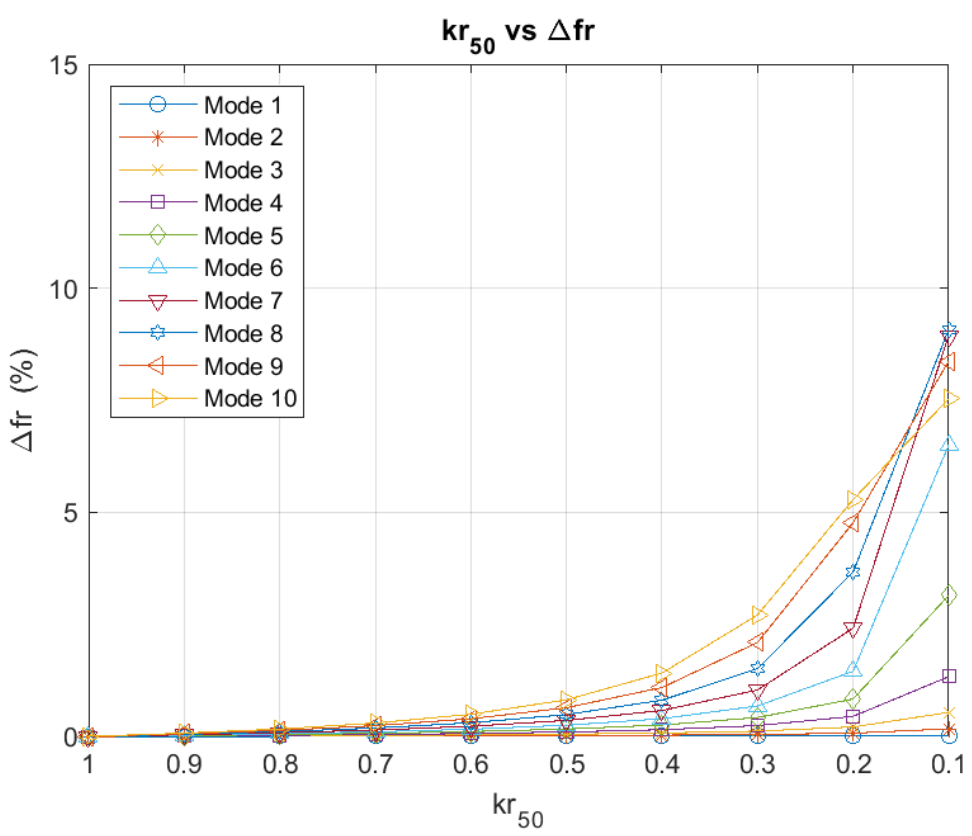
Figure 3-27 50-DOF System: Relative Stiffness (kr_{50}) vs. Relative Change in Frequencies
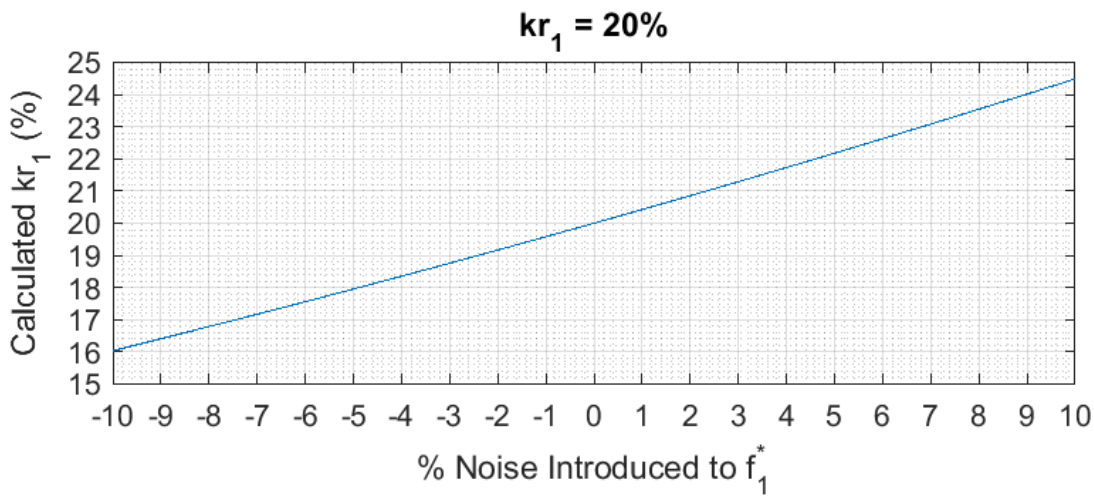
Figure 3-28 2-DOF: Noisy f_1^* and kr_1 (20%)
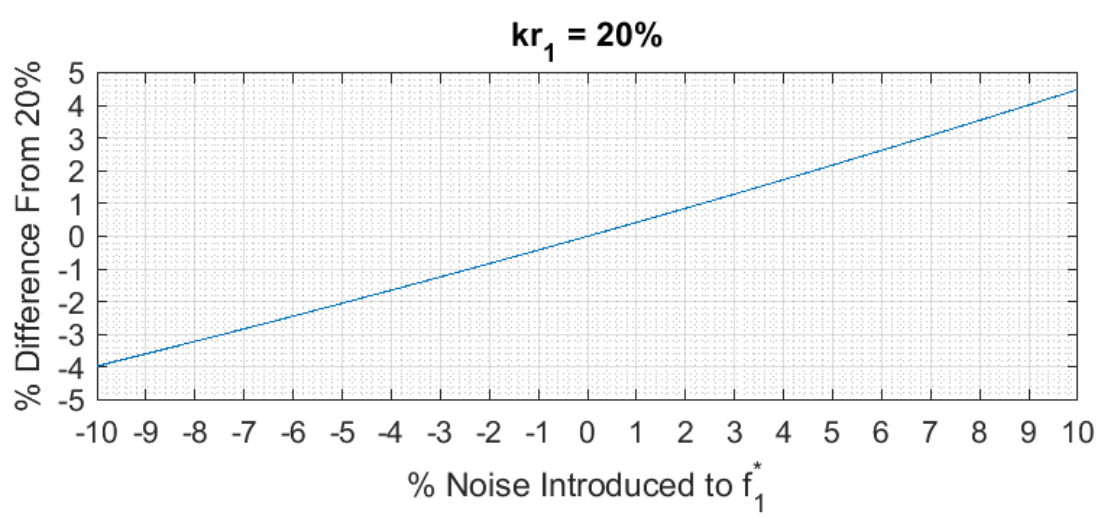
Figure 3-29 2-DOF: Noisy f_1^* and % Difference from kr_1 (20%)
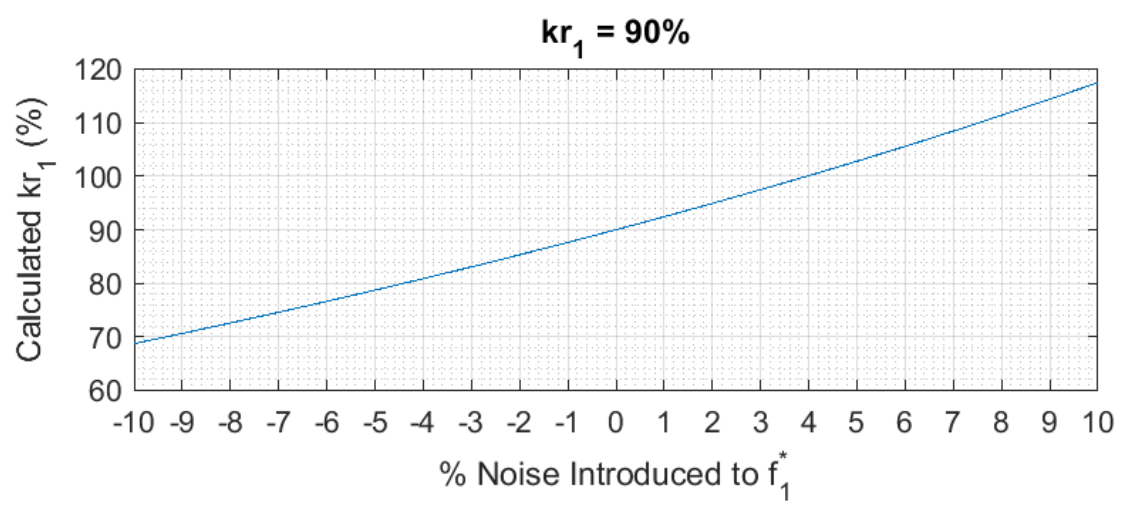
Figure 3-30 2-DOF: Noisy f_1^* and kr_1 (90%)
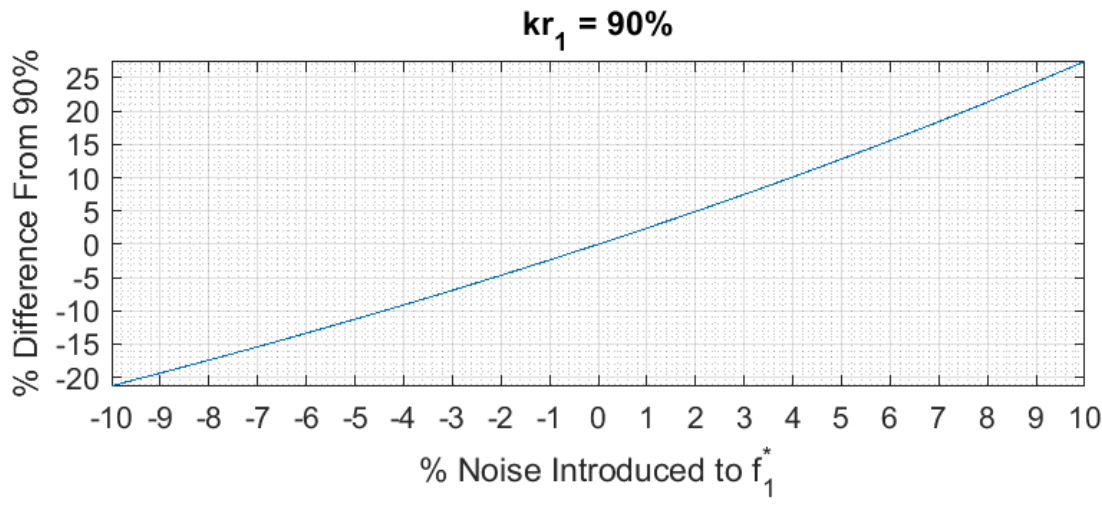
Figure 3-31 2-DOF: Noisy f_1^* and % Difference from kr_1 (90%)
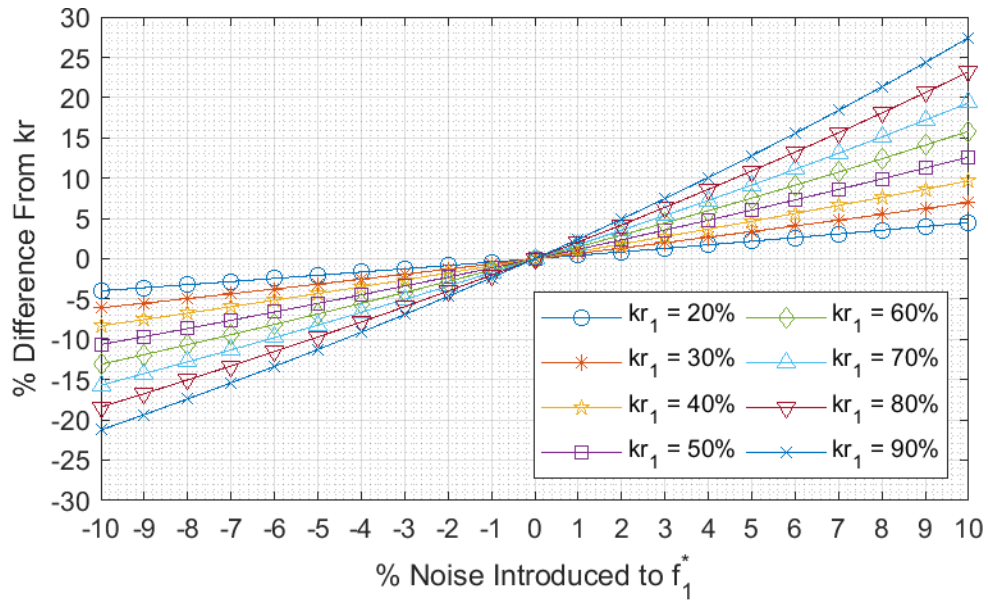
Figure 3-32 Noisy f_1^* and Different kr_1 Cases
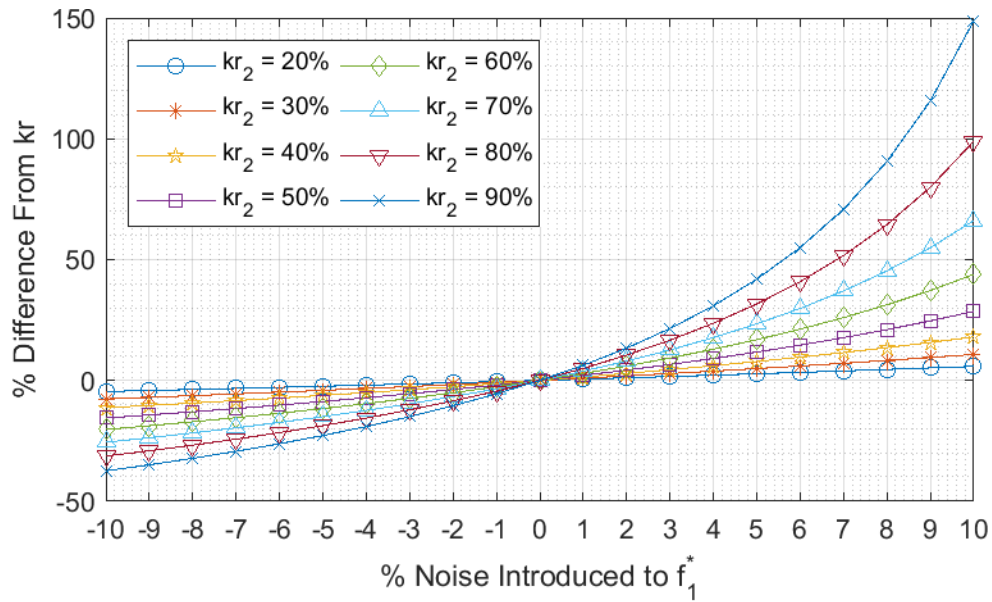
Figure 3-33 2-DOF: Noisy f_1^* and Different kr_2 Cases
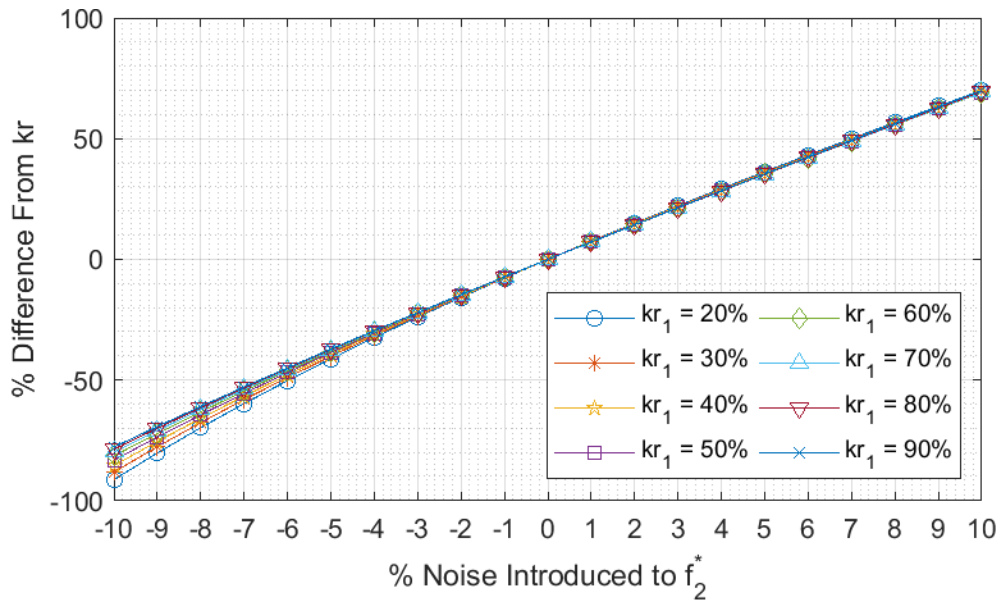
Figure 3-34 2-DOF: Noisy f_2^* and Different kr_1 Cases
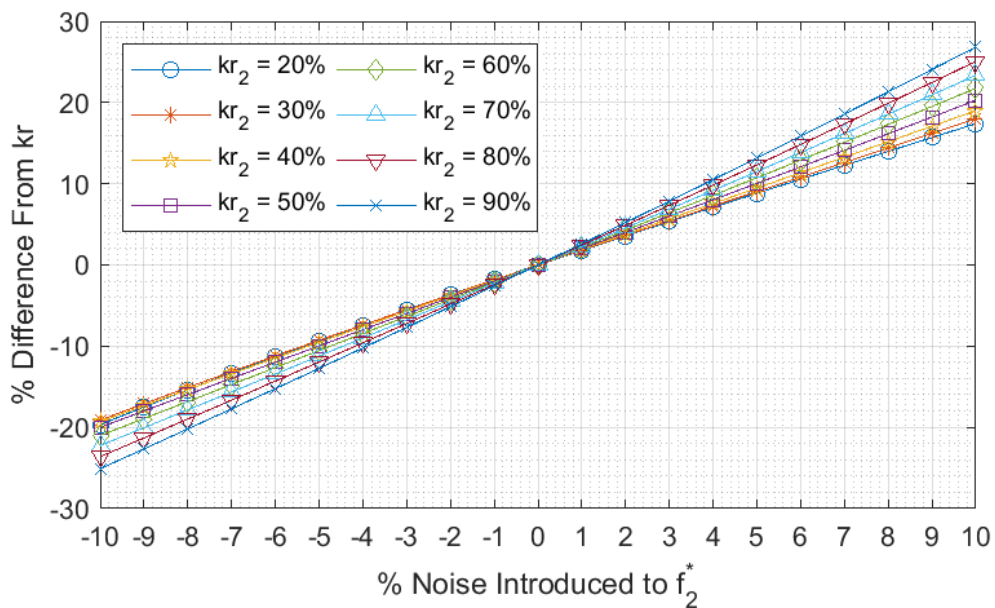
Figure 3-35 2-DOF: Noisy f_2^* and Different kr_2 Cases
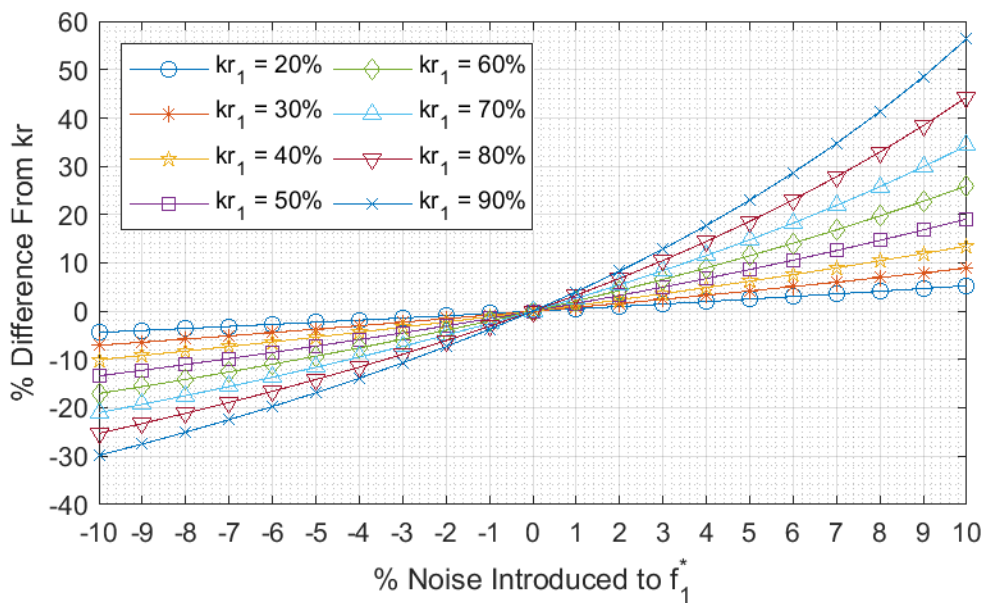
Figure 3-36 4-DOF: Noisy f_1^* and Different kr_1 Cases
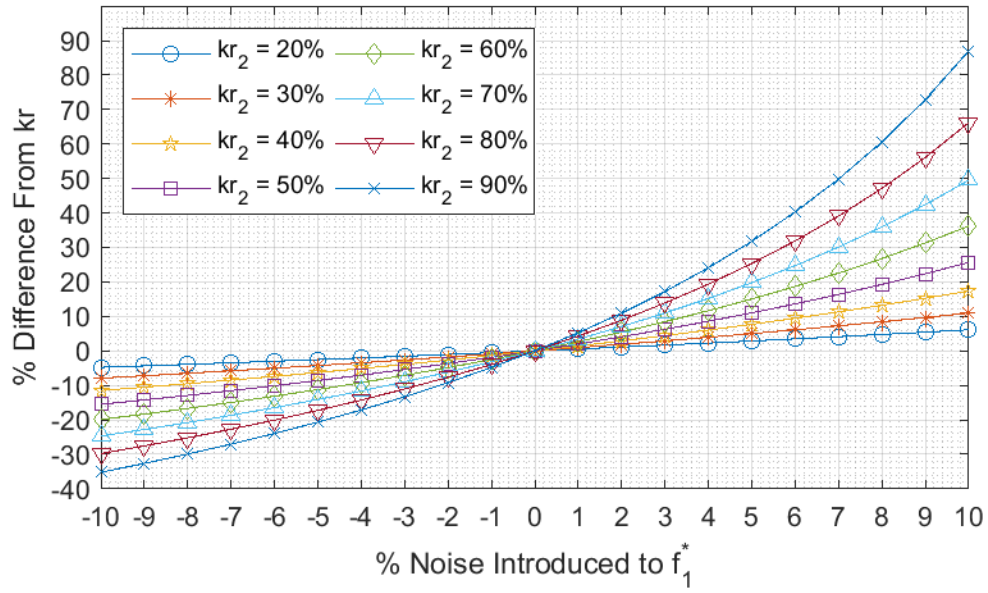
Figure 3-37 4-DOF: Noisy f_1^* and Different kr_2 Cases
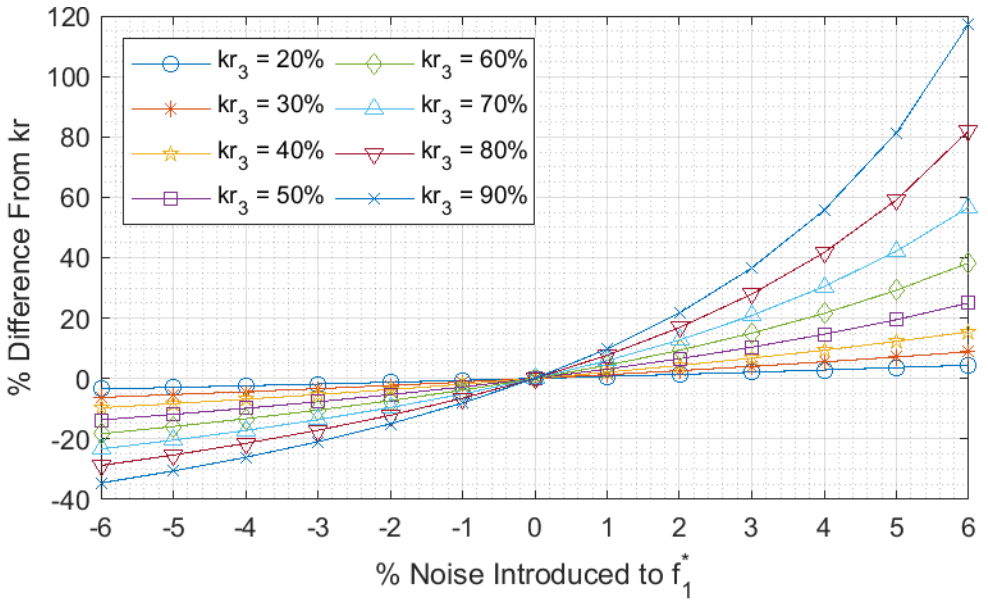
Figure 3-38 4-DOF: Noisy f_1^* and Different kr_3 Cases
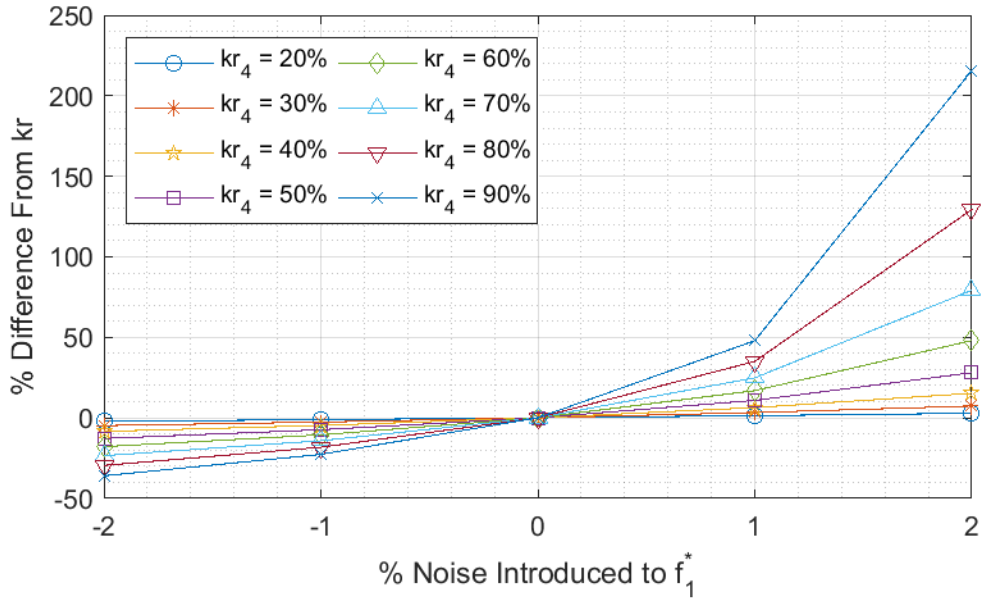
Figure 3-39 4-DOF: Noisy f_1^* and Different kr_4 Cases
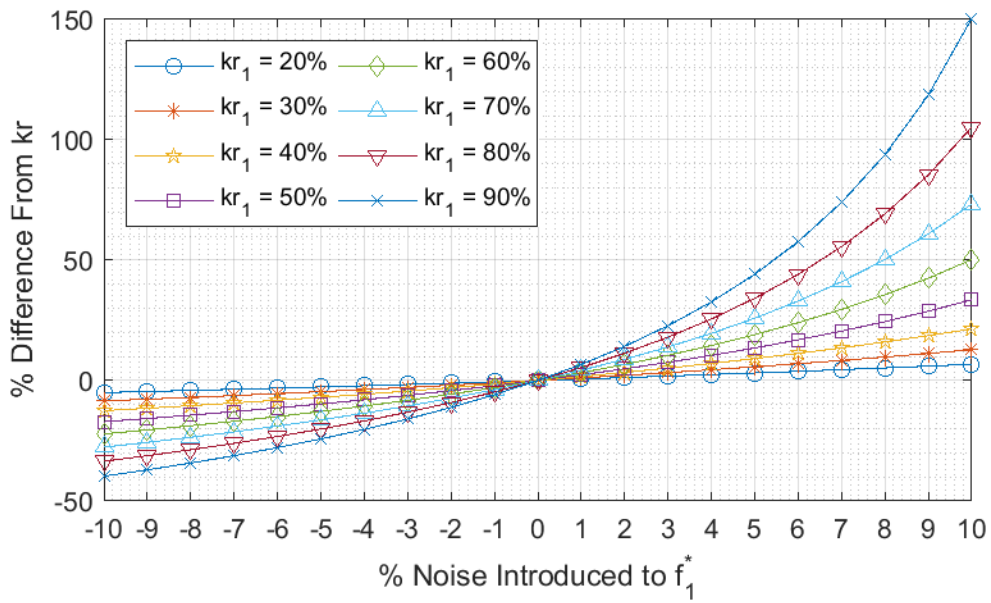
Figure 3-40 7-DOF: Noisy f_1^* and Different kr_1 Cases
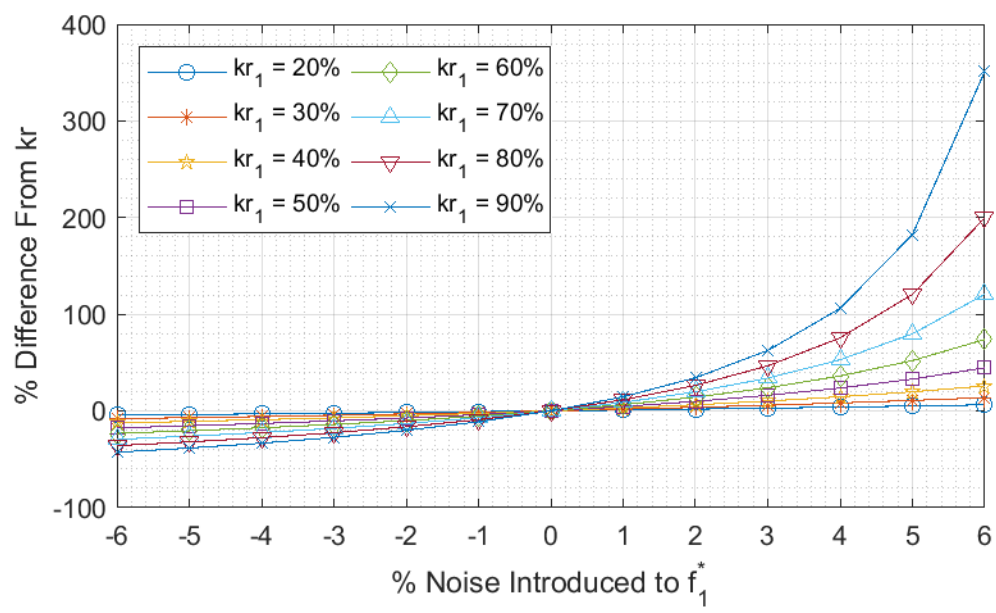
Figure 3-41 15-DOF: Noisy f_1^* and Different kr_1 Cases
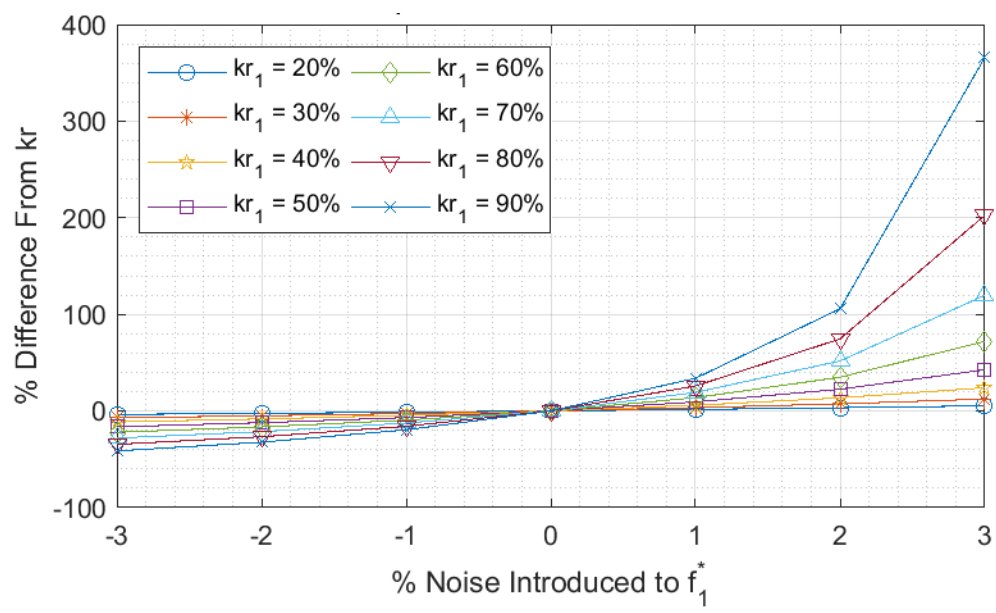
Figure 3-42 30-DOF: Noisy f_1^* and Different kr_1 Cases
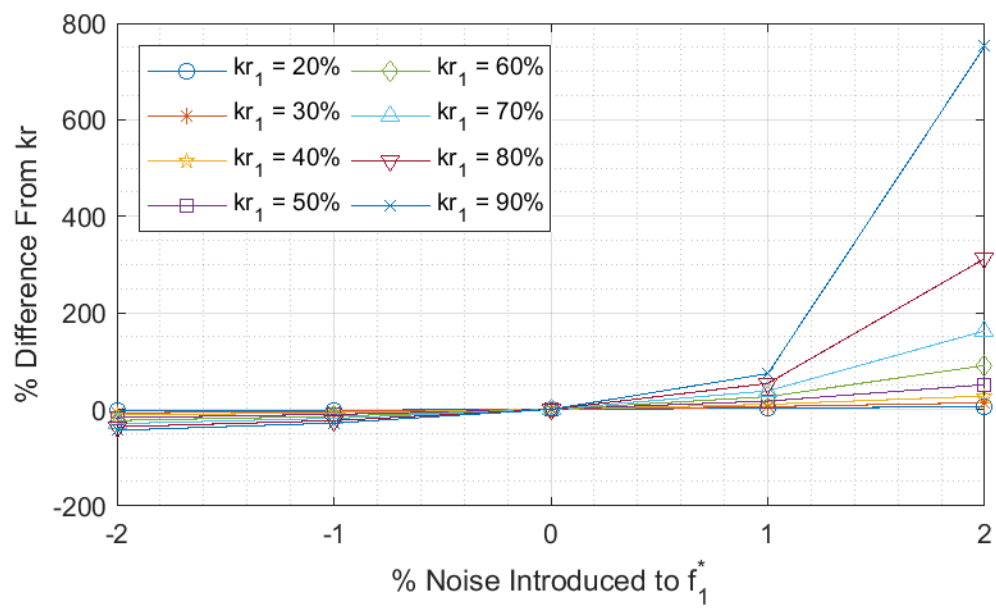
Figure 3-43 50-DOF: Noisy f_1^* and Different kr_1 Cases

Figure 4-1 Five-story Aluminum Model

Figure 4-2 Column and Plate Connections
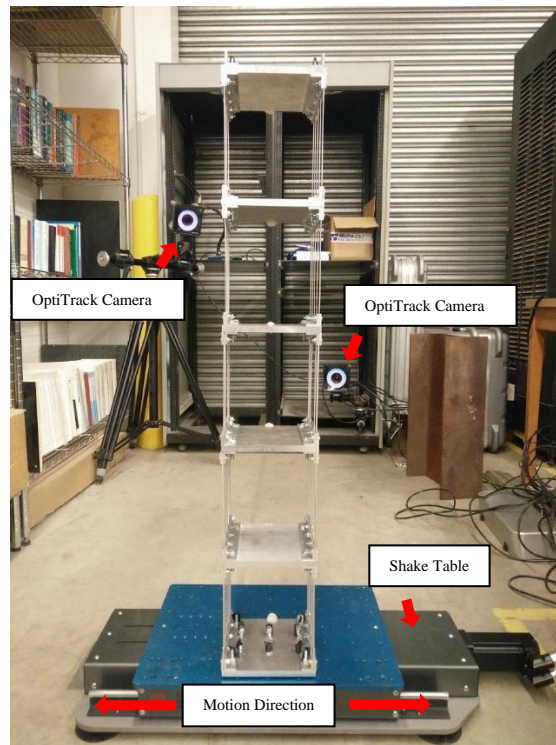
Figure 4-3 Test Setup (View 1)
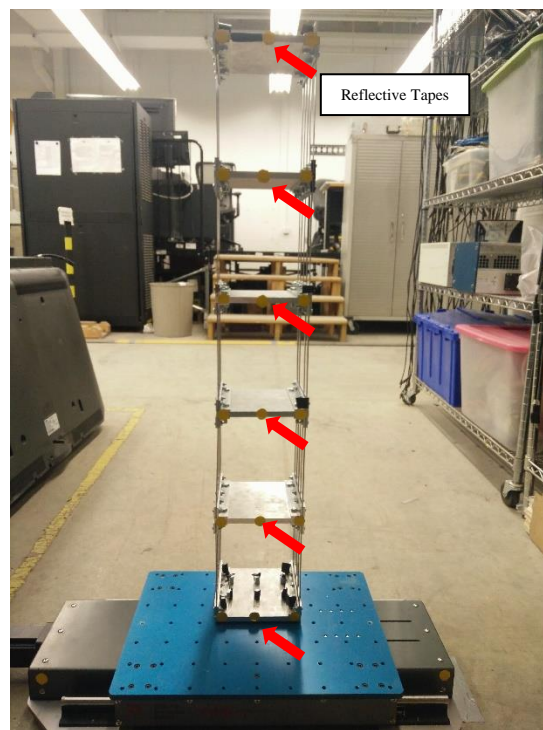
Figure 4-4 Test Setup (View 2)
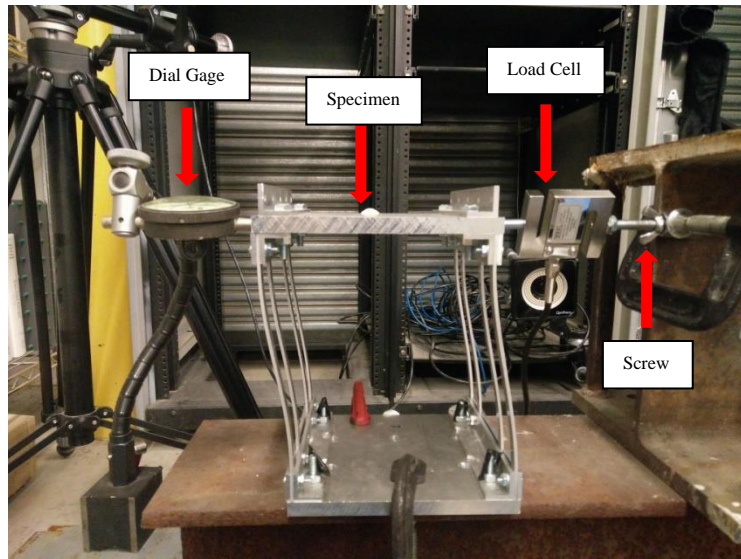
Figure 4-5 Individual Story Stiffness Test Setup (Front View)
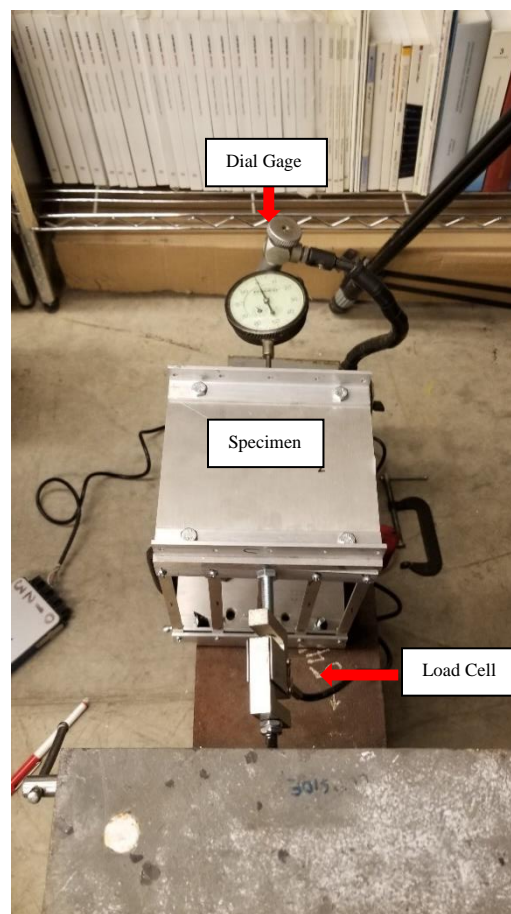
Figure 4-6 Individual Story Stiffness Test Setup (Top View)
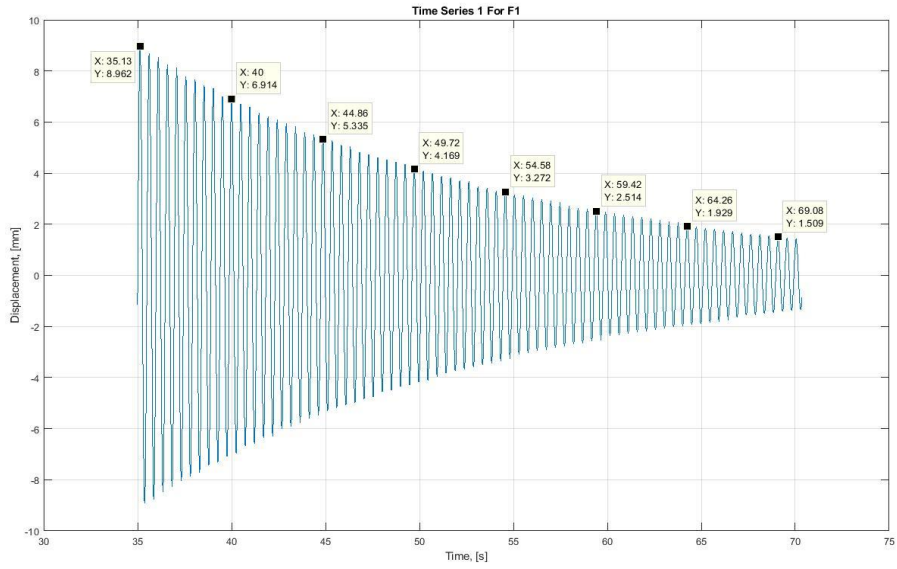
Figure 4-7 Free Vibration Signal for Mode 1 (Story 1)
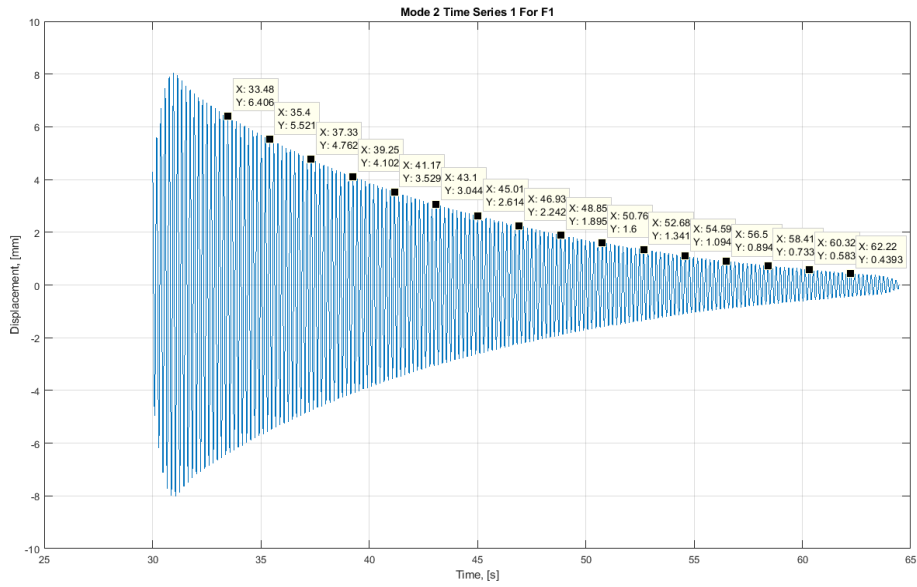
Figure 4-8 Filtered Free Vibration Signal for Mode 2 (Story 1)
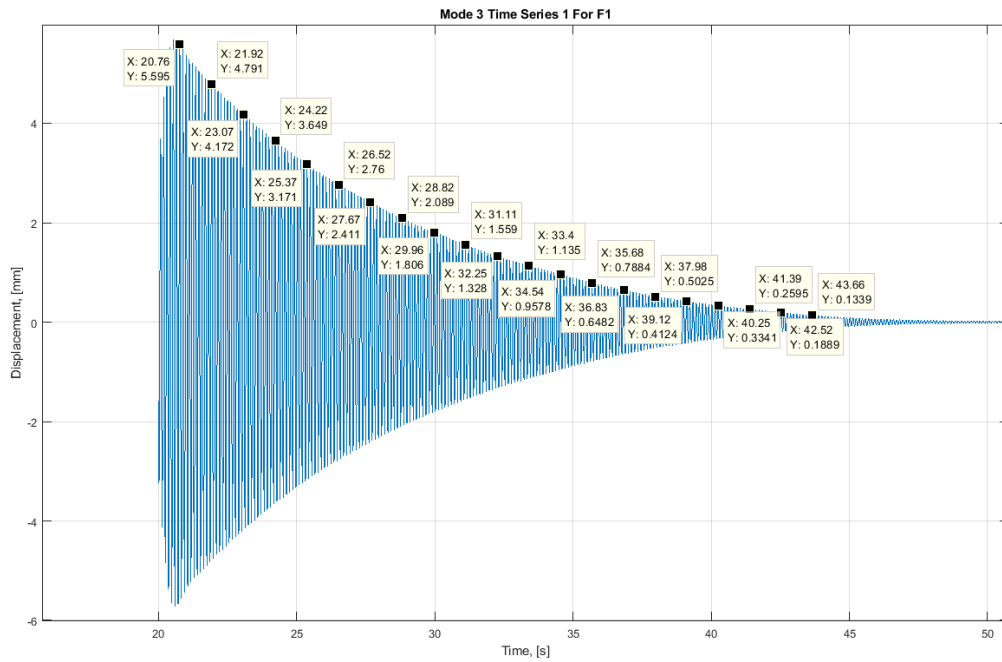
Figure 4-9 Filtered Free Vibration Signal for Mode 3 (Story 1)
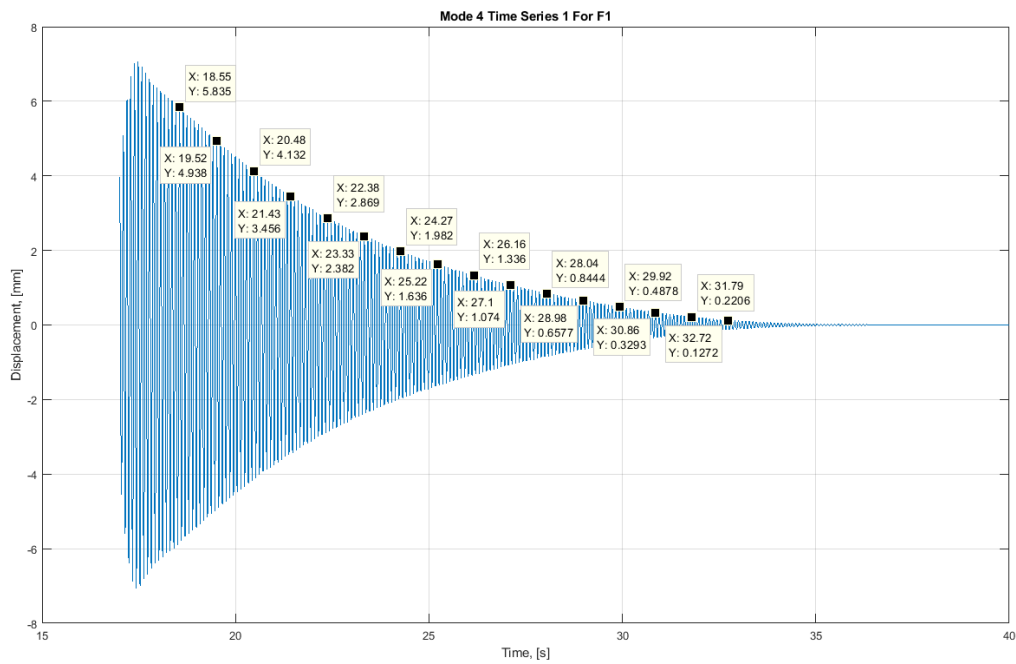
Figure 4-10 Filtered Free Vibration Signal for Mode 4 (Story 1)
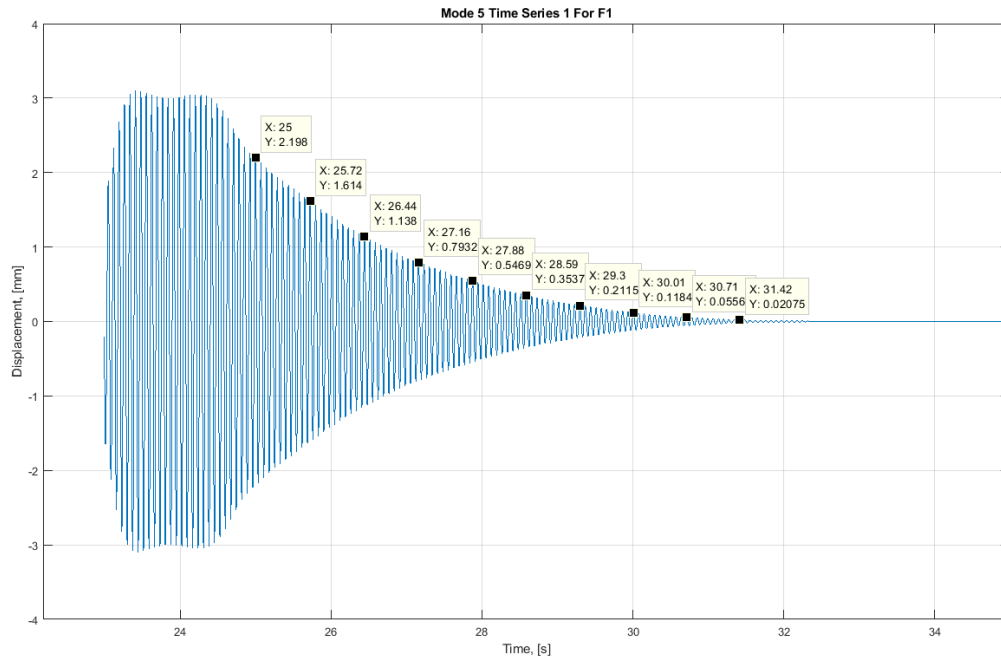
Figure 4-11 Filtered Free Vibration Signal for Mode 5 (Story 1)
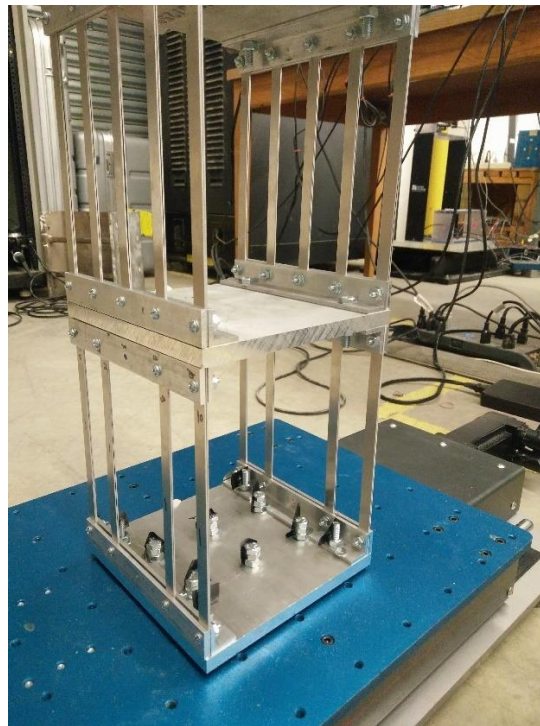
Figure 4-12 Experiment 1: Two Columns Removed from the First Story
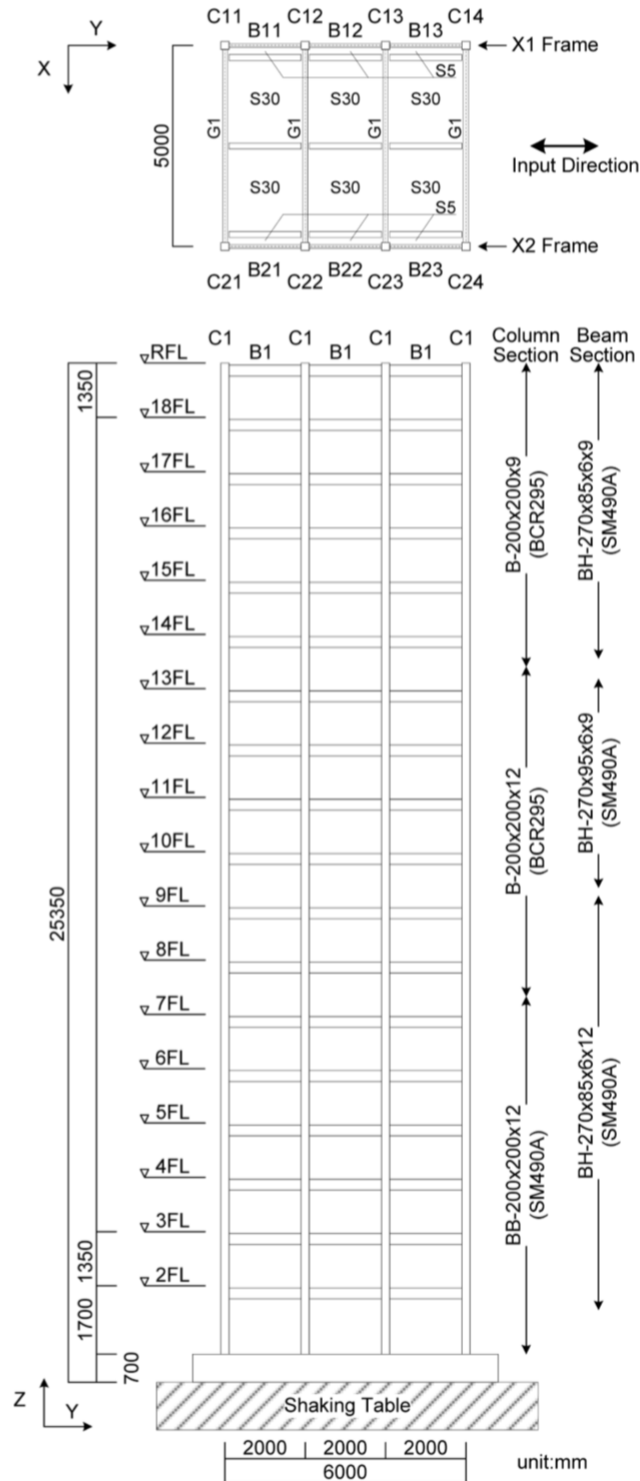
Figure 5-1 18-Story Steel Moment Frame Building Plan and Elevation (Suita et al., 2015)
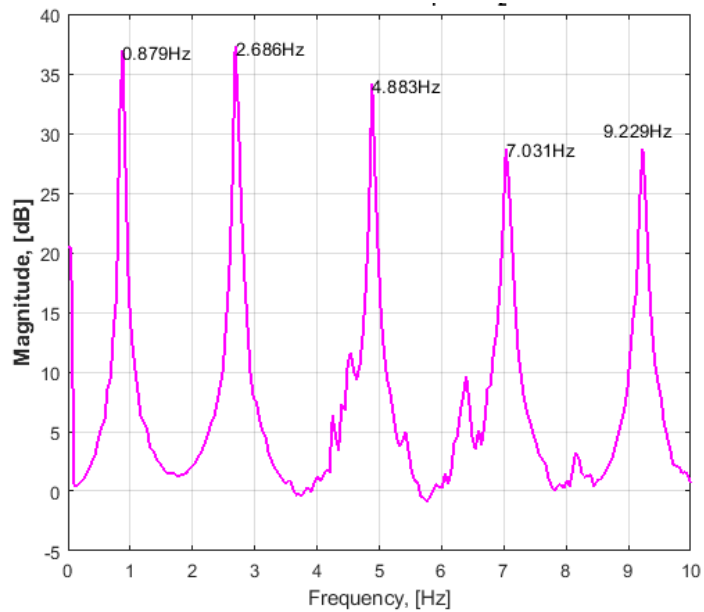
Figure 5-2 Transfer Function of the Average of the Responses of the Roof for 17cm/s Pseudo Velocity (Data from Suita et al., 2015)
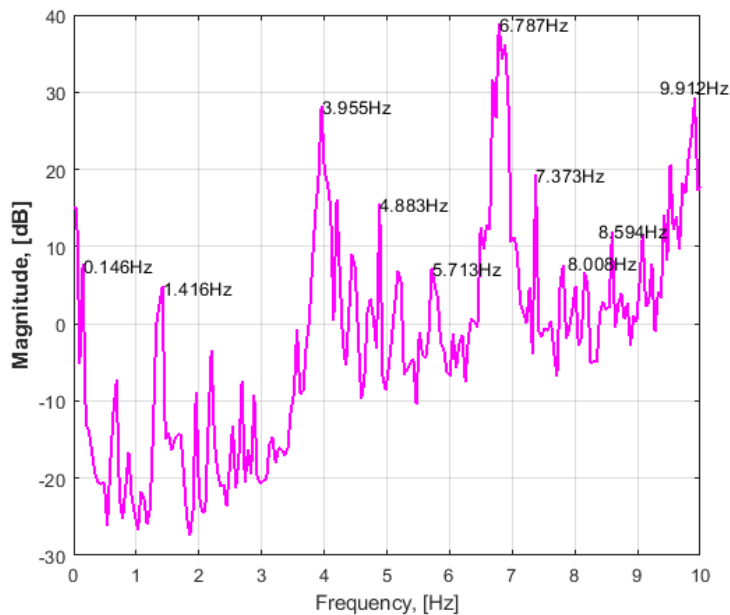
Figure 5-3 Transfer Function of Half Difference of Responses of the Roof for 17cm/s Pseudo Velocity (Data from Suita et al., 2015)
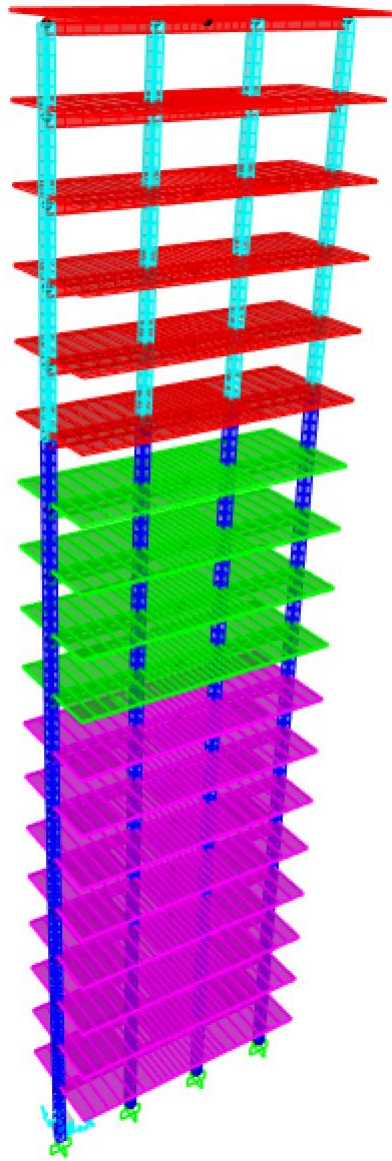
Figure 5-4 2D SAP2000 Model
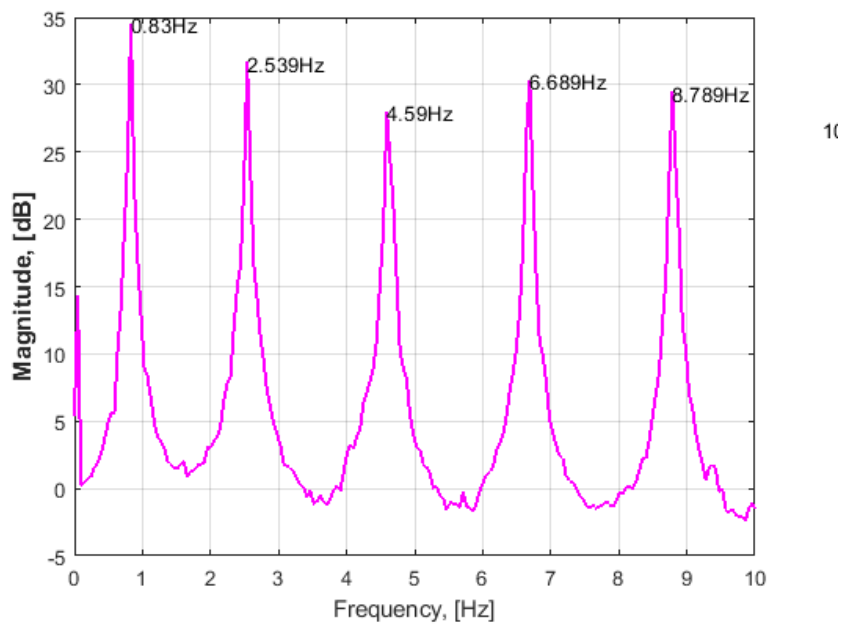
Figure 5-5 Transfer Function of the Average of the Responses of the Roof for 17cm/s Pseudo Velocity (Data from Suita et al., 2015)
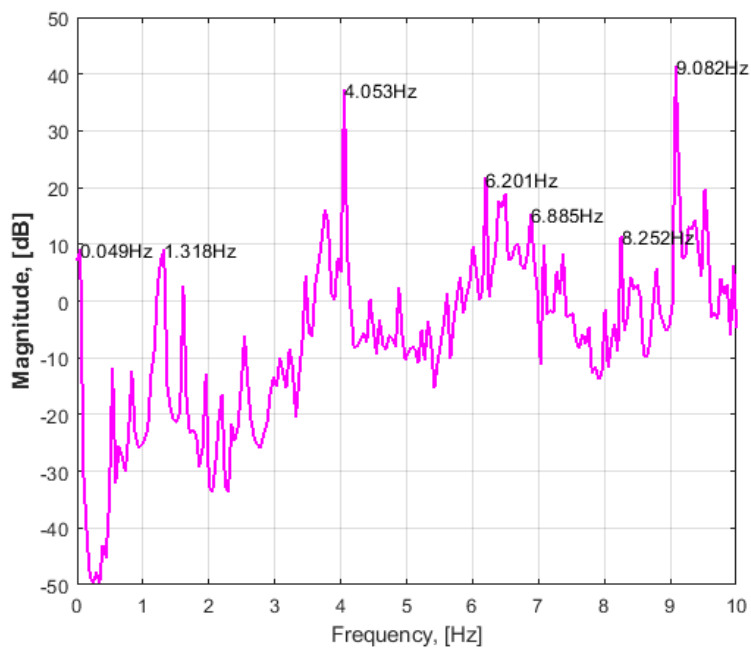
Figure 5-6 Transfer Function of Half Difference of Responses of the Roof for 17cm/s Pseudo Velocity (Data from Suita et al., 2015)

APPENDIX A. TWO-DEGREE-OF-FREEDOM SYSTEM EXAMPLE

For a two-degree-of-freedom system, it can be written as a linear combination of other matrices which have the coefficients as the stiffnesses.

$$A(m,k) = M^{-1}K = \begin{bmatrix} \dfrac{k_1}{m_1} + \dfrac{k_2}{m_1} & -\dfrac{k_2}{m_2} \\ -\dfrac{k_2}{m_1} & \dfrac{k_2}{m_2} \end{bmatrix} = k_1 \begin{bmatrix} \dfrac{1}{m_1} & 0 \\ 0 & 0 \end{bmatrix} + k_2 \begin{bmatrix} \dfrac{1}{m_1} & -\dfrac{1}{m_2} \\ -\dfrac{1}{m_1} & \dfrac{1}{m_2} \end{bmatrix}$$

Since masses are known, the parameters that need to be solved for are k_1 and k_2.

Let $m_1 = m_2 = 1$kg, and the given frequencies are $\omega_1 = 8.445$ rad/s and $\omega_2 = 21.182$ rad/s. Therefore, $\lambda_1 = \omega_1^2 = 71.318$ rad^2/s^2 and $\lambda_2 = \omega_2^2 = 448.677$ rad^2/s^2.

Step 1: Assign the initial value for stiffnesses

$$\text{Let } k^{(0)} = \begin{bmatrix} 200 \\ 200 \end{bmatrix} \text{N/m}$$

Step 2a: Determine $\left(A(k^{(p)}) - \lambda_i I\right)$

$$A(k^{(0)}) = M^{-1}K = \begin{bmatrix} \dfrac{1}{m_1} & 0 \\ 0 & \dfrac{1}{m_2} \end{bmatrix} \begin{bmatrix} k_1 + k_2 & -k_2 \\ -k_2 & k_2 \end{bmatrix} = \begin{bmatrix} \dfrac{k_1}{m_1} + \dfrac{k_2}{m_1} & -\dfrac{k_2}{m_2} \\ -\dfrac{k_2}{m_1} & \dfrac{k_2}{m_2} \end{bmatrix}$$

$$= \begin{bmatrix} 400 & -200 \\ -200 & 200 \end{bmatrix}$$

$$A(k^{(0)}) - \lambda_1 I = \begin{bmatrix} \dfrac{k_1}{m_1} + \dfrac{k_2}{m_1} - \lambda_1 & -\dfrac{k_2}{m_2} \\ -\dfrac{k_2}{m_1} & \dfrac{k_2}{m_2} - \lambda_1 \end{bmatrix} = \begin{bmatrix} 328.682 & -200 \\ -200 & 128.682 \end{bmatrix}$$

$$A(k^{(0)}) - \lambda_2 I = \begin{bmatrix} \dfrac{k_1}{m_1} + \dfrac{k_2}{m_1} - \lambda_2 & -\dfrac{k_2}{m_2} \\ -\dfrac{k_2}{m_1} & \dfrac{k_2}{m_2} - \lambda_2 \end{bmatrix} = \begin{bmatrix} -48.677 & -200 \\ -200 & -248.677 \end{bmatrix}$$

Step 2b: Determine $\left(A\left(k^{(p)}\right) - \lambda_i I\right)^{-1}$

$$\left(A\left(k^{(0)}\right) - \lambda_1 I\right)^{-1} = \begin{bmatrix} 328.682 & -200 \\ -200 & 128.682 \end{bmatrix}^{-1} = \begin{bmatrix} 0.056 & 0.087 \\ 0.087 & 0.143 \end{bmatrix}$$

$$\left(A\left(k^{(0)}\right) - \lambda_2 I\right)^{-1} = \begin{bmatrix} -48.677 & -200 \\ -200 & -248.677 \end{bmatrix}^{-1} = \begin{bmatrix} 0.009 & -0.007 \\ -0.007 & 0.002 \end{bmatrix}$$

Step 2c: Assemble the matrix $H\left(k^{(p)}\right)$

<u>Determine A_{ij}</u>

$$A_{11} = \frac{\partial (A(k) - \lambda_1 I)}{\partial k_1} = \begin{bmatrix} \dfrac{1}{m_1} & 0 \\ 0 & 0 \end{bmatrix} = \begin{bmatrix} 1 & 0 \\ 0 & 0 \end{bmatrix}$$

$$A_{12} = \frac{\partial (A(k) - \lambda_1 I)}{\partial k_2} = \begin{bmatrix} \dfrac{1}{m_1} & -\dfrac{1}{m_2} \\ -\dfrac{1}{m_1} & \dfrac{1}{m_2} \end{bmatrix} = \begin{bmatrix} 1 & -1 \\ -1 & 1 \end{bmatrix}$$

$$A_{21} = \frac{\partial (A(k) - \lambda_2 I)}{\partial k_1} = \begin{bmatrix} \dfrac{1}{m_1} & 0 \\ 0 & 0 \end{bmatrix} = \begin{bmatrix} 1 & 0 \\ 0 & 0 \end{bmatrix}$$

$$A_{22} = \frac{\partial (A(k) - \lambda_2 I)}{\partial k_2} = \begin{bmatrix} \dfrac{1}{m_1} & -\dfrac{1}{m_2} \\ -\dfrac{1}{m_1} & \dfrac{1}{m_2} \end{bmatrix} = \begin{bmatrix} 1 & -1 \\ -1 & 1 \end{bmatrix}$$

<u>Determine $H_{ij}^{(0)}$</u>

$$H_{11}^{(0)} = tr\left[\left(A\left(k^{(0)}\right) - \lambda_1 I\right)^{-1} \cdot A_{11}\right] = tr\left\{\begin{bmatrix} 0.056 & 0.087 \\ 0.087 & 0.143 \end{bmatrix}\begin{bmatrix} 1 & 0 \\ 0 & 0 \end{bmatrix}\right\} = tr\begin{bmatrix} -0.02 & 0 \\ -0.048 & 0 \end{bmatrix}$$

$$= 0.056$$

$$H_{12}^{(0)} = tr\left[\left(A\left(k^{(0)}\right) - \lambda_1 I\right)^{-1} \cdot A_{12}\right] = tr\left\{\begin{bmatrix} 0.056 & 0.087 \\ 0.087 & 0.143 \end{bmatrix}\begin{bmatrix} 1 & -1 \\ -1 & 1 \end{bmatrix}\right\}$$

$$= tr\begin{bmatrix} 0.028 & -0.028 \\ -0.044 & -0.044 \end{bmatrix} = 0.025$$

$$H_{21}^{(0)} = tr\left[\left(A\left(k^{(0)}\right) - \lambda_2 I\right)^{-1} \cdot A_{21}\right] = tr\left\{\begin{bmatrix} 0.009 & -0.007 \\ -0.007 & 0.002 \end{bmatrix}\begin{bmatrix} 1 & 0 \\ 0 & 0 \end{bmatrix}\right\}$$

$$= tr\begin{bmatrix} -0.02 & 0 \\ 0.008 & 0 \end{bmatrix} = 0.009$$

$$H_{22}^{(0)} = tr\left[\left(A(k^{(0)}) - \lambda_2 I\right)^{-1} \cdot A_{22}\right] = tr\left\{\begin{bmatrix} 0.009 & -0.007 \\ -0.007 & 0.002 \end{bmatrix}\begin{bmatrix} 1 & -1 \\ -1 & 1 \end{bmatrix}\right\}$$

$$= tr\begin{bmatrix} -0.028 & 0.028 \\ 0.016 & -0.016 \end{bmatrix} = 0.025$$

Construct $H(k^{(p)})$

$$H^{(0)} = \begin{bmatrix} H_{11}^{(0)} & H_{12}^{(0)} \\ H_{21}^{(0)} & H_{22}^{(0)} \end{bmatrix} = \begin{bmatrix} 0.056 & 0.025 \\ 0.009 & 0.025 \end{bmatrix}$$

Step 2d: Determine the next iteration $k^{(p+1)}$

$$k^{(1)} = k^{(0)} - \left[H^{(0)}\right]^{-1}\begin{bmatrix} 1 \\ 1 \end{bmatrix} = \begin{bmatrix} 200 \\ 200 \end{bmatrix} - \begin{bmatrix} 0.056 & 0.025 \\ 0.009 & 0.025 \end{bmatrix}^{-1}\begin{bmatrix} 1 \\ 1 \end{bmatrix} = \begin{bmatrix} 199.99 \\ 160 \end{bmatrix}$$

Step 2e/3:

For the first iteration, $k = \begin{bmatrix} 200 \\ 160 \end{bmatrix}$ N/m which also happens to be one of the solutions of the

problem. Nonetheless, if the solution has not converged, $k^{(1)}$ can be used for another iteration by

repeating the steps above. Another pair of solution which also produces the same frequency

response is $k = \begin{bmatrix} 320 \\ 100 \end{bmatrix}$ N/m. This solution can be found by choosing different initial

approximation.

APPENDIX B. MATHCAD ROUTINES FOR 4-DOF SYSTEM

B.1   Four Known Frequencies

If all the masses and frequencies are known, all four stiffnesses can be calculated directly.

Mass:	Frequencies:	Angular Frequencies:	Eigenvalues:
$m_1 := 1$	$f_1 := 2.233$	$\omega_1 := 2\pi \cdot f_1$	$\lambda_1 := \omega_1^2 = 196.851$
$m_2 := 1$	$f_2 := 6.634$	$\omega_2 := 2\pi \cdot f_2$	$\lambda_2 := \omega_2^2 = 1.737 \times 10^3$
$m_3 := 1$	$f_3 := 10.256$	$\omega_3 := 2\pi \cdot f_3$	$\lambda_3 := \omega_3^2 = 4.153 \times 10^3$
$m_4 := 1$	$f_4 := 12.666$	$\omega_4 := 2\pi \cdot f_4$	$\lambda_4 := \omega_4^2 = 6.333 \times 10^3$

Step 1: Initial Estimates for Stiffnesses

$$k_1 := 2000 \qquad k_2 := 2000 \qquad k_3 := 2000 \qquad k_4 := 2000$$

$$Km := \begin{pmatrix} k_1 \\ k_2 \\ k_3 \\ k_4 \end{pmatrix} \qquad \text{In vector form}$$

Step 2a:

$$i := 1 .. 4$$

$$B_i := \begin{pmatrix} \dfrac{k_1 + k_2}{m_1} - \lambda_i & -\dfrac{k_2}{m_2} & 0 & 0 \\[2ex] -\dfrac{k_2}{m_1} & \dfrac{k_2 + k_3}{m_2} - \lambda_i & -\dfrac{k_3}{m_3} & 0 \\[2ex] 0 & -\dfrac{k_3}{m_2} & \dfrac{k_3 + k_4}{m_3} - \lambda_i & -\dfrac{k_4}{m_4} \\[2ex] 0 & 0 & -\dfrac{k_4}{m_3} & \dfrac{k_4}{m_4} - \lambda_i \end{pmatrix}$$

Step 2b:

$IB_i := (B_i)^{-1}$

Step 2c:

Take partial derivative of B_i with respect to k_1

$$dB_{i,1} := \begin{pmatrix} \dfrac{1}{m_1} & 0 & 0 & 0 \\ 0 & 0 & 0 & 0 \\ 0 & 0 & 0 & 0 \\ 0 & 0 & 0 & 0 \end{pmatrix}$$

Take partial derivative of B_i with respect to k_2

$$dB_{i,2} := \begin{pmatrix} \dfrac{1}{m_1} & \dfrac{-1}{m_2} & 0 & 0 \\ \dfrac{-1}{m_1} & \dfrac{1}{m_2} & 0 & 0 \\ 0 & 0 & 0 & 0 \\ 0 & 0 & 0 & 0 \end{pmatrix}$$

Take partial derivative of B_i with respect to k_3

$$dB_{i,3} := \begin{pmatrix} 0 & 0 & 0 & 0 \\ 0 & \dfrac{1}{m_2} & \dfrac{-1}{m_3} & 0 \\ 0 & \dfrac{-1}{m_2} & \dfrac{1}{m_3} & 0 \\ 0 & 0 & 0 & 0 \end{pmatrix}$$

Take partial derivative of B_i with respect to k_4

$$dB_{i,4} := \begin{pmatrix} 0 & 0 & 0 & 0 \\ 0 & 0 & 0 & 0 \\ 0 & 0 & \dfrac{1}{m_3} & \dfrac{-1}{m_4} \\ 0 & 0 & \dfrac{-1}{m_3} & \dfrac{1}{m_4} \end{pmatrix}$$

$j := 1 .. 4$

$nH_{i,j} := IB_i \cdot dB_{i,j}$

$$Hm_{i,j} := \sum_{k=1}^{4} \left(nH_{i,j}\right)_{k,k}$$

$$Hm = \begin{pmatrix} 1.479 \times 10^{-3} & 1.251 \times 10^{-3} & 9.328 \times 10^{-4} & 6.456 \times 10^{-4} \\ 1.415 \times 10^{-3} & 4.587 \times 10^{-4} & 1.582 \times 10^{-3} & 1.729 \times 10^{-3} \\ 6.902 \times 10^{-4} & 1.838 \times 10^{-3} & 5.875 \times 10^{-4} & 1.933 \times 10^{-3} \\ -9.718 \times 10^{-5} & 1.127 \times 10^{-3} & 1.928 \times 10^{-3} & 1.923 \times 10^{-4} \end{pmatrix}$$

Step 2d:

$$dk := -Hm^{-1} \cdot \begin{pmatrix} 1 \\ 1 \\ 1 \\ 1 \end{pmatrix} = \begin{pmatrix} -171.523 \\ -323.607 \\ -333.359 \\ -47.133 \end{pmatrix}$$

$$Km := Km + dk = \begin{pmatrix} 1.828 \times 10^3 \\ 1.676 \times 10^3 \\ 1.667 \times 10^3 \\ 1.953 \times 10^3 \end{pmatrix} \quad \text{New stiffness vector}$$

Next Iteration:

$$k_1 := Km_1 \quad k_2 := Km_2 \quad k_3 := Km_3 \quad k_4 := Km_4$$

$$Km := \begin{pmatrix} k_1 \\ k_2 \\ k_3 \\ k_4 \end{pmatrix}$$

The new stiffness vector above can be used to iterate for new solution following the same steps until convergence.

B.2   Three Known Frequencies

Since only 3 frequencies are known, 1 stiffness is assumed known. The three known frequencies and masses are used to determine what the other three stiffness are.

Mass:	Frequencies:	Stiffnesses:
$m_1 := 1$	$f_1 := 2.233$	$k_4 := 2000$
$m_2 := 1$	$f_2 := 6.634$	
$m_3 := 1$	$f_3 := 10.256$	
$m_4 := 1$		

Angular Frequencies:

$\omega_1 := 2\pi \cdot f_1$

$\omega_2 := 2\pi \cdot f_2$

$\omega_3 := 2 \cdot \pi \cdot f_3$

Eigenvalues:

$$\lambda_1 := \omega_1{}^2 = 196.851$$

$$\lambda_2 := \omega_2{}^2 = 1.737 \times 10^3$$

$$\lambda_3 := \omega_3{}^2 = 4.153 \times 10^3$$

Step 1: Initial Estimates for Stiffness and Eigenvalues

$k_1 := 2000$ $k_2 := 2000$ $k_3 := 2000$ $\lambda_4 := 8 \cdot 10^3$

$$Km := \begin{pmatrix} k_1 \\ k_2 \\ k_3 \\ \lambda_4 \end{pmatrix} \quad \text{In vector form}$$

Step 2a:

$i := 1 .. 4$

$$B_i := \begin{pmatrix} \dfrac{k_1 + k_2}{m_1} - \lambda_i & -\dfrac{k_2}{m_2} & 0 & 0 \\[2em] -\dfrac{k_2}{m_1} & \dfrac{k_2 + k_3}{m_2} - \lambda_i & -\dfrac{k_3}{m_3} & 0 \\[2em] 0 & -\dfrac{k_3}{m_2} & \dfrac{k_3 + k_4}{m_3} - \lambda_i & -\dfrac{k_4}{m_4} \\[2em] 0 & 0 & -\dfrac{k_4}{m_3} & \dfrac{k_4}{m_4} - \lambda_i \end{pmatrix}$$

Step 2b:

$IB_i := \left(B_i\right)^{-1}$

Step 2c:

Take partial derivative of B_i with respect to k_1

$$dB_{i,1} := \begin{pmatrix} \dfrac{1}{m_1} & 0 & 0 & 0 \\[1em] 0 & 0 & 0 & 0 \\[0.5em] 0 & 0 & 0 & 0 \\[0.5em] 0 & 0 & 0 & 0 \end{pmatrix}$$

This matrix will be different depending what the assumed unknown stiffness are. In this case, k_1 k_2 and k_3 are assumed unknown.

Take partial derivative of B_i with respect to k_2

$$dB_{i,2} := \begin{pmatrix} \dfrac{1}{m_1} & \dfrac{-1}{m_2} & 0 & 0 \\[1em] \dfrac{-1}{m_1} & \dfrac{1}{m_2} & 0 & 0 \\[1em] 0 & 0 & 0 & 0 \\[0.5em] 0 & 0 & 0 & 0 \end{pmatrix}$$

Take partial derivative of B_i with respect to k_3

$$dB_{i,3} := \begin{pmatrix} 0 & 0 & 0 & 0 \\ 0 & \dfrac{1}{m_2} & \dfrac{-1}{m_3} & 0 \\ 0 & \dfrac{-1}{m_2} & \dfrac{1}{m_3} & 0 \\ 0 & 0 & 0 & 0 \end{pmatrix}$$

Take partial derivative of B_i with with respect to λ_4

$$dB_{i,4} := \begin{pmatrix} 0 & 0 & 0 & 0 \\ 0 & 0 & 0 & 0 \\ 0 & 0 & 0 & 0 \\ 0 & 0 & 0 & 0 \end{pmatrix} \qquad dB_{4,4} := \begin{pmatrix} -1 & 0 & 0 & 0 \\ 0 & -1 & 0 & 0 \\ 0 & 0 & -1 & 0 \\ 0 & 0 & 0 & -1 \end{pmatrix}$$

$j := 1 .. 4$

$nH_{i,j} := IB_i \cdot dB_{i,j}$

$$Hm_{i,j} := \sum_{k=1}^{4} \left(nH_{i,j}\right)_{k,k}$$

$$Hm = \begin{pmatrix} 1.479 \times 10^{-3} & 1.251 \times 10^{-3} & 9.328 \times 10^{-4} & 0 \\ 1.415 \times 10^{-3} & 4.587 \times 10^{-4} & 1.582 \times 10^{-3} & 0 \\ 6.902 \times 10^{-4} & 1.838 \times 10^{-3} & 5.875 \times 10^{-4} & 0 \\ -3.889 \times 10^{-4} & -1.5 \times 10^{-3} & -1.722 \times 10^{-3} & 1.667 \times 10^{-3} \end{pmatrix}$$

$$dk := -Hm^{-1} \cdot \begin{pmatrix} 1 \\ 1 \\ 1 \\ 1 \end{pmatrix} = \begin{pmatrix} -73.98 \\ -369.724 \\ -458.769 \\ -1.424 \times 10^3 \end{pmatrix}$$

$$Km := Km + dk = \begin{pmatrix} 1.926 \times 10^3 \\ 1.63 \times 10^3 \\ 1.541 \times 10^3 \\ 6.576 \times 10^3 \end{pmatrix}$$

Next Iteration:

$$k_1 := Km_1 \qquad\qquad k_2 := Km_2 \qquad\qquad k_3 := Km_3 \qquad\qquad \lambda_4 := Km_4$$

$$Km := \begin{pmatrix} k_1 \\ k_2 \\ k_3 \\ \lambda_4 \end{pmatrix}$$

The new stiffness and eigenvalue vector above can be used to iterate for new solution following the same steps until convergence.

B.3   Two Known Frequencies

Since only 2 frequencies are known, 2 stiffnesses are assumed known. The two known frequencies and masses are used to determine what the other two stiffness are.

Mass: Frequencies: Stiffnesses:

$m_1 := 1$ $f_1 := 2.23\varepsilon$ $k_3 := 200C$

                     $f_2 := 6.63\varepsilon$ $k_4 := 200C$

$m_2 := 1$ Eigenvalues:

                     Angular Frequencies:

$m_3 := 1$ $\omega_1 := 2 \cdot \pi \cdot f_1$ $\lambda_1 := \omega_1^2 = 196.851$

$m_4 := 1$ $\omega_2 := 2 \cdot \pi \cdot f_2$ $\lambda_2 := \omega_2^2 = 1.737 \times 10^3$

Step 1: Initial Estimates for Stiffness and Eigenvalues

$k_1 := 200C$ $k_2 := 200C$ $\lambda_3 := 4 \cdot 10^3$ $\lambda_4 := 8 \cdot 10^3$

$$Km := \begin{pmatrix} k_1 \\ k_2 \\ \lambda_3 \\ \lambda_4 \end{pmatrix}$$ In vector form

Step 2a:

$i := 1..4$

$$B_i := \begin{pmatrix} \dfrac{k_1 + k_2}{m_1} - \lambda_i & -\dfrac{k_2}{m_2} & 0 & 0 \\[3ex] -\dfrac{k_2}{m_1} & \dfrac{k_2 + k_3}{m_2} - \lambda_i & -\dfrac{k_3}{m_3} & 0 \\[3ex] 0 & -\dfrac{k_3}{m_2} & \dfrac{k_3 + k_4}{m_3} - \lambda_i & -\dfrac{k_4}{m_4} \\[3ex] 0 & 0 & -\dfrac{k_4}{m_3} & \dfrac{k_4}{m_4} - \lambda_i \end{pmatrix}$$

Step 2b:

$$IB_i := \left(B_i\right)^{-1}$$

Step 2c:

Take partial derivative of B_i with respect to k_1

$$dB_{i,1} := \begin{pmatrix} \dfrac{1}{m_1} & 0 & 0 & 0 \\ 0 & 0 & 0 & 0 \\ 0 & 0 & 0 & 0 \\ 0 & 0 & 0 & 0 \end{pmatrix}$$

This matrix will be different depending what the assumed unknown stiffness are. In this case, k_1 and k_2 are assumed unknown.

Take partial derivative of B_i with respect to k_2

$$dB_{i,2} := \begin{pmatrix} \dfrac{1}{m_1} & \dfrac{-1}{m_2} & 0 & 0 \\ \dfrac{-1}{m_1} & \dfrac{1}{m_2} & 0 & 0 \\ 0 & 0 & 0 & 0 \\ 0 & 0 & 0 & 0 \end{pmatrix}$$

This matrix will be different depending what the assumed unknown stiffness are. In this case, k_1 and k_2 are assumed unknown.

Take partial derivative of B_i with with respect to λ_3

$$dB_{i,3} := \begin{pmatrix} 0 & 0 & 0 & 0 \\ 0 & 0 & 0 & 0 \\ 0 & 0 & 0 & 0 \\ 0 & 0 & 0 & 0 \end{pmatrix} \qquad dB_{3,3} := \begin{pmatrix} -1 & 0 & 0 & 0 \\ 0 & -1 & 0 & 0 \\ 0 & 0 & -1 & 0 \\ 0 & 0 & 0 & -1 \end{pmatrix}$$

Take partial derivative of B_i with with respect to λ_4

$$dB_{i,4} := \begin{pmatrix} 0 & 0 & 0 & 0 \\ 0 & 0 & 0 & 0 \\ 0 & 0 & 0 & 0 \\ 0 & 0 & 0 & 0 \end{pmatrix} \qquad dB_{4,4} := \begin{pmatrix} -1 & 0 & 0 & 0 \\ 0 & -1 & 0 & 0 \\ 0 & 0 & -1 & 0 \\ 0 & 0 & 0 & -1 \end{pmatrix}$$

$$j := 1 .. 4$$

$$nH_{i,j} := IB_i \cdot dB_{i,j}$$

$$Hm_{i,j} := \sum_{k=1}^{4} \left(nH_{i,j}\right)_{k,k}$$

$$\text{Hm} = \begin{pmatrix} 1.479\times 10^{-3} & 1.251\times 10^{-3} & 0 & 0 \\ 1.415\times 10^{-3} & 4.587\times 10^{-4} & 0 & 0 \\ 5\times 10^{-4} & 1.5\times 10^{-3} & -1\times 10^{-3} & 0 \\ -3.889\times 10^{-4} & -1.5\times 10^{-3} & 0 & 1.667\times 10^{-3} \end{pmatrix}$$

$$\text{dk} := -\text{Hm}^{-1}\cdot\begin{pmatrix} 1 \\ 1 \\ 1 \\ 1 \end{pmatrix} = \begin{pmatrix} -725.648 \\ 58.493 \\ 724.916 \\ -716.674 \end{pmatrix}$$

$$\text{Km} := \text{Km} + \text{dk} = \begin{pmatrix} 1.274\times 10^{3} \\ 2.058\times 10^{3} \\ 4.725\times 10^{3} \\ 7.283\times 10^{3} \end{pmatrix}$$

Next Iteration:

$$k_1 := \text{Km}_1 \qquad k_2 := \text{Km}_2 \qquad \lambda_3 := \text{Km}_3 \qquad \lambda_4 := \text{Km}_4$$

$$\text{Km} := \begin{pmatrix} k_1 \\ k_2 \\ \lambda_3 \\ \lambda_4 \end{pmatrix}$$

The new stiffness and eigenvalue vector above can be used to iterate for new solution following the same steps until convergence.

B.4   One Known Frequency

Since only 1 frequency is known, 3 stiffnesses are assumed known. The one known frequency and masses are used to determine what the missing stiffness is.

Mass: Frequencies: Stiffnesses:

$m_1 := 1$ $f_1 := 2.23\vdots$ $k_2 := 2000$

$m_2 := 1$ Angular Frequencies: $k_3 := 2000$

$m_3 := 1$ $\omega_1 := 2 \cdot \pi \cdot f_1$ $k_4 := 2000$

$m_4 := 1$ Eigenvalues: $\lambda_1 := \omega_1^2 = 196.851$

Step 1: Initial Estimates for Stiffness and Eigenvalues

$k_1 := 2000$ $\lambda_2 := 2.5 \cdot 10^3$ $\lambda_3 := 4 \cdot 10^3$ $\lambda_4 := 8 \cdot 10^3$

$$Km := \begin{pmatrix} k_1 \\ \lambda_2 \\ \lambda_3 \\ \lambda_4 \end{pmatrix}$$ In vector form

Step 2a:

$i := 1..4$

$$B_i := \begin{pmatrix} \dfrac{k_1 + k_2}{m_1} - \lambda_i & -\dfrac{k_2}{m_2} & 0 & 0 \\[2ex] -\dfrac{k_2}{m_1} & \dfrac{k_2 + k_3}{m_2} - \lambda_i & -\dfrac{k_3}{m_3} & 0 \\[2ex] 0 & -\dfrac{k_3}{m_2} & \dfrac{k_3 + k_4}{m_3} - \lambda_i & -\dfrac{k_4}{m_4} \\[2ex] 0 & 0 & -\dfrac{k_4}{m_3} & \dfrac{k_4}{m_4} - \lambda_i \end{pmatrix}$$

Step 2b:

$IB_i := \left(B_i \right)^{-1}$

Step 2c:

Take partial derivative of B_i with respect to k_1

$$dB_{i,1} := \begin{pmatrix} \dfrac{1}{m_1} & 0 & 0 & 0 \\ 0 & 0 & 0 & 0 \\ 0 & 0 & 0 & 0 \\ 0 & 0 & 0 & 0 \end{pmatrix}$$

This matrix will be different depending what the assumed unknown stiffness is. In this case, k_1 is assumed unknown.

Take partial derivative of B_i with with respect to λ_2

$$dB_{i,2} := \begin{pmatrix} 0 & 0 & 0 & 0 \\ 0 & 0 & 0 & 0 \\ 0 & 0 & 0 & 0 \\ 0 & 0 & 0 & 0 \end{pmatrix} \qquad dB_{2,2} := \begin{pmatrix} -1 & 0 & 0 & 0 \\ 0 & -1 & 0 & 0 \\ 0 & 0 & -1 & 0 \\ 0 & 0 & 0 & -1 \end{pmatrix}$$

Take partial derivative of B_i with with respect to λ_3

$$dB_{i,3} := \begin{pmatrix} 0 & 0 & 0 & 0 \\ 0 & 0 & 0 & 0 \\ 0 & 0 & 0 & 0 \\ 0 & 0 & 0 & 0 \end{pmatrix} \qquad dB_{3,3} := \begin{pmatrix} -1 & 0 & 0 & 0 \\ 0 & -1 & 0 & 0 \\ 0 & 0 & -1 & 0 \\ 0 & 0 & 0 & -1 \end{pmatrix}$$

Take partial derivative of B_i with with respect to λ_4

$$dB_{i,4} := \begin{pmatrix} 0 & 0 & 0 & 0 \\ 0 & 0 & 0 & 0 \\ 0 & 0 & 0 & 0 \\ 0 & 0 & 0 & 0 \end{pmatrix} \qquad dB_{4,4} := \begin{pmatrix} -1 & 0 & 0 & 0 \\ 0 & -1 & 0 & 0 \\ 0 & 0 & -1 & 0 \\ 0 & 0 & 0 & -1 \end{pmatrix}$$

$j := 1..4$

$nH_{i,j} := IB_i \cdot dB_{i,j}$

$$Hm_{i,j} := \sum_{k=1}^{4} \left(nH_{i,j} \right)_{k,k}$$

$$Hm = \begin{pmatrix} 1.479 \times 10^{-3} & 0 & 0 & 0 \\ -4.53 \times 10^{-4} & 1.768 \times 10^{-3} & 0 & 0 \\ 5 \times 10^{-4} & 0 & -1 \times 10^{-3} & 0 \\ -3.889 \times 10^{-4} & 0 & 0 & 1.667 \times 10^{-3} \end{pmatrix}$$

APPENDIX C. EQUIPMENT AND CALIBRATION

C.1   Equipment List

C.1.1   Length and Displacement

- Full Jeweled Miracle Movement Dial Gage (Figure C-1)
  - Manufacturer: Federal
  - Precision: 0.001 in
  - Full scale Value: 1 in
- OptiTrack's Cameras

  Two OptiTrack's Prime 41 cameras were used. Each camera frame rate can be adjusted between 30 frames per second to 180 frames per seconds. The experiment setup, nevertheless, allowed the displacement data to be taken at 250 Hz with 0.001 mm precision. Detailed specifications can be found on the manufacturer's website. Motive 2.1 by OptiTrack software was used to operate and acquire the data from cameras. The systems were manufactured by NaturalPoint, Inc.
- Trimos LVDT
  - Manufacturer: Fowler High
  - Type: V1004+
  - Serial number: 10473/A
  - Precision: 0.001 mm
- Dial Caliper (Figure C-2)
  - Manufacturer: Pittsburgh
  - Precision: 0.0005 in
  - Full scale value: 6 in

C.1.2   Force

- S-Type Load Cell (Figure C-6 and Figure C-7 respectively)
  - Manufacturer: CALT, China

- o Model: DYLY-103
- o Serial number: 20180321
- o Output: 2.0 mV/V
- o Full Scale Value: 5 kg

C.1.2 Mass

- Ohaus SP6000 Scale
  - o Manufacturer: Ohaus
  - o Model: SP6000
  - o Precision: 0.1 g
  - o Full Scale Value: 6000 g

C.1.2 Seismic Simulator

- Table Top Earthquake System
  - o Manufacturer: MTS
  - o Frequency Range: 0.1 - 20 Hz
  - o Acceleration: ± 1 g (with 25 lb specimen)

The shake table was manufactured by MTS and controlled by a console called Table Top Earthquake System (Figure C-3). The console allows for sinusoidal or preloaded earthquake inputs. For a sinusoidal input, the frequency can be adjusted to a precision of 0.01 Hz. The amplitude can be controlled from 0% to 100% of ±3.2 inches for both sinusoidal and earthquake inputs. The specification of the model was shown in Table C-2.

C.2 Data Acquisition System

The load cell was connected to NI (National Instruments) 9219 Input Module, which in turn connected to cDAQ-9171. The details for both devices are shown in Table C-3, while the photos in Figure C-4 and Figure C-5. Full Wheatstone Bridge for the load cell with the internal excitation voltage of 2.5V provided by NI 9219. NI DAQExpress 3.0 Software was used obtain the output voltage, which translates to force by using the sensitivity from the calibration.

For the displacement, Motive 2.1 by OptiTrack software was used. The data were exported to CVS (Comma Separated Value) files for further processing. Other measured data were obtained manually with the either writing down the values or type in the spreadsheet.

C.3   Calibration

C.3.1   Load Cell Calibration

Before using the load cell in the experiment, it needs to be calibrated to determine its sensitivity and accuracy. Sensitivity of a sensor is the relationship between the output of the sensor, usually voltage, to the input of the sensor such as force, displacement, temperature, etc. Accuracy is the ratio of the maximum error to the maximum input value.

To calibrate the load cell, a static compressive or tensile force must be applied to the load cell. The voltage output is then recorded. The applied loads along with the corresponding voltage were shown in Table C-4 with the graph shown in Figure C-7. From the calibration data, the sensitivity was determined to be -0.0163 mV/V/N with an accuracy of 0.21%.

C.3.2   System Calibration

OptiTrack requires at least two cameras for triangulation. Prior to testing, the cameras must be first calibrated. The measured displacements also must be compared to another accurate displacement sensor to check whether the data from the cameras are acceptable to use.

To calibrate the cameras, the Trimos LVDT with 0.001mm precision was used. It measures vertical displacements, by moving the lever up and down on the side of the LVDT. A small circle was cut from a reflective tape and placed on the lever such that when it moves, the camera will be able to track it. Before the calibration, the camera lenses and exposure are adjusted such that only the reflective surfaces are visible to the camera. The calibration set up can be seen in Figure C-9.

Camera calibration is a two-step process. First, the two cameras were calibrated using the calibration wand provided by OptiTrack. The calibration wand features three reflective spheres set at a precise distance of 500 mm and 250 mm. The wand was slowly and methodically waved throughout the field of view. The second step defines the ground plane. An L-shaped wand with three reflective surfaces is laid down on the ground surface that defines the capture space. Once it is defined and calibrated, the cameras can triangulate where the reflective surface is relative to both cameras and calculate an average error. After the calibration process, the mean error was calculated to be 0.0370 mm.

Once the cameras have been calibrated, the accuracy of the OptiTrack measurements can be determined with the Trimos LVDT. The lever on the LVDT was moved up and down while the cameras followed the position of the reflective circle. The results are shown in Table C-5. The prescribed displacements are the displacements by the LVDT. Measured displacement refers to the displacements measured by the OptiTrack's cameras. The relative error was calculated at each displacement step. From the table, the maximum error was 0.101 mm while the average absolute error was 0.037 mm. This value is the same as the one given by the Motive software.

Table C-1 Model Elements' Properties

Element	Materials	Dimensions (in)
Thick Column Plate	6061 Aluminum Sheet (6061ASHT040)	0.375(W)x7(L)x0.04(T)
Thin Column Plate	6061 Aluminum Sheet (6061ASHT032)	0.375(W) x7(L)x0.032(T)
Floor Plate	6061 Aluminum Plate (6061ASH375)	6(W)x6 (L)x.375(T)
Connection Angle	6061 Aluminum Structural Angle Equal Leg	6(L)x3/4(W1) x3/4 (W2) x1/8(T)
Connection Bar	6061 Aluminum Flat Bar	6(L)x 3/4(W)x1/8 (T)
¼ in. Dia. Bolt with Nuts	Steel	1 in. Long
1/8 in. Dia. Bolt with Nuts and Washers	Steel	½ in. Long

Table C-2 Shake Table Specification

Table Dimensions	13 in x 17 in (1/4 -20UNC mounting holes on 2 in x 2 in grid)
Design payload	5-15 lbmm
Maximum Payload	25 lbm
Frequency Range	0.1 - 20 Hz
Displacement	+/- 3.2 inches
Velocity	+/- 20 inches/second
Acceleration	+1- 1.0g (with 25 lbm specimen)
Total weight of system	<60 lb
Overall dimensions	14 in (w) x 36 in (L) x 4 in (H)

Table C-3 DAQ System

Device	cDAQ-9171	NI 9219
Manufacturer	National Instruments	National Instruments
Serial Number	1631A58	162C1313

Table C-4 Load Cell Calibration's Data

Excitation Voltage = 2.5V

Load	Force	Voltage	Zeroed Voltage	Calculated Force	Calculated Error
Kg	N	mV	mV	N	N
0.00	0.00	-0.0350	0.0000	0	0.00
0.20	1.91	-0.1090	-0.0740	1.81	**-0.10**
0.77	7.56	-0.3390	-0.3040	7.46	**-0.10**
1.60	15.73	-0.6730	-0.6380	15.65	-0.08
2.18	21.34	-0.9030	-0.8680	21.29	-0.06
3.56	34.93	-1.4575	-1.4225	34.89	-0.05
4.38	42.96	-1.7835	-1.7485	42.88	-0.08
4.84	47.46	-1.9680	-1.9330	47.40	-0.06

Sensitivity =	-0.0408	mV/N
	-0.0163	**mV/V/N**
Max Error =	**0.10**	N
Accuracy =	**0.21%**	

Table C-5 OptiTrack Camera's Calibration Data

| Prescribed Displacement	Measured Displacement	Error
(mm)	(mm)	(mm)
0.000	0.005	0.005
12.295	12.342	0.047
22.430	22.420	-0.010
31.363	31.390	0.027
40.689	40.621	-0.068
52.090	51.989	-0.101
34.641	34.586	-0.055
20.916	20.941	0.025
8.402	8.400	-0.002
-1.153	-1.120	0.033
Average Absolute Error =		0.037

Figure C-1 Dial Gage

Figure C-2 Dial Caliper
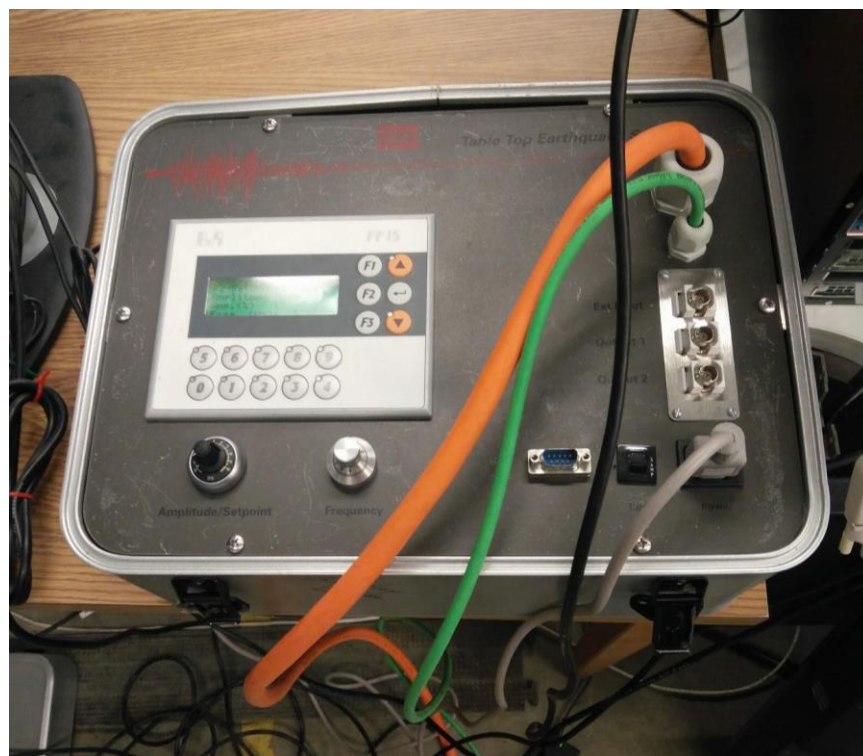
Figure C-3 Shake Table Control Box

Figure C-4 NI 9219 Input Module
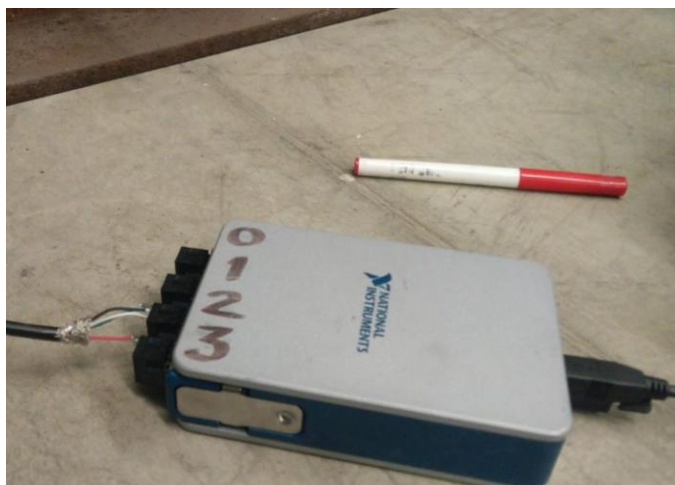
Figure C-5 NI 9219 Input Module and cDAQ-9171

Figure C-6 Load Cell

Parameter	Unit	Technical Specifications	Parameter	Unit	Technical Specifications
Sensitivity	mV/V	2.0±0.05	Temperature coefficient of sensitivity	≤%F·S/10℃	±0.03
Nonlinear	≤%F·S	±0.03	Operating temperature range	℃	-20℃～+80℃
Hysteresis	≤%F·S	±0.03	Input resistance	Ω	350±20Ω
Repeatability	≤%F·S	±0.03	Output Resistance	Ω	350±5Ω
Creep	≤%F·S/30min	±0.03	Safe Overload	≤%F·S	150% F·S
Zero output	≤%F·S	±1	Insulation resistance	MΩ	≥5000MΩ(50VDC)
Zero temperature coefficient	≤%F·S/10℃	±0.03	Excitation voltage	V	10V-15V
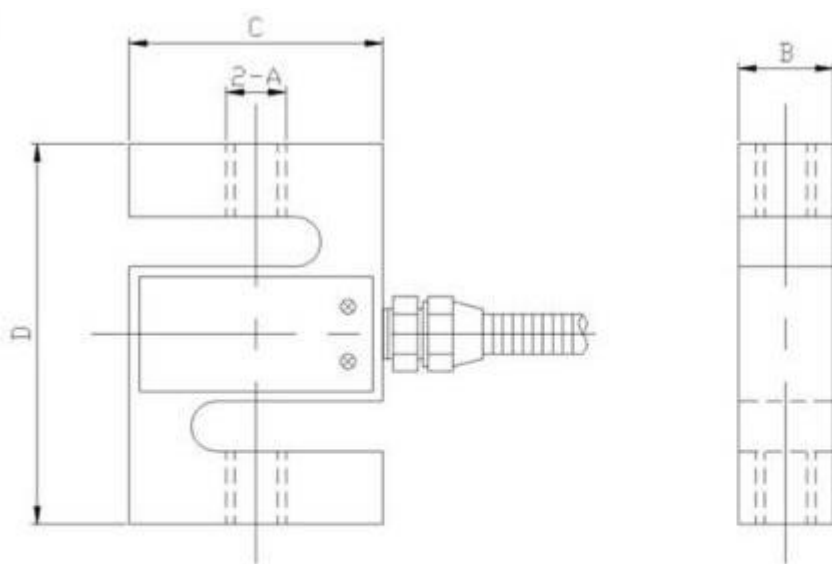
量程

| 量程 Range	A	B	C	D
5-50kg	M8×1.25	12.7	50.8	63.5
100-500kg	M12×1.75	19	50.8	76.2
1-1.5t	M16×2	25.4	50.8	76.2
2-5t	M18×1.5	25.4	76.2	108

Figure C-7 Load Cell Specification
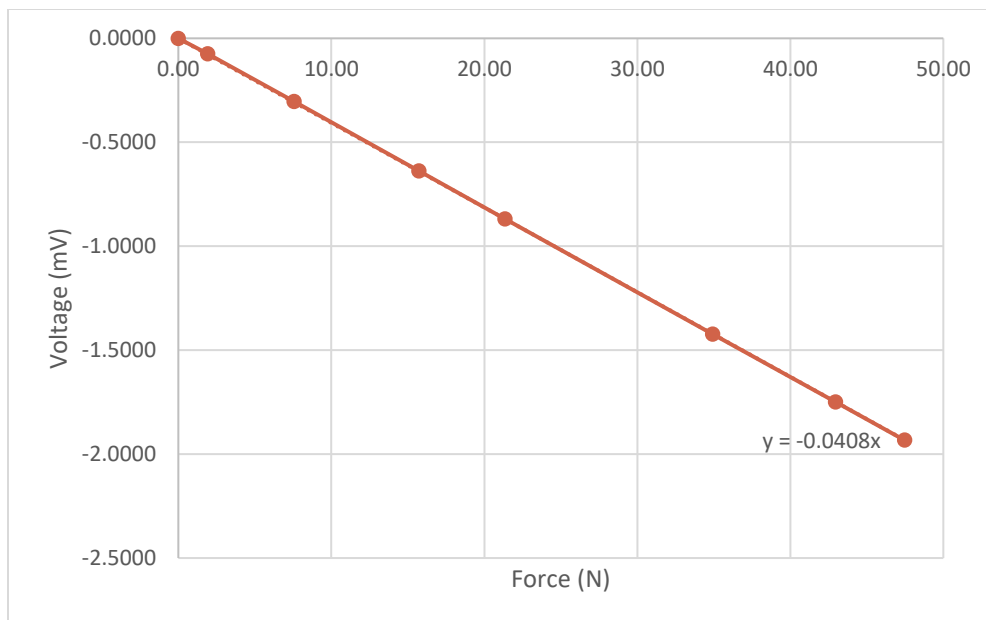
Figure C-8 Load Cell Calibration Graph
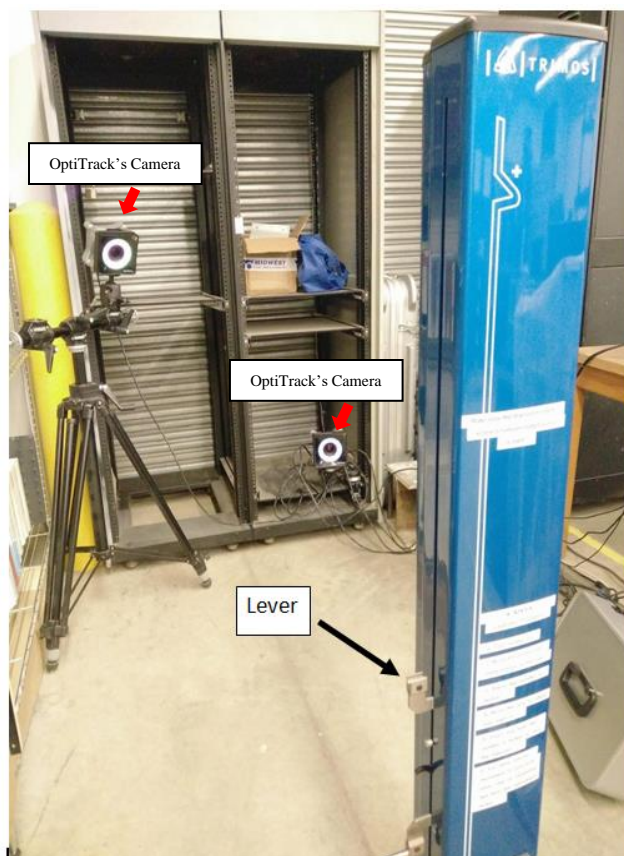
Figure C-9 Cameras' Calibration Setup

APPENDIX D. VAN NUYS HOTEL

The test structure is a 7-story reinforced concrete moment frame building located in Van Nuys, California. The building sustained severe damage during the 1994 Northridge earthquake. The intent is to determine the location and level of reductions in the story stiffnesses due to the Northridge earthquake. The structural system of the building is relatively simple, as describe below. The building was instrumented with 16 accelerometers. In the current application, the building is assumed to be a fixed-base spring-mass system with linear behavior and small amount of equivalent viscous damping.

D.1   Building Description

The building was constructed in 1966 and served as a hotel (Blume et al., 1973). The structural system of the building consists of flat slabs with perimeter beams supported by columns. Each column sits on two to four piles and the pile caps are tied together with ground beams (Figure D-1). The soil underneath is alluvium composing of mostly fine sandy silts and silty fine sands (Blume et al., 1973). Perimeter column-beam frames and interior column-slab frames provide lateral stiffness in each direction even though the exterior ones were stiffer. The typical building plan is symmetric, comprising of eight 18'9" bays on the east-west direction and two 20'1" outer bays, and one 20'10'' middle bay on the north-south direction. The typical floor plan is shown in Figure D-2, Figure D-3 and Figure D-4 show the typical transverse and longitudinal section of the building. From the figures, the first story height is 13'6'' and roof is 8'8'', while the rest is 8'8.5''. The dimensions of the structural elements are given in Table D-1. Properties of concrete used in the building are shown in Table D-2.

Gypsum wallboards were used in the interior partitions, while one-inch thick cement plasters were used at the exterior ends, and at the stairs and elevators. At the north side of the building on grid line D between the ground floor and second floor, there are also four full bays of masonry walls with 1-inch expansion joints to isolate from the columns, and 0.5-inch of the same joints to separate from the second floor's beams (Blume et al., 1973). As mentioned earlier, the lateral loads were

resisted by concrete frames; nonetheless, the nonstructural walls might also contribute to the lateral stiffness.

D.2   Earthquakes and Damages to the Building

Since its construction, the building has undergone several earthquakes. Some of the events are shown in Table D-3. The two major earthquakes the building experienced are the magnitude 6.6 1971 San Fernando earthquake and magnitude 6.5 1994 Northridge earthquake. The San Fernando earthquake caused inconsequential structural damage at north-east corner beam-column connection (Blume et al, 1973). This was repaired later by epoxy grouting. The nonstructural damage was substantial.

Before the 1994 Northridge earthquake, there were a series of smaller earthquakes none of which caused noticeable defects. The Northridge earthquake, however, caused heavy structural damage in the building, especially in the east-west (plan longitudinal) direction. Trifunac et al. (1999) surveyed the damage and reported substantial structural damage to the exterior frames in the east-west direction. Figure D-5 and Figure D-6 show the crack maps on the exterior frame A and frame D. In frame A, there were major cracks up to 5cm wide in five of the beam-column connections at the fifth floor. Trifunac et al. were not able to observe any damage in the first story due to obstructions. In frame D, on the first story, there were cracks in captive columns. Cracks in the masonry walls were also observed. Additionally, there were cracks in beam-column joints at the second floor to the fifth floor along gridline 5, 7 and 8. Cracks through columns were also observed on gridline 1 between the fourth floor and third floor, and gridline 9 between the third floor and second floor. They also noticed there were no observable cracks to the interior frames and no damage on the floor slabs except for minor cracks around the central columns on the 5th and 6th floor. It is interesting to note that story 6 and story 7 appeared to have suffered no or little damage.

D.3   Analysis Procedure

The building is to be idealized as a spring-mass system. Therefore, the initial masses and stiffnesses are estimated using data obtained prior to the 1994 Northridge earthquake.   The

approximations of the natural frequencies of the building before the earthquake will help calibrate the obtained stiffnesses, while the frequencies obtained after the earthquake will help determine what the reductions in the story stiffnesses are. This will be done on the east-west direction where the damage occurred.

D.3.1 Estimating the Building Frequencies

Todorovska & Trifunac (2006) tracked the fundamental frequency changes (Figure D-7) of the Van Nuys building. f_1 is the fixed-base fundamental frequency of the building and f_{sys} is the fundamental frequency of soil-structure system. f_{sys} was determined by the response of the building while f_1 by the analysis of the shear wave travel times. It was mentioned that using the f_{sys} to determine the reduction in the stiffness of the builing may not be accurate.

Nonetheless, there were also ambient frequency tests conducted on the building. The frequencies from the ambient tests may present less interaction from the soil. Mulhern and Maley (1973) did an ambient vibration test on the building after the San Fernando earthquake and after the building had been repaired. The fundamental frequency after the earthquake was 1.39Hz and after the repair it rose to 1.56 Hz on the east-west direction. The 1.56Hz frequency will be then assumed to be the fundamental frequency before Northridge earthquake. Ivanovic et al. (1999) did the ambient vibration 2.5 weeks after the Northridge earthquake and the frequencies on the EW direction of the buildings were 1.0Hz, 3.5Hz, 5.7Hz and 8.1Hz.

The building was instrumented with a total of 16 accelerometers. Accelerometers were placed at the ground floor, second floor, third floor, sixth floor and roof. The locations of the sensors are shown in Figure D-8. For the comparison, the frequencies determined directly from the building earthquake responses are also obtained and used to determine the reductions in the stiffnesses. To determine the frequencies of the building before the Northridge earthquake, the response records obtained during the 1992 Landers earthquake were used. The 1992 Landers earthquake produced a maximum of 0.15% roof drift ratio. The Phase Difference Index method of Cheng (2017) was used to estimate the natural frequencies of the building. The phase difference between the ground floor and roof responses are used to estimate the frequencies. The fundamental frequency is

estimated to be 0.9 Hz (fundamental period of 1.1s) (Figure D-9). Similarly, to determine the frequencies after the strong motion of 1994 Northridge event, the last 20 seconds of the ground floor and roof signal were used as the inputs for PDI. The maximum roof drift ratio was 0.14% during the last 20 seconds of the Northridge earthquake. The method provided estimates of the first four natural frequencies: 0.5Hz, 1.85Hz, 3.3Hz and 4.8Hz (Figure D-10).

D.3.2   Estimating the Building Mass and Story Stiffness

The mass can be lumped and estimated from the structural elements. Blume et al. (1973) did a study on the building for the San Fernando earthquake and the weights they used are given in Table D-4. For the story stiffnesses, because the building is composed of symmetric concrete frames, estimates can be obtained using the expression and correction factors given by Schultz (1992). The stiffnesses obtained are shown in Table D-5. With these two sets of information, the natural periods and frequencies of the building can be determined (Table D-6). The fundamental period is 1.12s with the corresponding frequency of 0.89Hz. This value is similar to the one obtained earlier using the response to the 1992 Landers earthquake. Schultz's expression should give the stiffnesses immediately after the construction and, as such, seems to underestimate the stiffnesses since 1.12s fundamental period is high for a 7-story building. The stiffness values obtained using Schultz's approach are scaled, using the same factor, so that the fundamental frequency is 0.9Hz as estimated from the 1992 Landers earthquake response using Cheng's (2017) approach, and 1.56Hz as given by the ambient fundamental frequency after the San Fernando earthquake. The result story stiffnesses are used in the baseline (pre-damage) model of the building (Table D-5).

D.3.3   Estimating the Reductions in the Stiffness

From the survey of Trifunac et al. (1999), the building appeared to have sustained damage in the first story through the fourth story. The top three stories (fifth, sixth and seventh stories) appeared undamaged even though there might be minor cracks on the fifth floor. It is then expected that the stiffnesses of the first 4 stories reduced due to the Northridge earthquake. Cases of four softened stories will be explored. If the damage in story 5, story 6, story 7 are small, the explored scenarios should be the most likely case.

D.4   Analysis Results and Discussion

D.4.1   Story Drift Ratio

Figure D-12 to Figure D-15 show story drift ratios for the 1994 Northridge earthquake. As there were no accelerometers on the fourth, fifth and seventh floors, the story drift ratios were calculated using displacement between those floors with available data and the total height between those floors. As can be seen from the plots, the maximum drift ratio for the first story was around 1%, the second story was just under 2%, third to fifth story just under 1.5% and sixth to seventh floor just under 0.6%. The 1% drift in the first story caused cracking in the captive columns at the story.

D.4.1   Stiffness Reductions

Table D-7 and Table D-8 shows relative stiffnesses for cases with four stories damaged based on the four frequencies obtained from 1) the ambient responses and 2) the Landers earthquake responses. In both cases, the fifth, sixth and seventh stories are assumed to remain unchanged. Cases where there are no solutions or infeasible solutions (e.g. increase in stiffness) are not shown. From Table D-7 which is for the ambient response, the relative stiffness for story 1 is 30%, 34% for story 2, 54% for story 3, 88% for story 4, and 100% for the rest. For the Landers earthquake responses, Table D-8, the relative stiffness for story 1 is 18%, 44% for story 2, 49% for story 3, 74% for story 4, and 100% for the rest. The two sets of values (based on the ambient response and the Landers earthquake response) do not agree because they start from different initial stiffness configurations. The numbers are not intended to be taken in absolute sense since many uncertainties and assumptions were made. The difficulties include the fact that the building was assumed to be a fixed-base linear spring-mass system without soil-structure interactions. The errors in the determination of the modal parameters, such as initial mass and stiffness, and the measured frequencies might also be a challenge.

A LARZ model (Lepage, 1997) was used to estimate the reductions in the story stiffnesses assuming that the structural elements are ductile. The response for the first 2.5 seconds and the last 5 seconds of the Northridge earthquake was used to determine the stiffness distributions. In calculating the stiffness values, story shear and story drifts, when the drifts are greater than 0.001in,

are used. The results are shown in Table D-9. From that table, the numerical simulation estimates that the story stiffness reductions are large and spread throughout the structure, including the sixth and seventh stories. This was different from what was observed at the building because the building suffered from brittle failures. Todorovska and Trifunac (2006) used wave travel times via impulse response function to estimate the reduction in stiffness. They suggest that the reductions were around 60% for the first story and around 30% to 40% for all other stories (Figure D-17).

Table D-1 Structural Elements' Dimension

Floor	Slab Thickness (in)	Column		Perimeter Beam	
		Exterior W(in) x D(in)	Interior W(in) x D(in)	EW Direction W (in) x D (in)	NS Direction W (in) x D (in)
1	4	14x20	18x18		
2	10	14x21	18x19	16x30	14x30
3	8.5	14x22	18x20	16x22.5	14x22.5
4	8.5	14x23	18x21	16x22.5	14x22.5
5	8.5	14x24	18x22	16x22.5	14x22.5
6	8.5	14x25	18x23	16x22.5	14x22.5
7	8.5	14x26	18x24	16x22.5	14x22.5
Roof	8			16x22	14x22

Table D-2 Concrete Properties (Blume et al., 1973)

Location	Compressive Strength, f'_c psi	Young's Modulus, E psi
Columns, 1st to 2nd floor	5000	4.2×10^6
Columns, 2nd to 3rd floor	4000	3.7×10^6
Beams and slabs, 2nd floor	4000	3.7×10^6
All other concrete, 3rd floor to roof	3000	3.2×10^6
Concrete Density = 150pcf		

Table D-3 Some Earthquakes Recorded at Van Nuys Building (Trifunac et al., 1999)

No.	Earthquake	Date	M	R (km)
1	San Fernando	2/9/1971	6.6	22
2	Whittier Narrows	10/1/1987	5.9	41
3	Whitter-Narrows Aftershock	10/4/1987	5.3	38
4	Pasadena	10/3/1988	4.9	32
5	Montebello	6/12/1989	4.1	34
6	Malibu	01/19//1989	5	36
7	Sierra Madre	6/28/1991	5.8	44
8	Landers	6/28/1992	7.5	186
9	Big Bear	6/28/1992	6.5	149
10	Northridge	1/17/1994	6.5	1.5
11	Northridge Aftershock	3/20/1994	5.2	1.2
12	Northridge Aftershock	12/6/1994	4.5	10.8

Table D-4 Building's Lumped Weight/Mass (Blume et al., 1973)

Floor	Weight (kip)	Mass (kg)
1		
2	1830	8.30E+05
3	1460	6.62E+05
4	1460	6.62E+05
5	1460	6.62E+05
6	1460	6.62E+05
7	1460	6.62E+05
Roof	1410	6.40E+05

Table D-5 Building's Stiffness

Story	Stiffness from Schultz's		Scaled Stiffness (Ambient Frequency)		Scaled Stiffness (Lander Frequency)	
	kip/in	N/m	kip/in	N/m	kip/in	N/m
1	2012.1	3.52E+08	6156.8	1.08E+09	2072.3	3.63E+08
2	3994.6	7.00E+08	12223.0	2.14E+09	4114.2	7.21E+08
3	2772.1	4.86E+08	8482.5	1.49E+09	2855.1	5.00E+08
4	2772.1	4.86E+08	8482.5	1.49E+09	2855.1	5.00E+08
5	2772.1	4.86E+08	8482.5	1.49E+09	2855.1	5.00E+08
6	2773.8	4.86E+08	8487.6	1.49E+09	2856.9	5.00E+08
7	2697.6	4.72E+08	8255.0	1.45E+09	2778.6	4.87E+08

Table D-6 Modal Frequencies/Periods

Mode	Frequencies (Hz)	Period (sec)
1	0.89	1.12
2	2.53	0.39
3	4.08	0.25
4	5.64	0.18
5	7.03	0.14
6	8.06	0.12
7	8.61	0.12

Table D-7 Relative Story Stiffness (Frequencies Form Ambient Response)

Cases	1
kr_1	**30%**
kr_2	**34%**
kr_3	**54%**
kr_4	**88%**
kr_5	100%
kr_6	100%
kr_7	100%

Table D-8 Relative Story Stiffness (Frequencies from Lander Earthquake Response)

Cases	1
kr_1	**18%**
kr_2	**44%**
kr_3	**49%**
kr_4	**74%**
kr_5	100%
kr_6	100%
kr_7	100%

Table D-9 Larz Model Stiffnesses

Story	Stiffness Before EQ kip/in	Stiffness After EQ kip/in	Relative Stiffness
1	3600	460	13%
2	5800	1050	18%
3	5000	970	19%
4	4900	910	19%
5	4800	920	19%
6	4800	860	18%
7	5200	960	18%
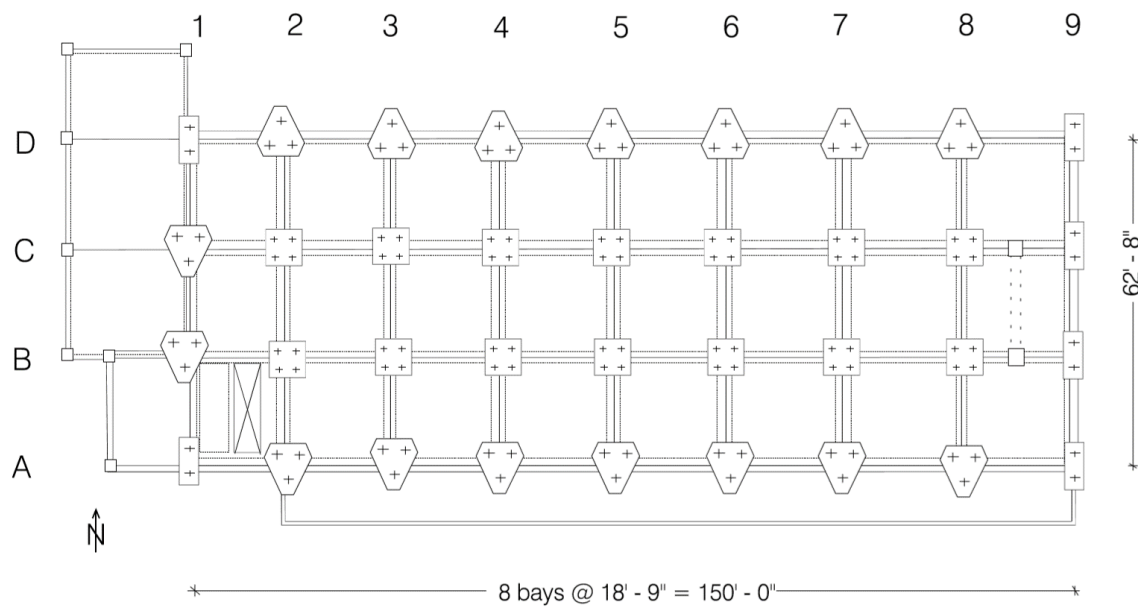
Figure D-1 Foundation Plan (Trifunac et al., 1999)
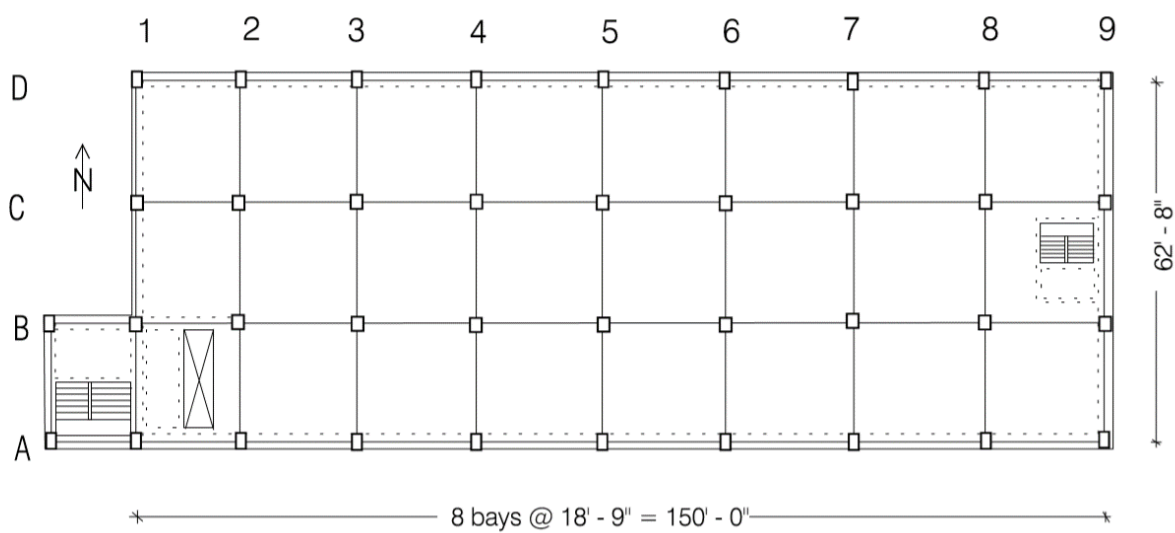
Figure D-2 Typical Floor Plan (Trifunac et al., 1999)
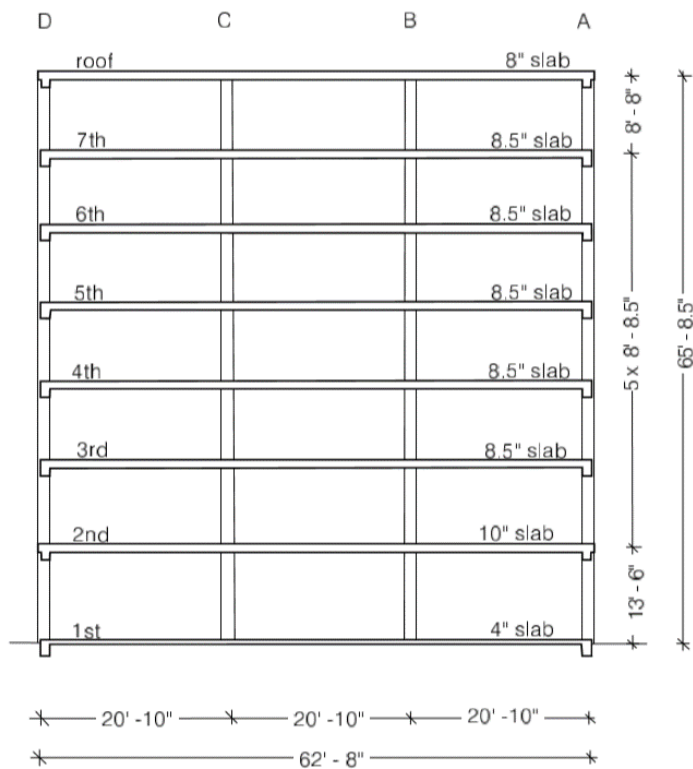
Figure D-3 Typical Transverse Section (Trifunac et al., 1999)
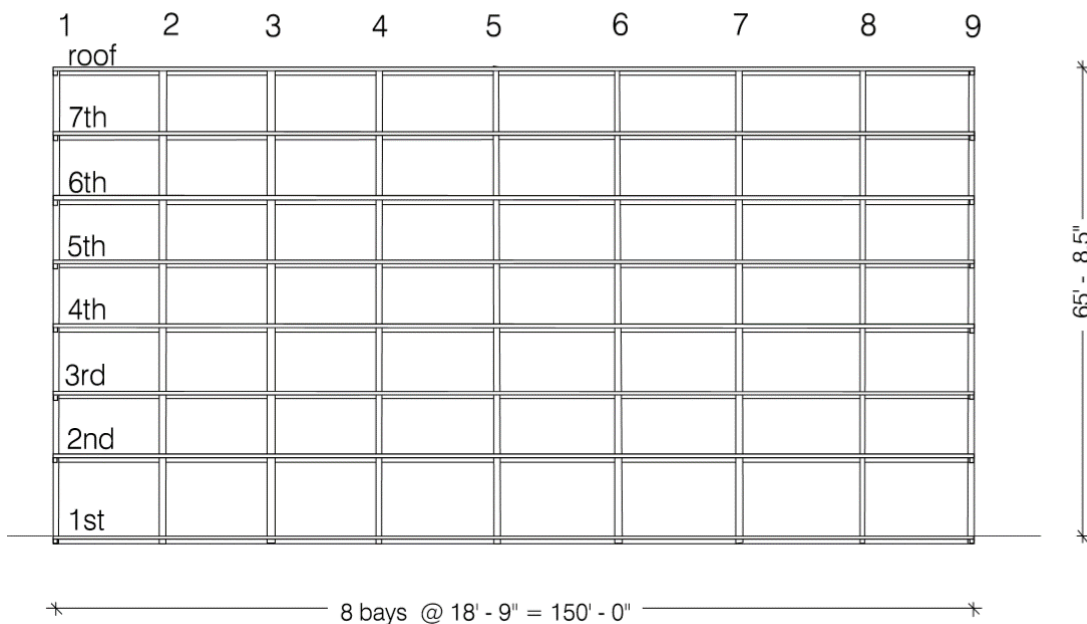
Figure D-4 Typical Longitudinal Section (Trifunac et al., 1999)
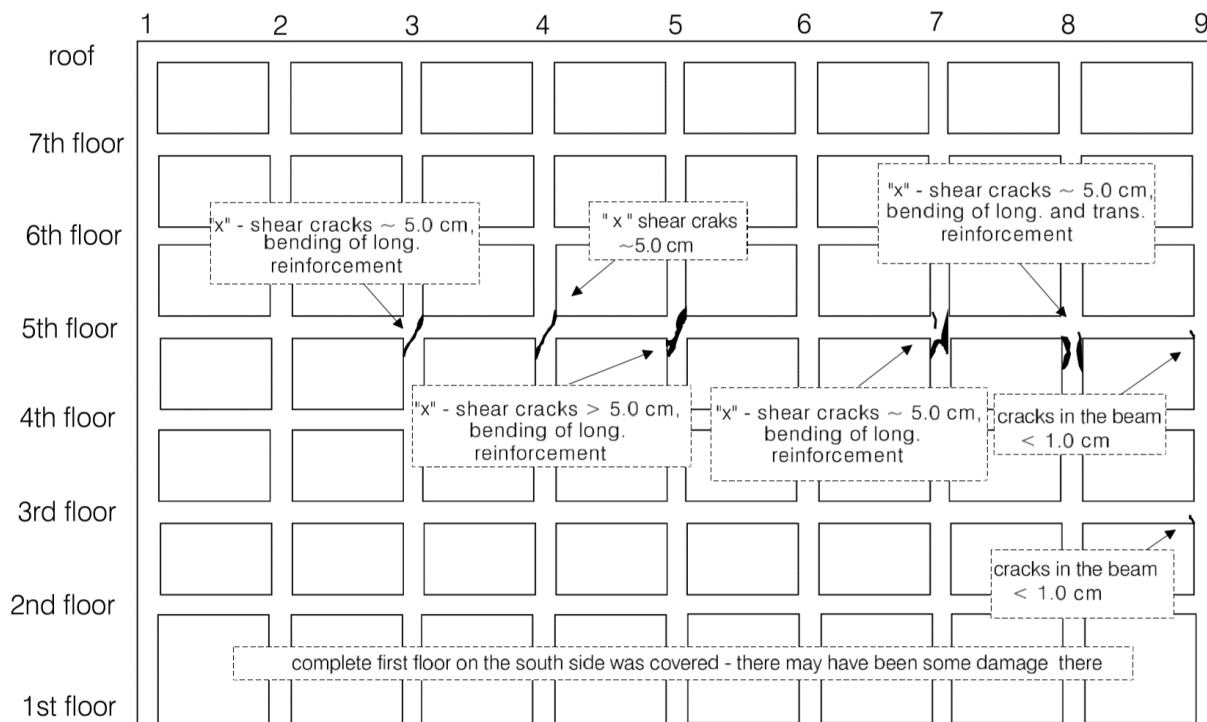
Figure D-5 Frame A Crack Map (Trifunac et al., 1999)
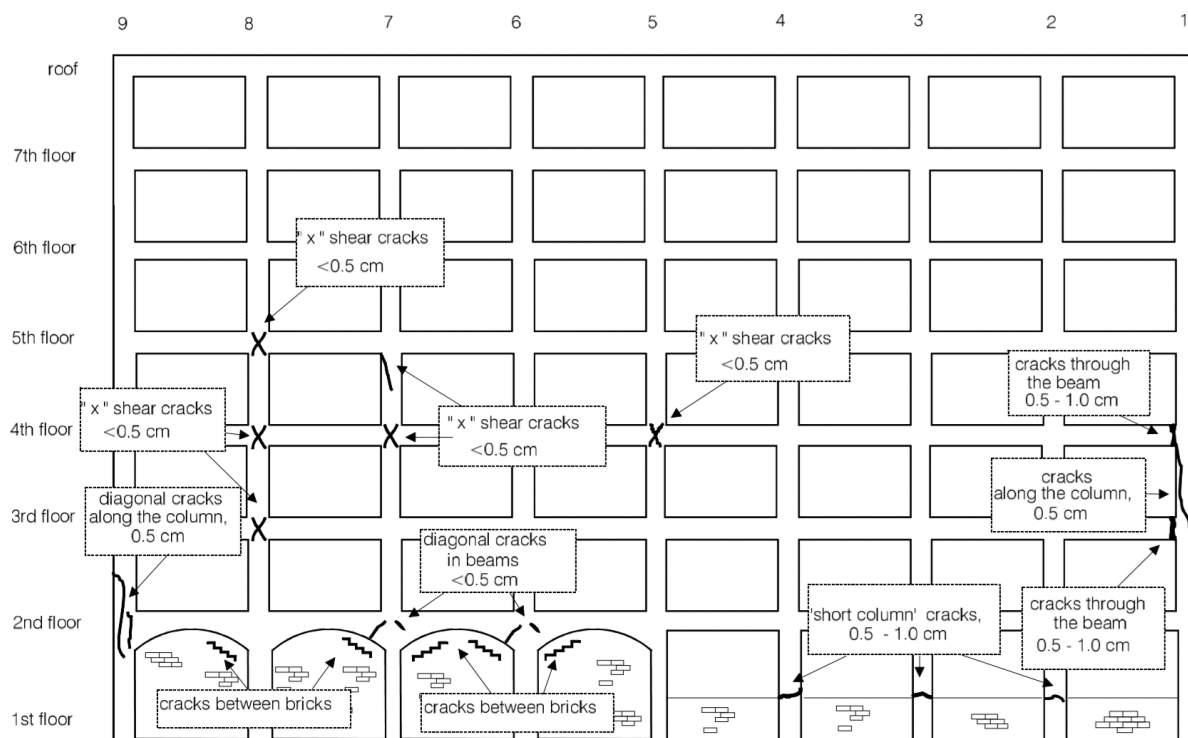
Figure D-6 Frame D Crack Map (Trifunac et al., 1999)
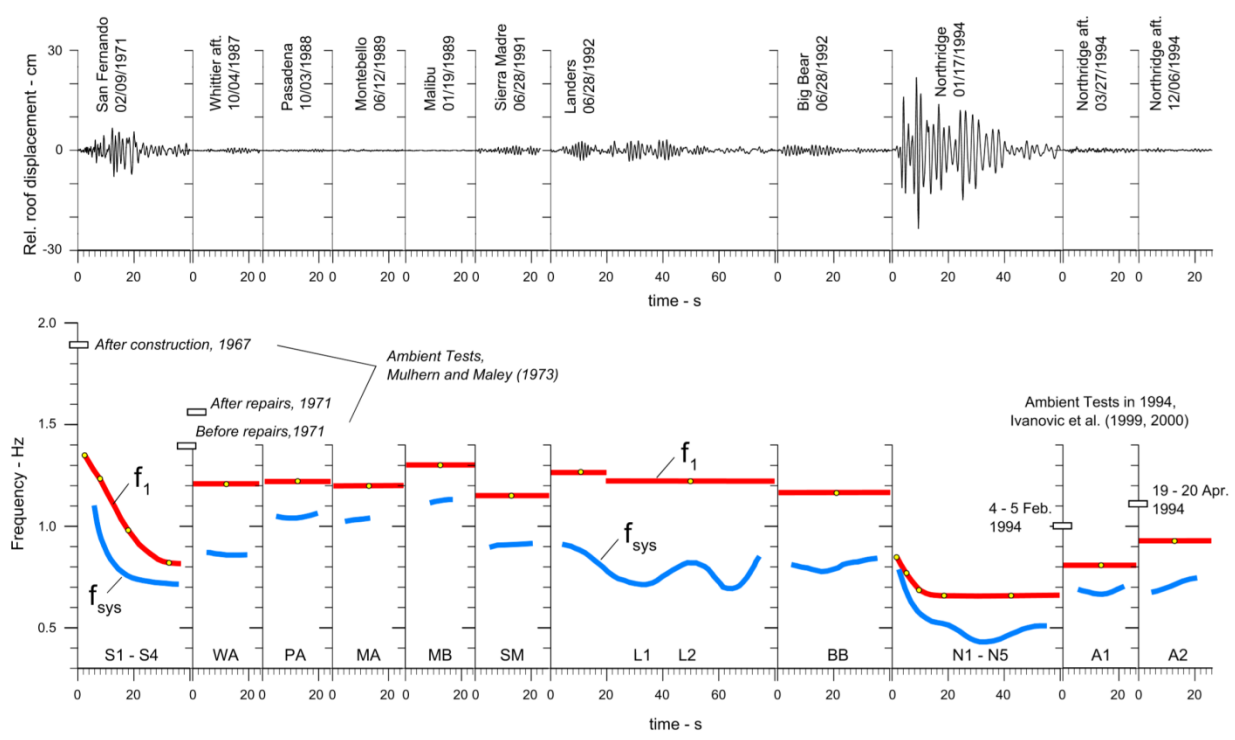
Figure D-7 Fundamental Frequency Variations (Todorovska & Trifunac, 2006)
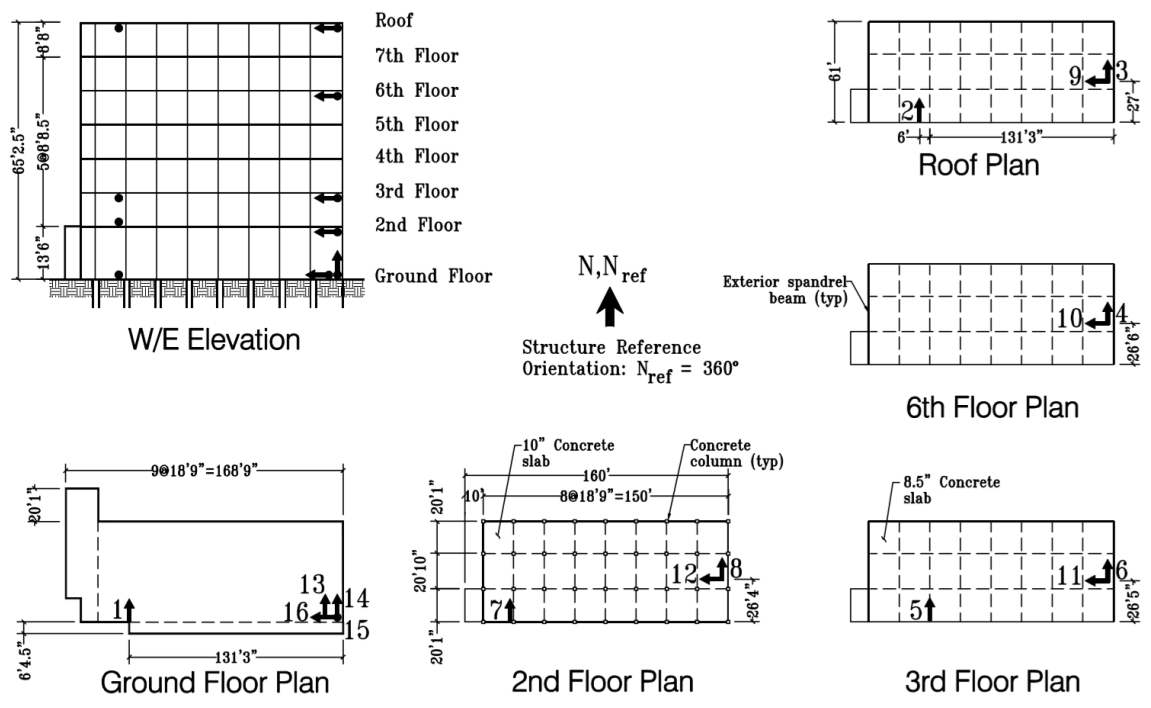
Figure D-8 Van Nuys Building's Sensor Locations (CESMD, 2019)
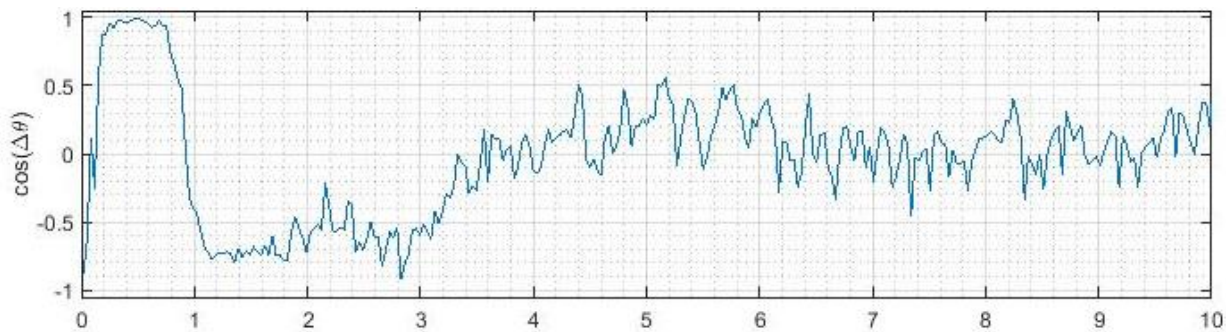
Figure D-9 PDI for 1992 Landers Earthquake
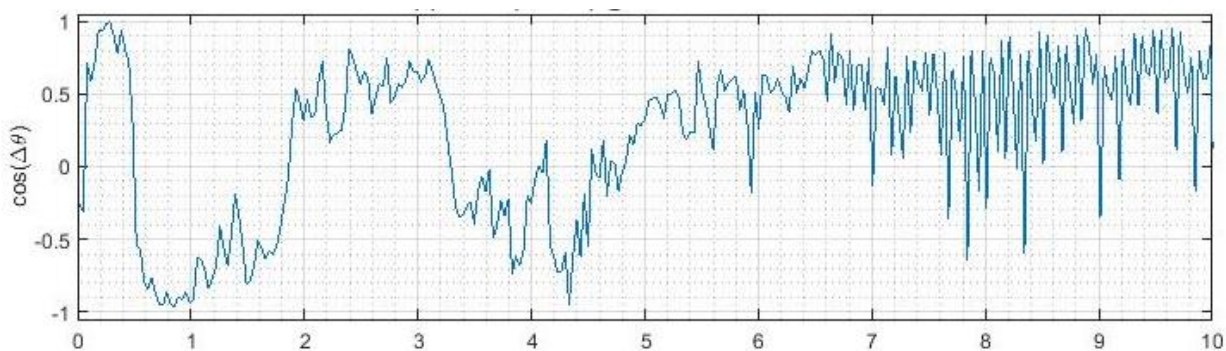

Figure D-10 PDI for 1994 Northridge Earthquake
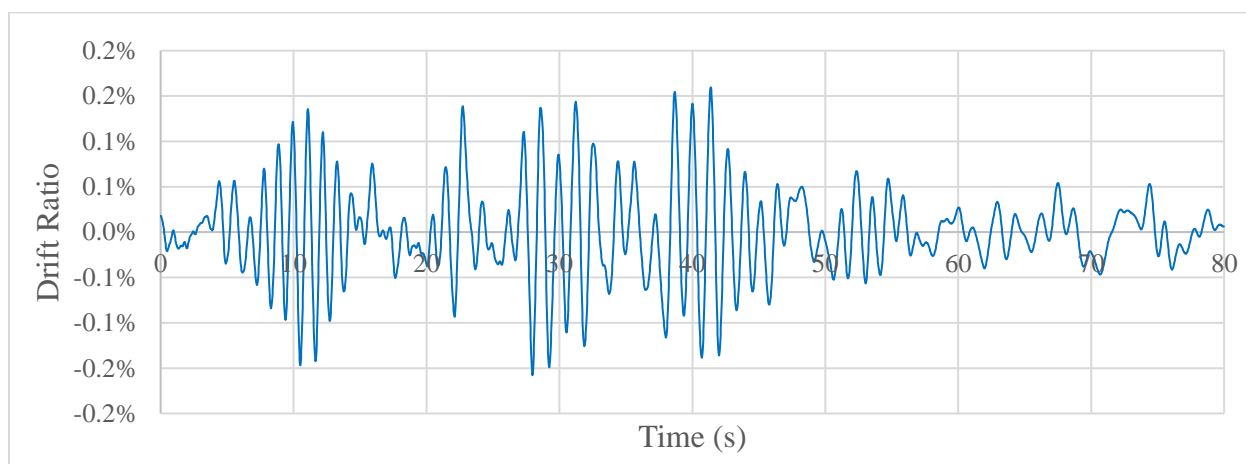

Figure D-11 Roof Drift Ratio During 1992 Lander Earthquake
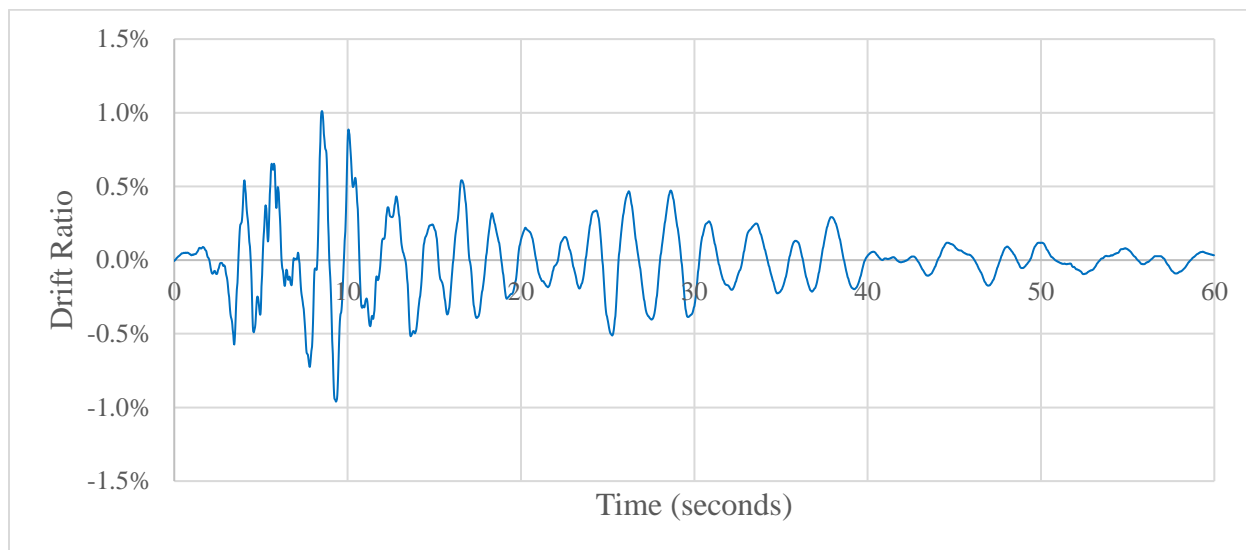
Figure D-12 First Story Drift Ratio During 1994 Northridge Earthquake
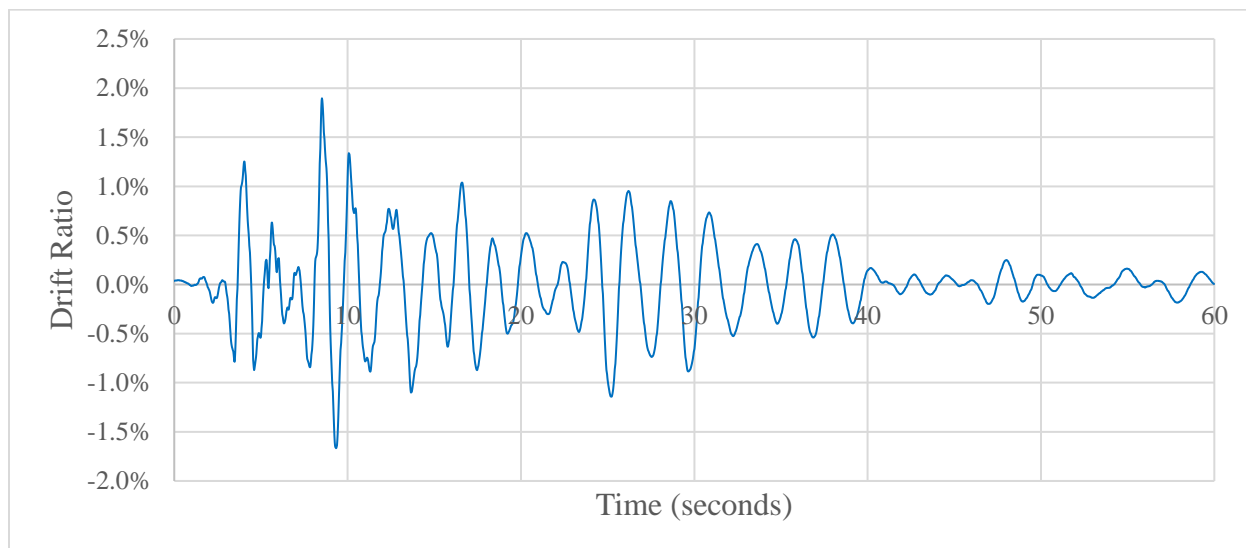
Figure D-13 Second Story Drift Ratio During 1994 Northridge Earthquake
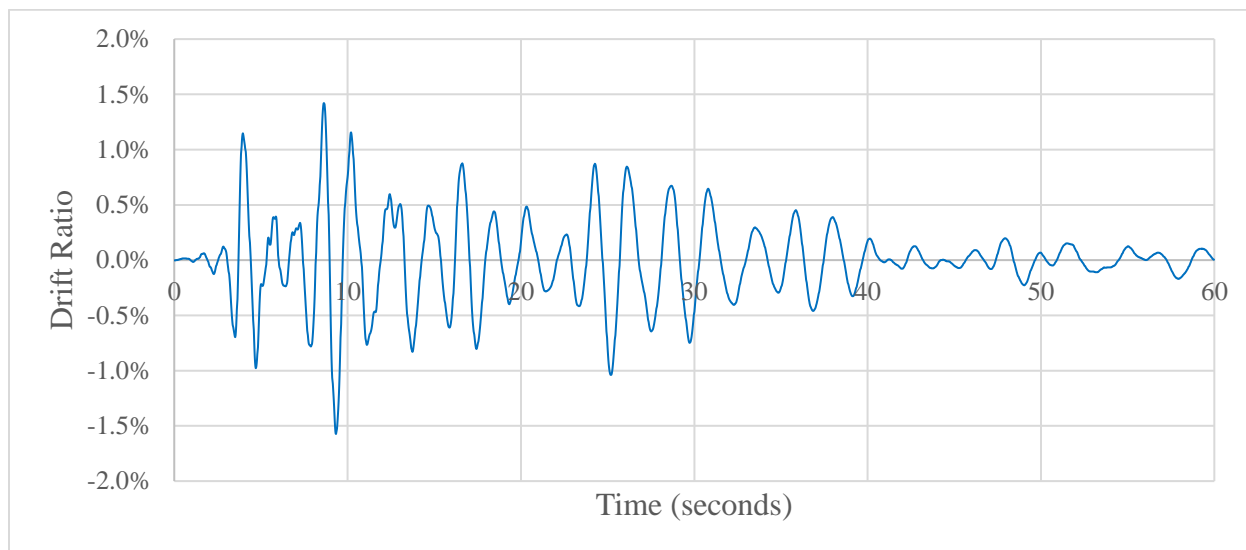
Figure D-14 Third to Fifth Story Drift Ratio During 1994 Northridge Earthquake
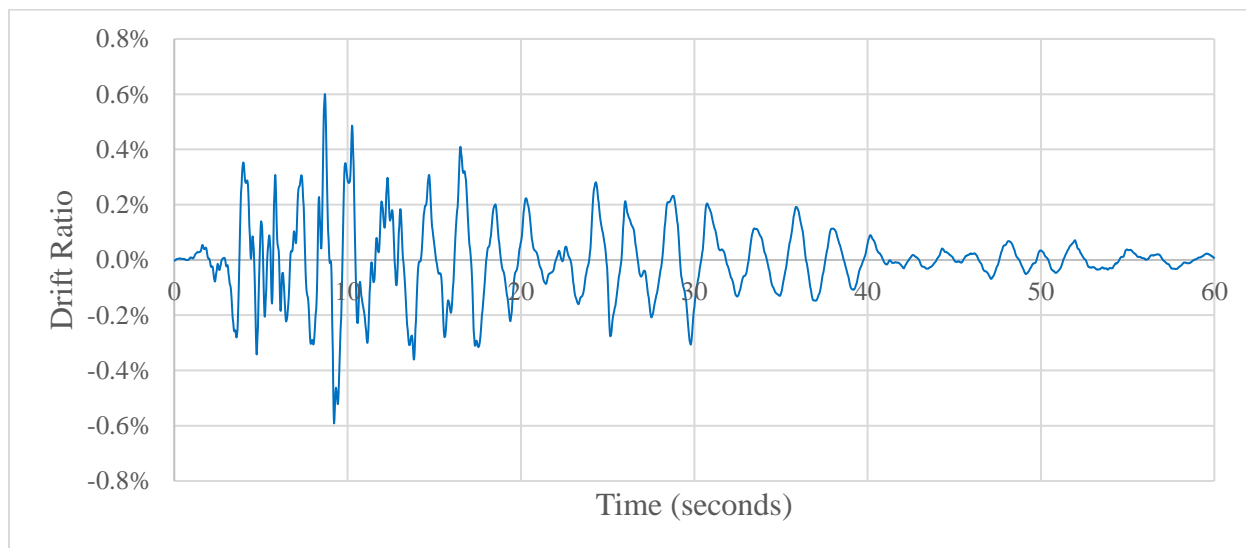

Figure D-15 Fifth to Sixth Story Drift Ratio During 1994 Northridge Earthquake
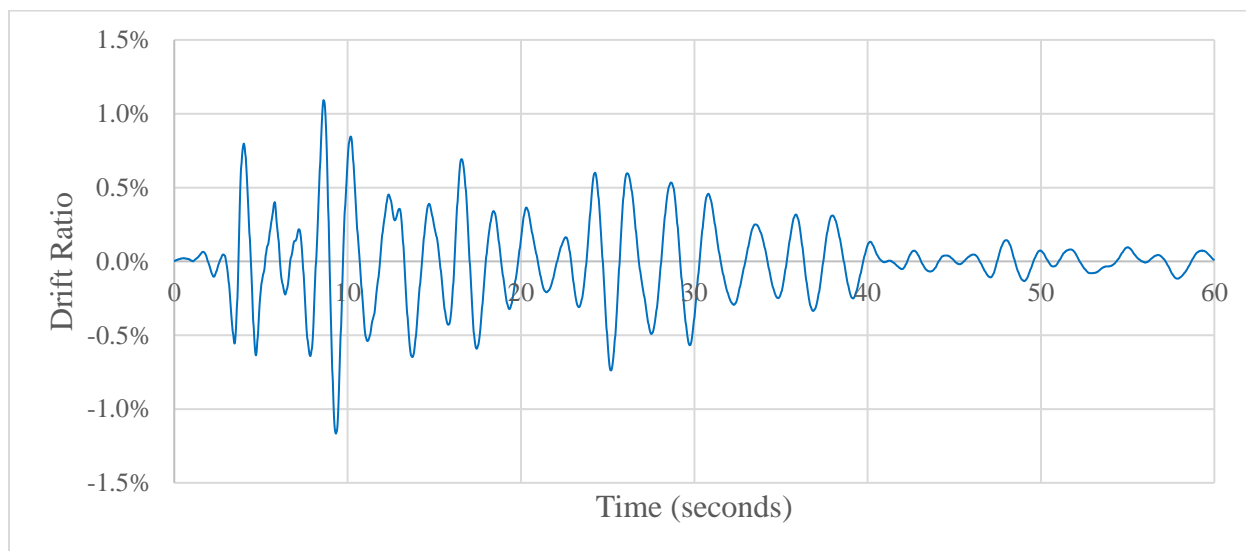
Figure D-16 Roof Drift Ratio During 1994 Northridge Earthquake
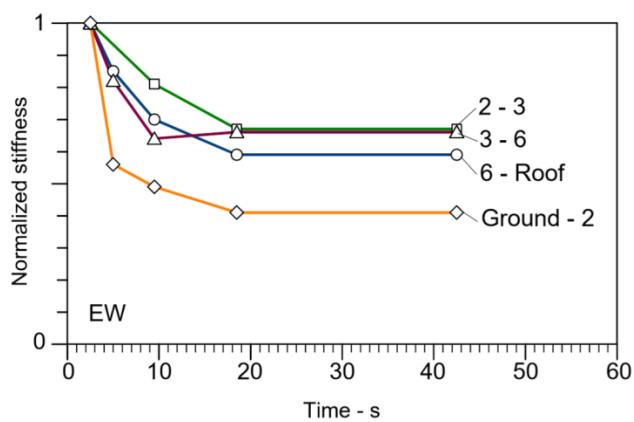

Figure D-17 Reductions in Stiffness for Van Nuys Building using Analysis of Wave Travel Times (Todorovska & Trifunac, 2006)

REFERENCES

Alvandi, A., & Cremona, C. (2006). Assessment of vibration-based damage identification techniques. *Journal of Sound and Vibration, 292*(1), 179-202. Retrieved 1 11, 2019, from https://sciencedirect.com/science/article/pii/s0022460x05004980

Biegler-König, F. W. (1981). A Newton iteration process for inverse eigenvalue problems. *Numerische Mathematik, 37*(3), 349-354. Retrieved 1 18, 2019, from https://link.springer.com/article/10.1007/bf01400314

Cawley, P., & Adams, R. (1979). The location of defects in structures from measurements of natural frequencies. *Journal of Strain Analysis for Engineering Design, 14*(2), 49-57. Retrieved 1 10, 2019, from http://journals.sagepub.com/doi/pdf/10.1243/03093247v142049

CESMD. (2019, 03 27). *Center for Engineering Strong Motion Data*. Retrieved from Information for Strong-Motion Station: https://strongmotioncenter.org/cgi-bin/CESMD/stationhtml.pl?staID=CE24386&network=CGS

Cheng, L.-H. (2017). *Phase Difference Index: A Frequency-Domain Analysis Tool.* West Lafayette: Purdue University.

Chopra, A. K. (2012). *Dynamics of Structures: Theory and Applications to Earthquake Engineering* (4th ed.). Prentice Hall.

Chu, M. T., & Golub, G. (2005). *Inverse Eigenvalue Problems: Theory, Algorithms, and Applications.* Oxford University Press.

Cornwell, P., Doebling, S. W., & Farrar, C. R. (1999). Application of the Strain Energy Damage Detection Method to Plate-like Structures. *Journal of Sound and Vibration, 224*(2), 359-374. Retrieved 1 11, 2019, from https://sciencedirect.com/science/article/pii/s0022460x99921636

CSI. (2019, 04 17). *SAP2000*. Retrieved from Computers and Structures Inc: https://www.csiamerica.com/products/sap2000

Das, S., Saha, P., & Patro, S. K. (2016). Vibration-based damage detection techniques used for health monitoring of structures: a review. *J. Civil Struct. Health Monit., 6*, 477-507.

Dawari, V. B., Kamble, P. P., & Vesmawala, G. R. (2015). *Structural Damage Identification Using Modal Strain Energy Method*. Retrieved 1 11, 2019, from https://link.springer.com/content/pdf/10.1007/978-81-322-2187-6_201.pdf

Doebling, S. W., Farrar, C. R., & Goodman, R. S. (1997). Effects of measurement statistics on the detection of damage in the Alamosa Canyon Bridge. *International modal analysis conference*, (pp. 919-929). Orlando, FL.

Doebling, S. W., Farrar, C. R., & Prime, M. B. (1998). A summary review of vibration-based damage identification methods. *The Shock and Vibration Digest, 30*(2), 91-105. Retrieved 1 10, 2019, from http://svd.sagepub.com/cgi/doi/10.1177/058310249803000201

Esfandiari, A., Bakhtiari-Nejad, F., & Rahai, A. (2013). Theoretical and experimental structural damage diagnosis method using natural frequencies through an improved sensitivity equation. *International Journal of Mechanical Sciences, 70*, 79-89. Retrieved 1 10, 2019, from https://sciencedirect.com/science/article/pii/s002074031300060x

Gomes, G. F., Mendéz, Y. A., Alexandrino, P. d., Cunha, S. S., & Ancelotti, A. C. (2018). A Review of Vibration Based Inverse Methods for Damage Detection and Identification in Mechanical Structures Using Optimization Algorithms and ANN. *Archives of Computational Methods in Engineering*, 1-15. Retrieved 1 12, 2019, from https://link.springer.com/article/10.1007/s11831-018-9273-4

Guan, H., & Karrbhari, V. (2008). Improved damage detection method based on element modal strain damage index using sparse measurement. *J. Sound Vib.*, 465-494.

Hassiotis, S., & Jeong, G. D. (1995). Identification of Stiffness Reductions Using Natural Frequencies. *Journal of Engineering Mechanics-asce, 121*(10), 1106-1113. Retrieved 1 10, 2019, from http://ascelibrary.org/doi/10.1061/(asce)0733-9399(1995)121:10(1106)

Ivanovic, S., Trifunac, M., Novikova, E., Gladkov, A., & Todorovska, M. (1999). *Instrumented 7-storey Reinforced Concrete Building in Van Nuys, California: Ambient Vibration Surveys Following the Damage From the 1994 Northridge Earthquake.* University of Southern California, Department of Civil Engineering, Los Angeles.

John A. Blume & Associates, E. (1973). Holiday Inn (29). *San Fernando, California, earthquake of February 9, 1971, I Part A*.

Kong, X., Cai, C.-S., & Hu, J. (2017). The State-of-the-Art on Framework of Vibration-Based Structural Damage Identification for Decision Making. *Applied Sciences, 7*(5), 497. Retrieved 1 10, 2019, from http://mdpi.com/2076-3417/7/5/497/pdf

Kublanovskaya, V. N. (2003). An Approach to Solving Inverse Eigenvalue Problems for Matrices. *Journal of Mathematical Sciences, 114*(6), 1808-1819.

Lancaster, P. (1966). *Lambda-Matrices and Vibrating Systems.* Oxford: PERGAMON PRESS.

Lee, J. S., Choi, I. Y., & Cho, H. N. (2004). Modeling and detection of damage using smeared crack model. *Engineering Structures, 26*(2), 267-278.

Lepage, A. (1997). *A Method for Drift-control in Earthquake-resistant Design of RC Building Structures.* Urbana: University of Illinios at Urbana-Champaign.

Pandey, A. K., Biswas, M., & Samman, M. M. (1991). Damage Detection From Changes In Curvature Mode Shapes. *Journal Of Sound and Vibration, 145*(2), 321-332.

Podlevskyi, B. M., & Yaroshko, O. S. (2013). Newton's Method for the Solution of Inverse Spectral Problems. *Journal of Mathematical Sciences, 194*(2), 156-165. Retrieved 1 10, 2019, from https://link.springer.com/content/pdf/10.1007/s10958-013-1516-1.pdf

Roy, K. (2017). Structural Damage Identification Using Mode Shape Slope and Curvature. *J. Eng. Mech., 143*(9), 04017110-1-04017110-12.

Roy, K., & Ray-Chaudhuri, S. (2013). Fundamental mode shape and its derivatives in structural damage localization. *Journal of Sound and Vibration, 332*(21), 5584-5593. Retrieved 1 11, 2019, from https://sciencedirect.com/science/article/pii/s0022460x13004082

Rytter, A. (1993). *Vibration Based Inspection of Civil Engineering Structures.* Aalborg, Denmark: Department of Building Technology and Structure Engineering, Aalborg University.

Salawu, O. (1997). Detection of structural damage through changes in frequency: a review. *Engineering Structures, 19*(9), 718-723. Retrieved 1 10, 2019, from https://sciencedirect.com/science/article/pii/s0141029696001496

Schultz, A. E. (1992). Approximating Lateral Stiffness of Stories in Elastic Frames. *Journal of Structural Engineering-asce, 118*(1), 243-263. Retrieved 3 21, 2019, from https://engineering.purdue.edu/~ce474/docs/schultz_1992.pdf

Shi, Z. Y., Law, S., & Zhang, L. M. (1998). Structural Damage Detection from Modal Strain Energy Change. *Journal of Sound and Vibration , 218*(5), 825-844.

Stubbs, N., & Osegueda, R. (1987). *Global nondestructive damage evaluation in solids.* Tech. Rep. No. TR-87-101, Texas A&M University, College Station.

Stubbs, N., Kim, J. T., & Farrar, C. R. (1995). Field verification of a nondestructive damage localization and severity estimation algorithm. *Proceedings of SPIE - The International Society for Optical Engineering (Proceedings of SPIE)*, *2460*, p. 210.

Suita, K., Suzuki, Y., & Takahashi, M. (2015). Collapse Behavior of an 18-Story Steel Moment Frame During a Shaking Table Test. *International Journal of High-Rise Buildings*, 171-180.

Todorovska, M. I., & Trifunac, M. (2006). *Impulse Response Analysis Of The Van Nuys 7-Story Hotel During 11 Earthquakes (1971-1994): One-Dimensional Wave Propagation And Inferences On Global And Local Reduction Of Stiffness Due To Earthquake Damage.* University of Southern California, Department of Civil Engineering, Los Angeles.

Trifunac, M., Ivanovic, S., & Todorovska, M. (1999). *Instrumented 7-Storey Reinforced Concrete Building in Van Nuys, California: Description of the Damage from the 1994 Northbridge Earthquake and Strong Motion Data.* University of Southern California, Department of Civil Engineer, Los Angeles.

West, W. M. (1986). *Illustration of the use of modal assurance criterion to detect structural changes in an Orbiter test specimen.* Retrieved 1 10, 2019, from https://ntrs.nasa.gov/search.jsp?r=19870041253

Whalen, T. M. (2008). The behavior of higher order mode shape derivatives in damaged, beam-like structures. *Journal of Sound and Vibration, 309*(3), 426-464. Retrieved 1 11, 2019, from https://sciencedirect.com/science/article/pii/s0022460x07005901

Zhu, H., Li, L., & He, X.-Q. (2011, May). Damage detection method for shear buildings using the changes in the first mode shape slopes. *Computers & Structures, 89*(9-10), 733-743.